Regulating the trafficking of the unfolded protein response (UPR) reporter ATF6

Wanida Tungkum

Supervisor: Professor Neil Bulleid

Submitted in fulfilment of the requirements for the Degree of Doctor of Philosophy

School of Molecular Biosciences

College of Medical, Veterinary and Life Sciences

University of Glasgow

2023

ABSTRACT

The activating transcription factor 6 (ATF6) is one of the three membrane proteins, which responds to misfolded protein induced stress, in the endoplasmic reticulum (ER). During ER stress, ATF6 dissociates from BiP, an ER chaperone, then transports to the Golgi apparatus where ATF6 undergoes proteolytic processing by site 1 protease (S1P) and site 2 protease (S2P). Up until now, the dissociation of BiP from ATF6 is reported to be the key factor that regulates the trafficking of ATF6 from the ER to Golgi in the unfolded protein response (UPR). However, our study suggests that the ATF6-BiP complex disassembly is not the only factor which controls ATF6 migration when cells get induced ER stress by standard inducers like dithiothreitol (DTT) and thapsigargin (TG). To identify the ATF6 protein complex, the stable cell-lines of the non-trafficking mutants ATF6α, D564G and Y567N, were created and compared with the wild type ATF6α. From our studies, the ATF6α mutants show specific characteristics, distinctively from the wild type ATF6α, which are likely to affect the ability of ATF6 to bind with other proteins and to form disulfides. The results of mass spectrometry indicate numerous proteins which seem to be interacted with ATF6 along with BiP such as 14-3-3E, Neudesin, TFG and ERdj3. Unfortunately, we can only properly investigate ERdj3. We investigated the interaction of ERdj3 protein with ATF6 by immunoisolation and western blot; the results show that ERdj3 interacts with ATF6. Subsequently, the lipotoxic stress inducers, dihydrosphingosine (DHS) and dihydroceramide (DHC), were used to induce ER stress and ATF6 pathway since it was reported that lipotoxic stress upregulates ATF6 differently compared with the mechanism of proteotoxic stress. However, the results from our study with the wild type ATF6α cell-line show that DHS and DHC did not upregulate the ATF6 stress response as previously reported. Taken together our results define the interactome of ER-localised ATF6α and suggest a role for ERdj3 during the ER stress response.

LIST OF CONTENTS Page Number

LIST OF TABLES **Page Number**

LIST OF FIGURES **Page Number**

ACKNOWLEDGEMENT

It is a great honour to complete my PhD research at the University of Glasgow. First of all, I would like to sincerely and heartily thank my supervisor, Professor Neil J. Bulleid, for tremendous support, guidance and patient during my PhD study, especially during the writing of my thesis. His enthusiasm for scientific research, rigorous work attitude, and extensive knowledge, are really a great model for me who has been assigned to be a lecturer after graduation. I also want to express my sincere thanks to all my colleagues in Professor Neil Bulleid's group, all the past and present members, Dr Ojore Oka, Dr Marcel Van Lith, Dr Philip Robinson, Dr Gregory Poet, Dr Zhenbo Cao, Dr. Xiaofei Cao, Marie Anne Pringle, Lorna Mitchell, Bethany Fleming and Arvin Pierre, for their advice, support, help, feedback and friendship. I am especially grateful to Dr Ojore Oka for practically teaching me several Molecular Biology techniques and also for his patience and precious advice. I owe my sincere and earnest thanks to my family and friends for their unlimited love and emotional support throughout my PhD time. I also would like to express my sincere thanks to Thai government and Ministry of Higher Education, Science, Research and Innovation of Thailand, for granting me a scholarship throughout the entire years of my PhD study at the University of Glasgow.

Lastly, I would like to thank our Institute of Molecular, Cell and System Biology, our College of Medical, Veterinary and life Sciences, and our University of Glasgow, for great support and great experiences during my study.

AUTHOR'S DECLARATION

I declare that, except where explicit reference is made to the contribution of others, this thesis is the result of my own work and has not been submitted for any other degree at the University of Glasgow or any other institution.

Printed Name: Wanida Tungkum

Signature:

ABBREVIATIONS

14-3-3E - 14-3-3 protein epsilon

ACOX1 - Acyl-CoA Oxidase 1

ARMET - Arginine-rich, mutated in early-stage tumour

ASK1 - Apoptosis signal regulating kinase 1

ATF4 - Activating transcription factor 4

ATF6 - Activating transcription factor 6

ARMET - Arginine-rich, mutated in early-stage tumour

Bak - Bcl-2 homologous antagonist/killer

Bax – Bcl-2-associated X protein

Bcl2 - B-cell lymphoma 2

Bim – Bcl-2-like protein 11

BiP - Glucose-regulated protein 78 (Grp78)

BSA - Bovine serum albumin

bZIP - Basic leucine zipper

CHO cells - Chinese hamster ovary cells

CHOP - Transcription factor C/EBP-homologous protein

CL – Total cell lysate

CNX – Calnexin

COP II - Coat protein complex II

CRT – Calreticulin

DHC - Dihydroceranmide

DHS - Dihydrosphingosine

DMEM – Dulbecco's modified Eagle's medium

DMSO – Dimethyl sulfoxide

DOC – Isolating stress-induced genes that are downstream of CHOP

DR5 – Death receptor 5

DSP – dithiobis(succinimidyl propionate)

DTT - 1,4-Dithiothreitol

EDTA – Ethylene diamine tetraacetic acid

EGTA – Ethylene glycol-bis(ß-aminoethyl ether) or N,N,N′,N′-tetraacetic acid

eIF2 - Eukaryotic initiation factor 2

Endo H - Endoglycosidase H

ER - Endoplasmic reticulum

ER stress - Endoplasmic reticulum stress

ERAD - ER-associated degradation

ERdj3 - DnaJ heat shock protein family member B11 (DNAJB11)

ERN1 - ER to nucleus signalling 1

ERN2 - ER to nucleus signalling 2

ERO1 – ER oxidoreductin 1

ERp18 - Thioredoxin Domain-Containing Protein 12 (TXNDC12)

Erp29 – Endoplasmic reticulum resident protein 29

Erp57 – Protein disulfide isomerase A3 (PDIA3)

Erp72 – Protein disulfide isomerase A4 (PDIA4)

ERSE - ER stress response element

FBS - Fetal Bovine Serum

FITC - Fluorescein isothiocyanate

FW – Forward primer

FXR - Farnesoid X receptor

GADD34 - Growth arrest and DNA damage-inducible 34

GLP1 - Glucagon-like peptide-1

Gpx - Glutathione peroxidase

GRP94 - Glucose-regulated protein 94

Grp170 - Glucose-regulated protein 170

GSH - Reduced Glutathione

GSSG - Oxidized Glutathione disulfide

HCl - Hydrochloric acid

HDAC2 - Histone Deacetylase 2

HDL – High Density Lipoprotein

HEK-239 cells - Human embryonic kidney cells

HEPES – 4-(2-hydroxyethyl)-1-piperazineethanesulfonic acid

HSP70 or DnaK - Heat shock protein 70

HSP70s - Heat shock protein 70 family

HT-1080 cells - Human fibrosarcoma cells

IP – Immunoprecipitation

IRE1 - Inositol requiring enzyme

JNK - c-Jun NH2-terminal kinase

KO – Knockout

MS - Mass spectrometry

Na_2CO_3 - Sodium Carbonate

NaCl - Sodium Chloride

NaH_2PO_4 - Sodium Phosphate

NaOH - Sodium hydroxide

NEM - N-Ethylmaleimide

$(NH_4)_2SO_4$ - Ammonium Sulphate

Ox - Oxidized

P – Phosphate

P5 - Protein disulfide isomerase P5

PAS - Protein A-sepharose

PBS - Phosphate-buffered saline

PDI - Protein disulfide isomerase

PDILT or PDIA7 - Protein disulfide-isomerase-like protein of the testis

PDIR or PDIA5 - Protein disulfide isomerase-related

PDIs - Protein disulfide isomerase family

Pen-Strep – Penicillin and streptomycin

PERK - Double-stranded RNA-activated protein kinase-like ER kinase

PMSF – Phenylmethylsulfonyl fluoride

PP1 - Protein phosphatase 1

PPAR – Peroxisome proliferator-activated receptor

Prx4 - Peroxiredoxin

Red - Reduced

RER - Rough endoplasmic reticulum

RIDD - Regulated IRE1-dependent decay

ROS – Reactive oxygen species

RW – Reverse primer

S1P - Site 1 protease

S2P - Site 2 protease

SCD1 - Stearoyl-Coenzyme A desaturase 1

SDS - Sodium dodecyl sulfate

SER - Smooth endoplasmic reticulum

SFA - Saturated fatty acid

SRP - Signal recognition particle

sXbp1 - Spliced Xbp1 mRNA

TBST/TBS – Tris buffered saline

TCA - Trichloroacetic acid

TEMED – N,N,N′,N′-Tetramethylethylenediamine

TFG – Trafficking from ER to Golgi regulator

TG – Thapsigargin

Thbs4 - Thrombospondin 4

TLR4 - Toll-like receptor 4

TRAF2 - TNF receptor-associated factor 2

UPR - Unfolded protein response

uXbp1 - Unspliced Xbp1 mRNA

VCP – Valosin-containing protein or transitional endoplasmic reticulum ATPase (TER ATPase)

VKOR - Vitamin K epoxide reductase

VLDLR – Very-low-density-lipoprotein receptor

WT – Wild type

Xbp1 - X-box-binding protein 1

CHAPTER I: MAIN INTRODUCTION

1. 1. The endoplasmic reticulum (ER)

The endoplasmic reticulum (ER) is a membrane-bound organelle, which can only be found in the cytoplasm of eukaryotic cells. In the animal cells, the ER accounts for more than half of the cells content. Basic structure of the ER is a membrane network of flattened sacs and tubules, which is contiguous with the outer membrane of the nuclear envelope (English and Voeltz, 2013; Watson, 1955). In the spaces of this sac, also known as the ER lumen, contains the fluid portion and here is where a lot of proteins, specifically secretory and membrane proteins, are synthesis and modified (Fig.1.1). The function of ER is varied, depends on cell type, cell function and cell need, however the most well-known function is protein synthesis, modified, and secretion (Reid and Nicchitta, 2015; Westrate et al., 2015; Braakman and Hebert, 2013; Rapoport, 2007). However, several studies suggested that lipid synthesis is also a prominent role of the ER (Fagone and Jackowski, 2009; Baumann and Walz, 2001). According to physical and functional characteristics, the ER can be differentiated into two types: rough ER and smooth ER, however, ER structure is very dynamic and could be altered upon changes to the cellular conditions and environment (Westrate et al., 2015; English, Zurek and Voeltz, 2009; Shibata, Voeltz and Rapoport, 2006; Voeltz et al., 2002; Baumann and Walz, 2001). The ratio of rough ER (RER) and smooth ER (SER) is varied in different cell types, based on the role of the cells. For example, pancreatic cells will contain more RER rather than SER, since the cells need to produce and secrete numerous amounts of proteins like insulin. Meanwhile, cells with the role of lipid synthesis such as liver cells and adrenal cells, have more SER (Baumann and Walz, 2001).

Rough endoplasmic reticulum. This type of ER is having ribosomes attach to the membrane on the cytoplasmic side; therefore, it appears rough on the surface under electron microscopy (West et al., 2011, Shibata et al., 2010). This type of the ER is primarily found connected to the nuclear membrane. Ribosome makes the RER to have specific role in protein synthesis, protein modification and secretion of protein entering the secretory pathway (Reid and Nicchitta, 2015; Prinz et al., 2000, Rolls et al., 2002, Simon and Blobel, 1991). It has been suggested that almost one third of the proteins within the human genome are targeted for synthesis at the ER (Kaufman, 1999). During secretion, the RER

collaborates with the Golgi complex by trafficking the mature protein to the Golgi and then from the Golgi, the secretory vesicles will carry the protein to cell membrane or the outside of the cell. RER can be mostly found in secretory cells such pancreatic cells, liver cells, B lymphocytes and osteoblasts (Baumann and Walz, 2001; Dallner et al., 1963). The proteins which are synthesised in and retained in the ER, have varied functions such as regulating calcium release from the ER, integrating proteins into the cell membrane, protein synthesis, protein folding and post-translational modification (Braakman and Hebert, 2013, Meldolesi and Pozzan, 1998).

Smooth endoplasmic reticulum. It is more tubular and curved like than the RER. This type of ER is named as a smooth ER since it does not have the ribosomes attached to the ER membrane on the cytosolic site, therefore the membrane texture appears smoother than the RER membrane. Since the lack of ribosomes on the membrane surface, the general function of SER is more involved with the synthesis of lipids such as oils, phospholipids and steroids, metabolism of carbohydrates, regulation of calcium concentration, detoxification of drugs and poisons, transport of ions and also secretion of proteins and products from cells (Gao et al., 2017; Guo, Sirkis and Schekman, 2014; West et al., 2011; Fagone and Jackowski, 2009; Glick and Nakano, 2009; Black et al., 2005; Baumann and Walz, 2001; Ishizuki et al., 1983). Higher prevalence of the SER can be found in many cell types such as cells in the adrenal gland, ovaries, and testis (Voeltz et al., 2002, Fagone and Jackowski, 2009).

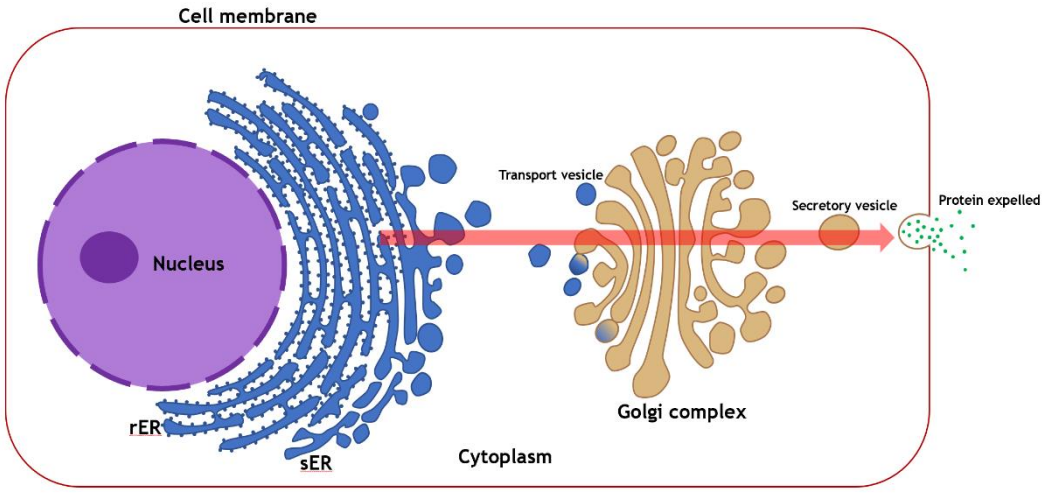

Fig. 1.1. Endoplasmic reticulum (ER) structure and proteins secretory pathway.

1. 2. Protein synthesis and folding in the ER

The major role of the ER in cells is protein synthesis and this role is the focus for our study. While only some of the intracellular proteins are synthesised at the ER, the majority of extra-cellular and membrane proteins are synthesised at the ER and go through the secretory pathway (Reid and Nicchitta, 2015; Jan, Williams and Weissman, 2014). The ER is considering as a first compartment in the secretory pathway by regulating the synthesis, modification, and delivery of proteins to its proper target sites (Vitale and Denecke, 1999; Jin et al., 2017). For protein synthesis, ribosomes are required, therefore, protein synthesis only occurs in the RER which has ribosomes attached to the cytosolic side of the membrane. However, the post-translational modification and proteins folding could occur in both SER and RER (Braakman and Hebert, 2013; Rapoport, 2007). The folding process and post-translational modification such as oligomerization, N-linked glycosylation, and disulfide formation, take place in the ER lumen with the help of chaperones and folding enzymes and are very important processes for most proteins to be functional (Braakman and Hebert, 2013). The initiation of protein synthesis of the secretory and membrane proteins at the ER starts with the translation of a nascent polypeptide with a signal sequence which is recognised and bonded with the signal recognition particle (SRP) (Gilmore, Blobel and Walter, 1982; Walter, Ibrahimi and Blobel, 1981). Then the complex attaches to the ER membrane via the SRP receptor (Alder et al., 2005). The growing polypeptide chain is translocated co-translationally through the ER translocon, a channel which contains several Sec proteins on the ER membrane, and the growing polypeptide chain will move across the ER membrane into the ER lumen (Braakman and Bulleid, 2011; Dejgaard et al., 2010; Rapoport, 2007; Sitia and Braakman, 2003, Helenius et al., 1992; Deshaies et al., 1991). While translation is running or when it completed, the exposed polypeptide chain will interact with folding factors and/or modification enzymes (Braakman and Bulleid, 2011; Rutkevich et al., 2010; Sitia and Braakman, 2003). If the translated protein is a membrane protein, it will be integrated to the ER membrane and translocated to a target location with the ER membrane (Braakman and Hebert, 2013; Blobel, 1980). Meanwhile, the secreted proteins or the other non-membrane proteins will be cleaved to release the signal peptide before being transported to a target place via Golgi complex (Potter and Nicchitta, 2002; Seiser and Nicchitta, 2000).

In the ER lumen, the synthesised proteins undergo post-translational modifications and fold into their native form with the help of ER chaperones and enzymes such as the protein disulfide isomerase (PDI) family and N-linked glycosylated enzymes (Ariyasu et al., 2017; Poet et al., 2017; Rutkevich et al., 2010, Ron and Walter, 2007). Only properly folded proteins can be exported to their final destination, with misfolded proteins being retained in the ER for refolding or for targeting to the ER-associated degradation (ERAD) pathway (Ariyasu et al., 2017; Ruggiano, Foresti and Carvalho, 2014; Hebert and Molinari, 2007; Ellgaard and Helenius, 2003). Despite the fact that there are numerous factors that could help the synthesised proteins to be folded to their native form, the disruption of these processes by internal and external stimuli still happens and cause the accumulation of unfolded or misfolded proteins in the ER lumen resulting in ER stress and/or cell death (Ruggiano et al., 2014; Hebert and Molinari, 2007; Credle et al., 2005). To overcome this situation, cells have developed specific processes collectively called the unfolded protein response (UPR) or ER stress response, with two main adaptive mechanisms; increasing of protein folding capacity in the ER and decreasing protein load. The folding capacity is upregulated by expanding organelle size and inducing newly synthesised protein-folding machinery such as ER chaperone and folding enzymes (Ariyasu et al., 2017; Schuck et al., 2009; Ron and Walter, 2007; Yoshida, 2007). Meanwhile, protein loading into the ER is restrained by downregulating on a transcriptional and translational level of protein synthesis, and the permanently misfolded proteins will be targeted for ERAD pathway to clear unfolded proteins from the ER (Smith, Ploegh and Weissman, 2011; Ellgaard and Helenius, 2003; Martínez and Chrispeels, 2003; Pakula et al., 2003; Friedlander et al., 2000; Travers et al., 2000; Harding, Zhang and Ron, 1999). Moreover, long term ER stress can lead to apoptosis and cell death to protect the whole organism (Tabas and Ron, 2011; Hacker, 2000). Therefore, several studies suggest that the upregulation or the absence of the UPR is related to several human diseases, for example, cancer, diabetes, inflammation, achromatopsia, and neurodegenerative disorders (Chianga et al., 2017; Honjo et al., 2017; Chen et al., 2015; Ruggiano et al., 2014; Ozcan, and Tabas, 2012; Yoshida, 2007). The UPR senses and manipulates the ER conditions via three types of stress sensors, inositol requiring enzyme α (IRE1α), double-stranded RNA-activated protein kinase-like ER kinase (PERK) and activating transcription factor 6 (ATF6), which regulate three individual branches of downstream signalling

pathways (Fig. 1.2). In mammalian cells, these three signal transducers are ER transmembrane proteins which can sense and transmit stress signals across the ER membrane in parallel (Ron and Walter, 2007; Schröder, and Kaufman, 2005).

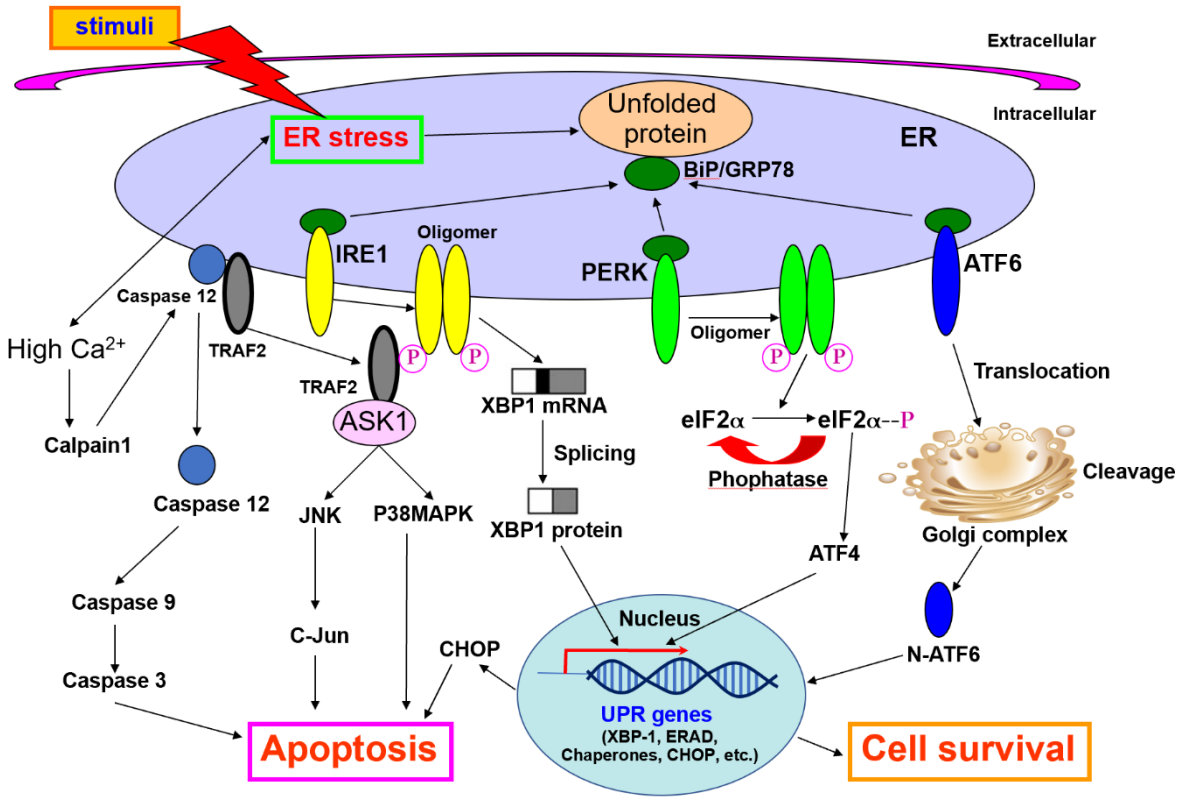

Fig. 1.2. The three branches of the unfolded protein response (UPR); ATF6, PERK, and IRE1.

1. 3. Endoplasmic reticulum stress (ER stress) and unfolded protein response (UPR)

The endoplasmic reticulum (ER) is the site of synthesis, folding and modification of proteins in the cell and is the major source of intracellular calcium (Ca^{2+}). In different physiological, pathological, chemical, or biological stimulation, such as hypoxia, abnormal Ca^{2+} homeostasis, viral infections, high-fat diet, oxidative injury, hypoglycemia, protein synthesis and folding in the ER lumen are disturbed, leading to the accumulation of unfolded protein in the ER lumen. The proteotoxicity of the unfolded protein which accumulated in the ER lumen, leads to stress of the ER (Jin et al., 2017; Hotamisligil, 2010; Yoshida, 2007; Alder et al., 2005; Schroder and Kaufman, 2005). In the response to ER stress, cell activates a signalling transduction pathway that attempts to cope with the altered

conditions and restore a favourable folding environment, called the unfolded protein response (UPR) (Ariyasu et al., 2017; Schuck et al., 2009; Ron and Walter, 2007). The target of the UPR is to upregulate the refolding process in the ER, downregulate the protein translation, and upregulated the ERAD pathway to clear the misfolded protein from the ER lumen and restore cell homeostasis. However, the effect of the UPR and the prolonging of ER stress will activate an apoptosis pathway and lead to cell death (Dandekar et al., 2015; Tabas and Ron, 2011; Hacker, 2000).

The UPR has three specific-signalling pathways initiate by three ER transmembrane proteins: inositol requiring enzyme α (IRE1α), double-stranded RNA-activated protein kinase-like ER kinase (PERK) and activating transcription factor 6 (ATF6) (Jin et al., 2017; Karagoz et al., 2017; Walter and Ron, 2011; Adachi et al., 2008; Lai, Teodoro and Volchuk, 2007; Ron and Walter, 2007; Schröder and Kaufman, 2005). These three branches of the UPR regulate three individual downstream signalling pathways which work distinctively free from each other. However, it is still not fully understood how each branch selectively response to ER stress. The main regulator of these three mediators is BiP, the ER chaperone of the heat shock protein HSP70 family, which also known as Grp78 (glucose-regulated protein 78) (Walter and Ron, 2011; Ron and Walter, 2007; Schröder and Kaufman, 2005). BiP has an important role as a masking of the UPR transducer proteins to inactivate it and has a key role in restoring the misfolded and/or unfolded proteins into the right form in the ER lumen. Without stress, BiP binds with the luminal domain of the ER stress sensors: IRE1, PERK and ATF6, and inactivates the downstream signalling. When ER stress occurs and the unfolded protein accumulates in the ER lumen, BiP dissociates from ER transducers to bind with the unfolded proteins and restore it (Schröder, and Kaufman, 2005; Dorner and Kaufman, 1994; Flynn et al., 1991). Meanwhile, the ER-stress sensors which are free from BiP, will activate the downstream signalling pathways of the UPR by upregulating the UPR genes such as ER chaperones (Lai, Teodoro and Volchuk, 2007; Yoshida, 2007; Adachi et al., 2008; Walter and Ron, 2011; Woehlbier and Hetz, 2011).

1.3.1. IRE1 pathway

IRE1 is a type 1 ER transmembrane protein (serine/threonine kinase), consists with an N-terminal as an ER stress sensor luminal domain, and a C-terminal as a cytosolic effector region which contains serine/threonine kinase domain and endoribonuclease (RNase) domain, the domains respond to the upregulation of ER-stress response genes. In humans, there are two types of IRE1: IRE1α and IRE1ß, which encoded from the ER to nucleus signalling 1 and 2 (ERN1 and ERN2), respectively (Fu et al., 2021; Sheng et al., 2019; Almanza et al., 2019; Lin et al., 2007; Iwawaki et al., 2001; Tirasophon, Welihinda and Kaufman, 1998). Reports suggested that the knockout of ERN1 or ERN2 genes in mice can lead to embryonic lethal and severe diseases (Iwawaki et al., 2009; Bertolotti et al., 2001). However, the expression of the IRE1α is immensely, meanwhile, the expression of IRE1ß is restricted (Fu et al., 2021; Martino et al., 2013; Bertolotti et al., 2001). IRE1 is the most conservative pathway of the UPR signalling pathways in the eukaryotic cells. In the resting stage, the luminal domain of IRE1 binds with BiP, which will dissociate upon the occurrences of ER stress. Activation of IRE1 in mammalian cells is typical of receptor kinase proteins, which is IRE1 oligomerization, followed by trans-autophosphorylation (Prischi et al., 2014; Oikawa, Kimata and Kohno, 2007). The activation of kinase domain on the C-terminal catalyses the X-box-binding protein 1 (Xbp1) mRNA splicing by removing a 26 nucleotides sequence from uXbp1 (unspliced Xbp1) and produced mature sXbp1 (spliced Xbp1) mRNA (Calfon et al. 2002; Yoshida et al. 2001; Tirasophon et al. 1998). Therefore, the sXbp1 mRNA will encode an active leucine zipper (bZIP) transcription factor sXbp1 which translocates to the nucleus and upregulates transcription of genes that are involved in increasing the ER protein-folding capacity and relieving ER stress such as chaperones, ER expansion elements, ER/Golgi transport components, ER-associated degradation (ERAD) proteins, redox homeostasis regulated proteins and also oxidative stress response proteins (Bhardwaj et al., 2020; Hetz, 2012; Marciniak and Ron, 2006; Lee, Iwakoshi and Glimcher, 2003; Travers et al., 2000). Moreover, the RNase domain of IRE1 also has an important role in downregulating the translation processes to reduce protein loading into the ER by cleavage of ER-targeted mRNAs, including its own mRNA, and/or cleavage of the 28s ribosomal subunit (Hollien and Weissman, 2006; Schröder, and Kaufman, 2005; Iwawaki et al., 2001; Tirasophon et al., 2000). This

mechanism of IRE1 is also known as the regulated IRE1-dependent decay (RIDD). Additionally, the interaction of TNF receptor-associated factor 2 (TRAF2), an E3 ubiquitin ligase, with IRE1 is capable to transmit a MAP kinase activation cascade which leads to the activation of apoptosis signal regulating kinase 1 (ASK1), a MAP3K of the JNK/p38 MAPK pathway (Homma et al., 2009; Matsuzawa and Ichijo, 2008; Urano et al., 2000). Recent studies also suggested that the IRE1 pathway is likely to play an essential role in tumors and cancers cells proliferation, invasion and migration (Sheng et al., 2019; Liu et al., 2017; Rajapaksa et al., 2015).

1.3.2. PERK pathway

PERK is also a type I ER-transmembrane protein, which consists of a luminal sensing domain and a cytosolic serine/threonine kinase domain. In the resting condition, PERK binds to the ER chaperone protein BiP and is retained within the ER membrane. The dissociation of BiP upon ER stress leads to auto-phosphorylation and dimerization of PERK, similar to the activation of IRE1 (McQuiston and Diehl, 2017; Bertolotti et al. 2000; Liu, Schroder and Kaufman, 2000). The active PERK is targeting a eukaryotic initiation factor 2α (eIF2α) by phosphorylation on serine-51, resulting in inhibition of protein synthesis in general and a decrease of protein load in the ER lumen (Woehlbier and Hetz, 2011; Ron and Walter, 2007; Ron, 2002; Harding et al., 2000; Prostko, Brostrom and Brostrom, 1993). In parallel, the translation of an activating transcription factor 4 (ATF4) is significantly increased. ATF4 directly upregulates the expression of genes involved in antioxidant stress responses, amino acid synthesis and transport functions to maintain ER homeostasis, and also upregulates apoptosis genes such as a transcription factor C/EBP-homologous protein (CHOP) (Hiramatsu et al., 2014; Han et al., 2013; Kanemoto and Wang, 2012; Harding et al., 2003; Ron, 2002; Novoa et al., 2001). In addition, the role of PERK can switch to promoting apoptosis and cell death during prolonged stress by upregulating the expression of apoptotic proteins such as CHOP and the growth arrest and DNA damage-inducible 34 (GADD34), and also repressing the expression of cyclin D and p53 at the same time (Lee et l., 2017; Rajesh et al., 2015; Walter and Ron, 2011; Zhang et al., 2006; Boyce et al., 2005; Schröder, and Kaufman, 2005; Ron, 2002; Brewer and Diehl, 2000). Moreover, several studies also suggested that the PERK pathway is

required for normal physiological control of ER protein synthesis, as well as for normal development of several tissues (Deng et al., 2004; Jiang et al. 2003).

1.3.3. ATF6 pathway

ATF6 is a type II ER-transmembrane protein which has two isoforms in mammals: ATF6α and ATF6β, which consist of 670 and 703 amino acids respectively. ATF6α is playing the main role in the UPR upon ER stress, meanwhile, ATF6β is considered as a very poor UPR mediator (Correll et al., 2019; Hillary and FitzGerald, 2018). ATF6 is identified as a member of the basic leucine zipper (bZIP) family (Haze et al., 1999 and 2001) since it consists the bZIP sequence on the cytosolic domain (N-terminal), which works as a transcription factor to upregulate the ER stress response element (ERSE) such as BiP, XBP1, glucose-regulated protein 94 (GRP94), and protein disulfide isomerase (Okada et al., 2002; Haze et al., 1999; Yoshida et al., 1998). Meanwhile, the luminal domain (C-terminal) of ATF6 contains molecular disulfide bonds which senses the change of ER environment and responses to the ER stress. Similar to other ER stress sensors, IRE1 and PERK, a signal transduction of ATF6 is mainly regulated by BiP which binds to the luminal domain of ATF6. Upon ER stress response, BiP dissociates from ATF6 to bind with unfolded protein, a higher affinity substrate, which overly accumulates in the ER lumen. Nevertheless, it is different from IRE1 and PERK, BiP regulates the activation of the Golgi localization sequences in ATF6, rather than the oligomerisation domains. Therefore, the dissociation of BiP from ATF6 luminal domain does not cause oligomerization and phosphorylation of ATF6, but leads to a translocation of ATF6 from ER membrane to Golgi compartment for proteolytic process (Adachi et al., 2008; Shen and Prywes, 2004; Shen et al., 2002). After the dissociation of BiP, ATF6 will be packaged into a coat protein complex II (COPII) vesicle and then migrates to the Golgi complex (Schindler and Schekman, 2009; Nadanaka et al., 2004). There, ATF6 is cleaved by the Golgi serine proteases: site 1 protease (S1P) and site 2 protease (S2P), Therefore, the product of cleavage process, a 50 kDa cytosolic bZIP fragment of ATF6, translocates into the nucleus where it forms the active homodimers or dimerizes with other bZIP transcription factors, such as NF-Y (CAAT binding factor) and Xbp1s, to upregulate the transcription processes of ER stress response genes such

as ER chaperone and folding enzymes, including BiP, glucose-regulated protein 94 (Grp94), protein disulfide isomerase (PDI) and Xbp1 (Woehlbier and Hetz, 2011; Adachi et al., 2008; Schröder, 2008; Ron and Walter, 2007; Yoshida, 2007; Nadanaka, 2006; Schröder and Kaufman, 2005; Shen and Prywes, 2004; Wang et al., 2000; Ye et al., 2000; Haze et al., 1999; Yoshida et al., 1998). Moreover, ATF6 also conducts apoptosis in term of chronic stress response by upregulating the translation of genes involved in cell death such as CHOP and the endoplasmic reticulum protein 29 (ERp29) (Hirsch et al., 2014; Tabas and Ron, 2011; Yoshida et al., 2000).

Regarding the broad studies of ATF6, the understanding of the trafficking process of ATF6 from the ER to the Golgi upon ER stress response remains unclear and still not being fully investigated. Recent studies suggested that the dissociation of BiP from ATF6 is not enough for ATF6 to translocate from the ER to the Golgi apparatus and undergo proteolysis (Nadanaka et al., 2004; Antonny and Schekman, 2001). There are a number of additional elements such as ATP, COPII cargo protein, protein disulfide isomerases (PDI), thrombospondin (Thbs), and also a conformational change of the ATF6 itself, are required for this process. For example, ATP has been identified as an importance cofactor for BiP in protein refolding process, therefore lack of ATP could inhibit the dissociation of BiP from ATF6 under stress conditions (Vishnu et al., 2014; Mirazimi and Svensson, 2000; Dorner and Kaufman, 1994; Braakman, Helenius, and Helenius 1992). Moreover, researcher suggested that the reduced monomer form of ATF6, which is formed only after the departure of BiP, is likely to be the most preferable form of ATF6 for packaging into COPII vesicles and also the most preferable substrate form of the S1P. This redox change might help to prevent an unnecessary activation of the UPR pathway when ATF6 migrates by mistake to the Golgi complex in the absence of ER stress (Schindler and Schekman, 2009; Nadanaka et al., 2007). In addition, several studies suggested that the reduction of ATF6 is likely to be assisted by proteins in PDI family such as the protein disulfide isomerase A5 (PDIA5 or PDIR) (Higa et al., 2014; Nadanaka et al., 2004). PDIs seem to be involved in both inter- and intra-molecular disulfide bonds rearrangement of ATF6 during the UPR. Besides, the transport vesicles which carry ATF6 from the ER to the Golgi, are also required specific proteins such as Thbs4 to be added. Therefore, the COPII vesicles could be formed properly and complete the migration process of ATF6 upon stress

response (Brodya et al., 2016; Lynch et al., 2012). However, the translocation of ATF6 to the Golgi also does not guarantee that the future downstream of the UPR will be triggered, since the cleaved process of ATF6 in the Golgi is regulating by several factors as well, for instance the disulfide formation of ATF6 and the S1P recognition region. Consequently, the abnormal changing of those factors will affect the binding of S1P and the cleaved process to produce the free form of cytosolic bZIP domain of ATF6 (Sun et al., 2015; Ye et al., 2000). Therefore, despite the amount of information obtained until now, the mechanisms underlying ATF6 transport in the UPR still remain elusive and require more study to understand it better.

1.3.4. BiP, the trigger of the UPR

BiP or immunoglobulin-binding protein, which is also known as 78 kDa glucose-regulated protein (GRP78), is a member of the heat shock protein 70 (HSP70) family and consists of 654 amino acids. BiP is also one of the most well-known ER chaperones, which has an important role in regulating the accumulation of the unfolded proteins in the ER lumen and being the key factor in the UPR during ER stress to maintain ER homeostasis (Sweeney et al., 2017; Ron and Walter, 2007). In the non-stressed condition, most of BiP binds to the luminal domain of the UPR mediator proteins such as ATF6, PERK and IRE1 to inactivate the proteins and maintain them in the ER membrane, then, when ER stress occurred, BiP is induced to release from the UPR mediators by the accumulation of the unfolded proteins in the ER lumen (Cuevas et al., 2017; Sweeney et al., 2017; Chen and Brandizzi, 2013; Ron and Walter, 2007; Schröder and Kaufman, 2005). According to the structure of BiP, which comprises two distinct functional domains, an ATP-binding domain and a peptide-binding domain, therefore, BiP is also known as an ATP-dependent chaperone (Karlin and Brocchieri, 1998; Munro et al., 1986). For protein folding and quality control, BiP has to bind with ATP in advance, so it could be released from the UPR mediators, before binding to exposed hydrophobic side chains of the unfolded protein clients. In addition, depletion of ATP could inhibit protein folding activity of BiP and prolong the association of the UPR proteins with BiP (Morris et al., 1997). Studies suggested that for recruiting the unfolded proteins, BiP requires co-chaperone, mainly the

members of DnaJ family (HSP40) such as DNAJB9/ERdj4 and DNAJC10/ERdj5, to assist the process (Terrab and Wipf, 2020; Pobre, Poet, and Hendershot, 2019; Chen et al.,2017; Braakman and Hebert, 2013; Oka et al., 2013; Otero, Lizák, and Hendershot, 2010). However, the mechanism of BiP dissociation from the UPR sensors during ER stress, is still not fully understand and the accessing of ATP is insufficiently to induce the departure of BiP. In the past, the dissociation of BiP from the UPR reporters was identified as a simple competitive process between two types of BiP client proteins; the UPR reporters and the unfolded proteins that accumulate in the ER lumen upon stress, since the unfolded proteins are appeared to be a strong competitor substrate of BiP than the UPR reporter proteins (Shen et al., 2002; Bertolotti et al., 2000; Bukau and Horwich, 1998). Nonetheless, recent studies proved that BiP binds with the UPR mediators tightly and the complex is very stable. The accumulation of a strong competitor like the unfolded proteins, upon ER stress or the presence of ATP alone, cannot simply lead the dissociation of BiP from the complex, in conclusion, the departure of BiP requires more additional factors than it was expected before (Schindler and Schekman, 2009; Shen et al., 2005). The promising factors for regulating the detached BiP is ER oxidoreductases such as P5, PDIR and ERp18, which are members of the protein disulfide isomerase family (PDIs) (Fass, 2019; Oka et al., 2019; Zeng et al., 2019; Zhang et al., 2019; Honjo et al., 2017; Mathew, 2015). The ER oxidoreductase was suggested to create the thiol modification in the structure of BiP and the redox changing might affect the stability of the BiP binding the UPR mediators, therefore, BiP can detach from the binding complex easier (Wang and Sevier, 2016; Higa et al., 2014; Wei et al., 2012). In addition, the dissociation of BiP will unmask the luminal domain sequence of the UPR reporters, leading to the downstream of the UPR pathways to be activated. Once detached from BiP, the free form of IRE1 and PERK will respond to the stress signal by structuring the oligomers, then followed by autophosphorylation to activate their downstream targets (Adams et al., 2019; Kopp etal., 2019; Hetz and Papa, 2018; Pincus et al., 2010; Wu and Kaufman, 2006). However, the response of ATF6 after the dissociation of BiP is different from the other two UPR mediators. The dissociation will lead to the packaging of ATF6 into COP II vesicle and transport from the ER to the Golgi apparatus, in which ATF6 will get cleavaged to the active form that can upregulate the downstream pathway of the UPR (Xu et al., 2021; Oka et al., 2019; Hetz and Papa, 2018; Higa et al., 2014; Lynch et al., 2012; Wu and Kaufman, 2006;

Shen et al., 2002). Indeed, the overexpression of BiP could either inhibit the downstream pathways of the UPR in the presence of ER stress or increase the capacity of the ER to cope with the accumulation of unfolded proteins (Shen et al., 2002).

1. 4. ER stress and apoptosis

All three UPR pathways can switch from a survival pathway to apoptosis pathway when the initial cellular responses fail to restore ER homeostasis and the stress continues for a long time (Read and Schröder, 2021; Lai, Teodoro and Volchuk, 2007; Szegezdi et al., 2006; Schröder and Kaufman, 2005). Several studies have demonstrated that the pathway of ER stress-induced apoptosis is involved with many diseases, such as diabetes, nervous system disorders and cancer (Chalmers et al., 2017; Kanemoto and Wang, 2012; Matus, Glimcher and Hetz, 2011; Scheper and Hoozemans, 2009; Lindholm, Wootz and Korhonen, 2006). The C/EBP homologous protein transcription factor (CHOP), c-Jun NH2-terminal kinase (JNK) and caspase are the main pathway that is implicated in ER stress-mediated apoptosis. However, the molecular mechanisms of this response are still not fully investigated and need more future study to clarify (Fig. 1.3).

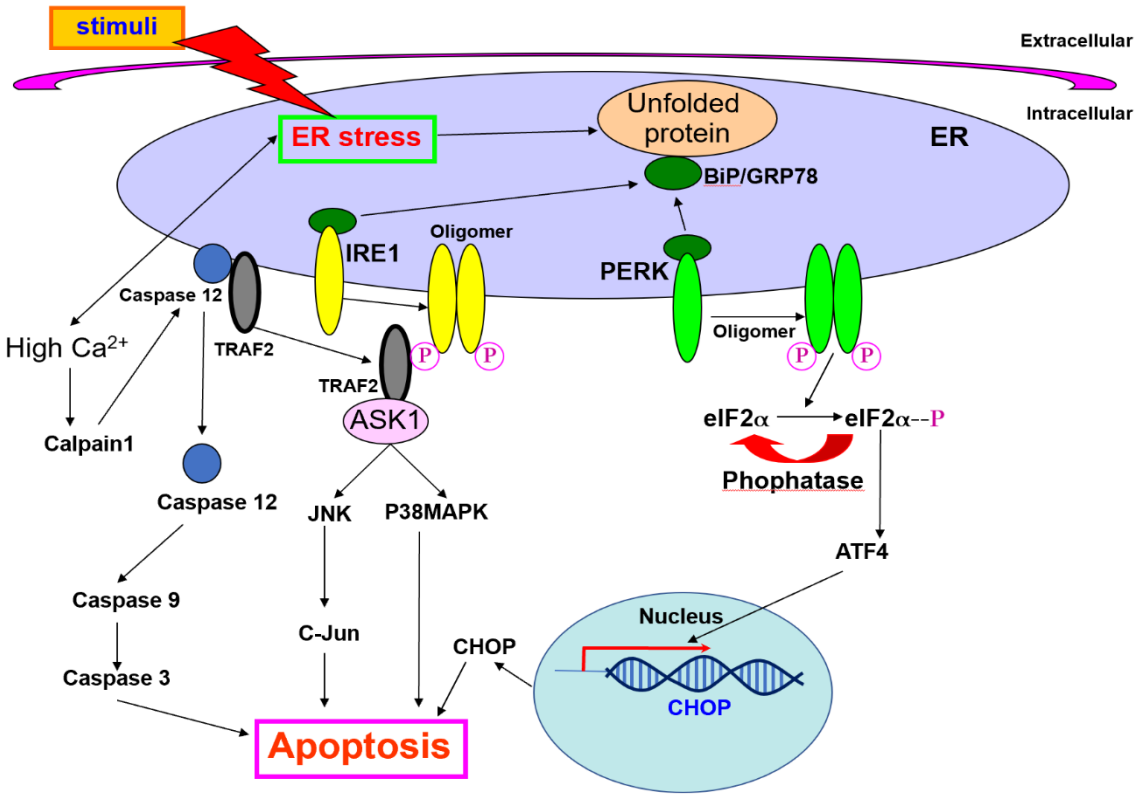

Fig. 1.3. ER stress-induced apoptosis. The unsuccessfully renewing ER homeostasis during stress response could lead to chronic ER stress and cell death by inducing the expression of multiple proapoptotic proteins such as Bax, Bak and caspase 12, as well as inhibiting the expression of antiapoptotic protein Bcl-2.

1.4.1. CHOP/GADD153

CHOP or GADD153 is bZIP-containing transcription factor and counted as one of the members in the CCAAT/enhancer binding protein (C/EBP) family. Although CHOP is known as growth-arrest and DNA-damage-inducible gene 153 (Wang et al., 1996), the protein is lower expressed under normal physiological conditions, like growth arrest or DNA damage, and only highly expressed under the inducing of ER-stress conditions (Okada T. at al. 2002; Harding H.P. et al. 2000). In the chronic ER stress, CHOP can be upregulated by all three UPR signalling pathways (Hu etal., 2019; Oyadomari and Mori, 2004; Harding et al., 2003). However, the PERK pathway is likely to play a key role in the induction of CHOP expression. The overexpression of CHOP could induce apoptosis for ER-stress response by upregulating a variety of genes (Malhi and Kaufman, 2011; Tabas and

Ron, 2011; Walter and Ron, 2011), such as GADD34 and ERO1α, but CHOP could not induce apoptosis directly. Furthermore, GADD34 is a regulatory subunit of protein phosphatase 1 (PP1) that leads PP1 to dephosphorylate eIF2α on serine 51, which recovers protein translation. If the condition of ER has not been recovered to the normal state, inhibition of protein synthesis will increase protein load in the ER and promote ER stress (Marciniak et al., 2004). Moreover, CHOP-mediated ERO1α expression causes hyperoxidizing conditions in ER which will increase misfolded proteins in ER (Schröder, 2008; Harding et al., 2003). In addition, CHOP can regulate the expression of some proteins in Bcl-2 family, such as downregulating the expression of anti-apoptotic protein Bcl-2 and upregulating the expression of proapoptotic BH3-only protein Bim, and also induce cellular reactive oxygen species (Malhi and Kaufman, 2011; Harding et al., 2003; McCullough et al., 2001).

1.4.2. JNK and p38 MAPK

c-Jun N-terminal kinase (JNK) and p38 MAP kinase are similar to the members of the stress-responsive MAP kinase family (Matsuzawa and Ichijo, 2008; Schröder and Kaufman, 2005). The two proteins will be upregulated by apoptosis signal-regulating kinase 1 (ASK1). Under ER stress conditions, IRE1α will interact with TNF receptor-associated factor 2 (TRAF2) and ASK1, causing activation of downstream JNK and p38 MAPK pathways leading to apoptosis (Homma et al., 2009; Nishitoh et al. 2002; Urano et al., 2000). The recent studies are still not completely clear about the downstream mechanism of JNK and p38 MAPK but it is thought that this might be involved with the regulation of proteins in Bcl-2 family. However, it has been already reported that JNK and p38 MAPK pathways also function as regulator of autophagy pathway and inflammatory response under ER stress (Read and Schröder, 2021; Malhi and Kaufman, 2011; Bueter, Dammann and Leviton, 2009; Rzymski et al., 2009; Gargalovic et al., 2006; Hu et al., 2006).

1.4.3. Caspase

Several studies have demonstrated that caspase 12 and caspase 7 play an important role in ER stress-induced apoptosis and are activated specifically only under ER-stress conditions, but not by other apoptotic signals (Read and Schröder, 2021; Gotoh, Endo and Oike, 2011; Malhi and Kaufman, 2011; Schröder and Kaufman, 2005; Szegezdi, Fitzgerald and Samali, 2003; Nakagawa et al., 2000). Pro-caspase 12 is located on the cytoplasmic side of the ER membrane and interacts with TRAF2, on the other hand, caspase 7 is localized on the cytosol side of ER membrane. In response to ER stress, the interaction between TRAF2 and caspase 12 is inhibited by overexpression of IRE1α (Yoneda et al. 2001), and then caspase 7 is translocated from the cytosol to the cytoplasmic side of ER membrane to interact with pro-caspase 12 and cleave it, causing its activation (Rao et al. 2001). Moreover, caspase 12 can be activated by calpains, a family of Ca2+-dependent cysteine protease. Compared with mice, human caspase 12 is lack of function, but however, Hitomi and colleagues have suggested that caspase 4 in human, which is a homologous to mouse caspase 12, also performs the function of caspase 12 (Hitomi et al., 2004). Recent studies have demonstrated that caspase 12 can activate caspase 9 (Lai, Teodoro and Volchuk, 2007; Morishima et al. 2002), but function and downstream pathway of caspase 12 are still remained unclear.

1. 5. Protein disulfide isomerase (PDI) family

The protein disulfide isomerase family (PDIs) is a group of thiol-disulfide oxidoreductase enzymes that comprises more than 20 members which are mainly located in the ER, however few members are intervene within the ER membrane, moreover the proteins in this group could be either catalytically active or inactive (Okumura, Kadokura and Inaba, 2015; Tannous et al., 2015). It was suggested for decades that the PDIs have an importance role in the oxidative protein folding and in the stabilization of proteins structure in the ER lumen, since a lot of intracellular proteins and almost one-third of the secreted human proteins consisted of disulfide bond either in the intra- or inter-molecule. However, the studies of the PDIs over the decades shown that the PDIs is not only playing critical role in protein translation in the ER, but also involving with the other processes

according to the role of the ER, for examples, protein trafficking, ERAD, calcium homeostasis and proteins homeostasis, which all required the disulfide conformation change of the proteins (Matsusaki et al., 2020; Okada et al., 2019; Arai et al., 2017). Therefore, the PDIs is obviously one of the main characters in the UPR during ER stress as well, since the disulfide formation change of the signaling proteins like ATF6 are also necessary in this process.

It is commonly understood that the disulfide formation in the native structure of several proteins is important for its performance and transportation. However, the non-native disulfide formation is also commonly found in the protein translation process as a transition form of the native product of the normal protein folding as well. In addition, such non-native disulfides are also notable in the misfolded protein formation during ER stress (Bulleid and Ellgaard, 2011; Hatahet and Ruddock, 2009; Jansens et al., 2002). This non-native disulfide bond can prevent the correct folding of protein and must be reduced to form the native structure, or the protein will be targeted to degrade. Therefore, oxidoreductase enzymes like PDIs, which can oxidise, reduce, or isomerise their substrate proteins by accepting or donating electrons, are required for the post-translation modification and protein refolding (Kosuri et al., 2012; Feige and Hendershot, 2011; Hatahet and Ruddock, 2009; Jansens et al., 2002). For PDIs, the oxidised form of the enzyme will catalyse the disulfide formation in the substrate protein by transferring the disulfide bond from its active site to substrate. Meanwhile, the reduced form of PDIs will work in the rearrangement of the non-native disulfide formation, the process also known as isomerization (Fig. 1.4). However, the process of disulfide formation is relatively more well-studied than the process of isomerisation (Bulleid and Ellgaard, 2011; Appenzeller-Herzog and Ellgaard, 2008).

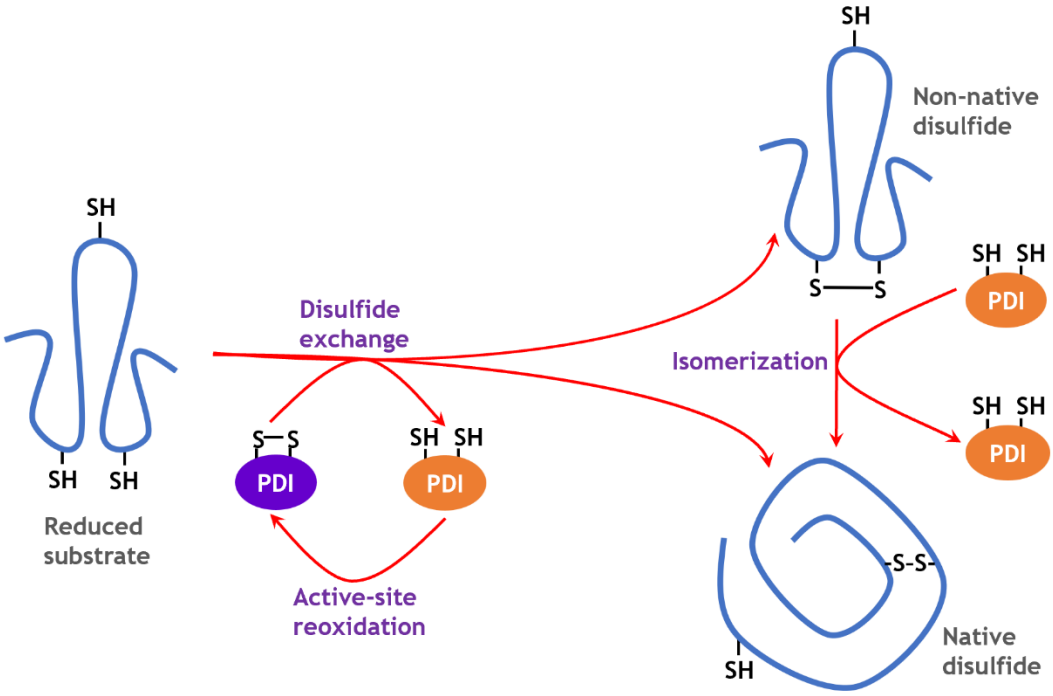

Fig. 1.4. The processes of protein disulfide isomerase family (PDIs) members exchange disulfides with its substrate proteins (Bulleid and Ellgaard, 2011). In these processes, PDIs members could be either reduced or oxidised form, depending on the substrates.

The published structure of PDIs shown that all comprise at least one thioredoxin-like domain, which is the main character for its grouping (Kozlov et al., 2010; Maattanen et al., 2006; Sevier and Kaiser, 2006). Even though, the name of the family indicates a protein disulfide isomerisation function, this property is not applied to all of the members in this group, for instance, a protein disulfide-isomerase-like protein of the testis (PDILT or PDIA7) which has only one cysteine in the active site shows no oxidoreductase activity (van Lith et al., 2007). The thioredoxin-like domain which was mentioned before and used to categorize members of the PDIs, appears to be either catalytic or non-catalytic. The domain classified as a- and b-type domains afterwards (Appenzeller-Herzog and Ellgaard, 2008). The a-type domains usually have a CXXC active-site motive which consists of two cysteines and another two random amino acids found in the middle of the sequence. However, some of the a-type domains might contain only one cysteine or none of it since the classification is based on the sequence similarity rather than the redox function of the domain. Meanwhile all the members in the b-type

domain group have none of cysteines on the active site. In addition, there appeared to be another two domains which could be found in the PDIs structure; the J- and D-domain, however these are very rare domains and until now only two PDIs members are found to carry these domains, ERdj5 with the J-domain and ERp29 with the D-domain (Lippert et al., 2007; Hosoda et al., 2003).

The catalytic function or the redox activity of the PDIs members is found to be related with the CXXC sequence on the active site of a-type domain. Therefore, only members consisting of at least one a-domain with this specific sequence, could show catalytic property. Studies shown that the catalytic members of PDIs can generate the native disulfides or isomerise the non-native disulfides by dithiol-disulfide exchange with substrate proteins within the ER (Hatahet and Ruddock., 2007; Jensens, Duijn, and Braakman., 2002; Walker and Gilbert., 1997). Generally, the disulfide bond formation and isomerisation processes require different forms of PDIs, either the oxidised or reduced form, depending on the inter- or intra-molecular disulfide arrangement. Therefore, redox changing of the PDIs need to be produced in advance before performing its catalytic activity. Even though the mammalian PDIs are still poorly investigated, several studies suggested that the appearance of the human PDIs in vivo can be both reduced and oxidised state, despite the condition in the ER is generally more oxidizing. In addition, studies suggested that several enzymes such as Ero1, peroxiredoxin (Prx4), glutathione peroxidase (Gpx 7 and 8), and vitamin K epoxide reductase (VKOR) are also involved with the regulation of redox changing status of the disulfide exchange proteins like PDIs (Nguyen et al., 2011; Tavender et al., 2010; Schulman et al., 2010). Some PDIs also require functional partners for client recognition since they cannot recruit substrates by themselves. For instance, ERP57 needs signaling proteins like the lectin chaperones calnexin (CNX) and calreticulin (CRT) to bind with the client proteins prior, therefore ERp57 can recognize and bind with the protein complex. Meanwhile, the other PDIs such as PDI, can directly recruit its substrates without the assist of other proteins (Kanemura et al., 2020; Gestaut et al., 2019). Even though, the regulatory pathway of redox changing of the PDIs is still not fully investigated, in human, nowadays the most acknowledgement pathway of redox regulation of the PDIs is reportedly to be the process of electron flow to and from PDIs, which is regulated

by the Ero1 and glutathione (Fig. 1.5) (Jha et al., 2021; Port et al., 2017; Deponte, 2013; Appenzeller-Herzog and Ellgaard, 2008; Thorpe and Coppock, 2007).

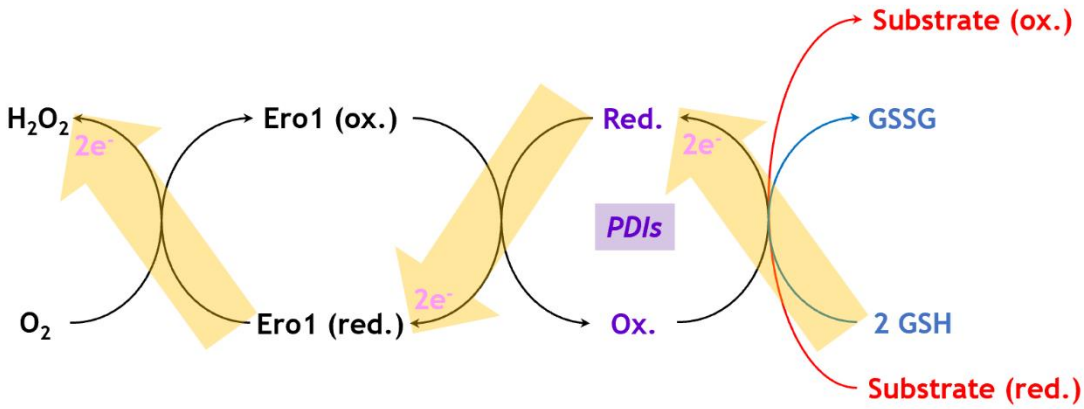

Fig. 1.5. Overview of redox changing and electron flow pathways to and from PDIs. The processes are regulated by Ero1 and glutathione for oxidation and reduction respectively. Red = reduced, Ox = oxidized, GSH = reduced Glutathione, GSSG = oxidized Glutathione disulfide (Appenzeller-Herzog and Ellgaard, 2008).

1. 6. ERdj3 or DnaJ heat shock protein family member B11 (DNAJB11)

ERdj3 or DnaJ heat shock protein family member B11 (DNAJB11) is an ER chaperone in DnaJ family, also known as HSP40 family, with a conservation of ~70 amino acid J domain, which contains specific His-Pro-Asp (HPD) motif. Research proposed that the conserved J-motif among DnaJ family members plays an important role in the interaction with chaperones in the 70-kDa heat shock protein (HSP70 or DnaK) family, including BiP. Therefore, mutation in this specific-motif sequence can interrupt the function of DnaJ as the HSP70 co-chaperone. In addition, studies suggested that the members of the DnaJ family, including ERdj3, are highly involved with folding, trafficking, disaggregation, and degradation of proteins in the ER lumen as well as an extracellular proteostasis (Adams et al., 2021; Chen et al., 2017; Nillegoda and Bukau, 2015; Kim et al., 2013). The DnaJ proteins are mainly working as HSP70s co-factors which can stimulate the interaction of HSP70s and the unfolded client proteins. Some of the members in this family also can directly bind with the unfolded proteins and lead it to ERAD. However, it was reported that most of DnaJ proteins will depart from the HSP70-

unfolded protein complex before the refolding process is completed. According to this information, the role of DnaJ proteins is likely to help HSP70s recruit the unfolded proteins than help BiP refolding the unfolded substrates (Terrab and Wipf, 2020; Pobre, Poet, and Hendershot, 2019; Chen et al.,2017). However, there is still a lack of information about the regulation pathways of DnaJ proteins over HSP70s in many aspects, including the knowledge about regulation of BiP, which is the ER chaperone mainly working in proteins refolding during ER stress, is also remained elusive and not fully examined until now.

For ERdj3, recent studies illustrated that the protein could interact with BiP and regulate the function of BiP in the UPR during ER stress, mainly in the protein's refolding processes. ERdj3 appears to assist BiP by recruiting the unfolded-protein substrates to BiP for ATP-dependent processes, after the dissociated of BiP from the UPR mediators upon ER stress (Hanafusa, Wada, and Hosokawa, 2019; Romine and Wiseman, 2019; Genereux et al., 2015; Guo F, Snapp 2013; Jin, Zhuang and Hendershot., 2009; Jin et al., 2008; Shen and Hendershot, 2005). Moreover, the binding of ERdj3 with the unfolded proteins is not for delivery the client proteins to BiP or promoting the role of BiP, research suggested that the binding of ERdj3 could prevent aggregation of unfolded proteins in the ER lumen and ERdj3 is also found to be co-secreted with the unfolded proteins from ER when unfolded proteins arehighly accumulated in the ER lumen in stress condition. The secretion of this ERdj3-unfolded protein complex from ER is likely to be related with the activation of PERK during the UPR, because the absence of PERK can cause the accumulation of the complex in the ER lumen more than the presence of PERK (Hanafusa, Wada, and Hosokawa, 2019; Romine and Wiseman., 2019). However, the mechanism of PERK regulating the secretion of the ERdj3-unfolded protein complex still requires additional study for more information. Meanwhile, for the other UPR mediators such as ATF6 and IRE1, here is still no report of the direct interaction between ERdj3 and these two proteins of the UPR in the presence of ER stress. Despite the fact that ER stress activates ERdj3 and the known function of ERdj3 as BiP co-chaperone, it is still a debate, whether ERdj3 is serving as a pro-folding or pro-degradation factor in the ER. However, it is a possibility that the ERdj3 may have function in both pathways.

1. 7. Lipotoxic stress

Recently, new research suggested that proteotoxicity is not the only inducer of ER stress to upregulate the UPR. New evidence indicates that lipotoxic stress also causes ER stress and can upregulate the UPR pathway. Even though lipotoxic stress acts as an ER stress inducer, the mechanism of induction is different from the mechanism during proteotoxic stress (Tam et al., 2019; Volmer and Ron, 2015; Promlek et al., 2011). In general, when proteotoxic stress activates the ER stress response, the UPR sensors IRE1, PERK and ATF6 sense the ER stress signal via its luminal domain. Then the downstream mechanism is to upregulate the protein refolding process and ERAD for clearing the misfolded/unfolded protein from the ER lumen. Meanwhile, the lipotoxic stress will upregulate the activity of the UPR mediators via their transmembrane domain, which causes an increase of membrane fluidity during stress (Fig. 1.6) (Tam et al., 2019; Halbleib et al., 2017; Volmer and Ron, 2015; Volmer et al., 2013; Promlek et al., 2011).

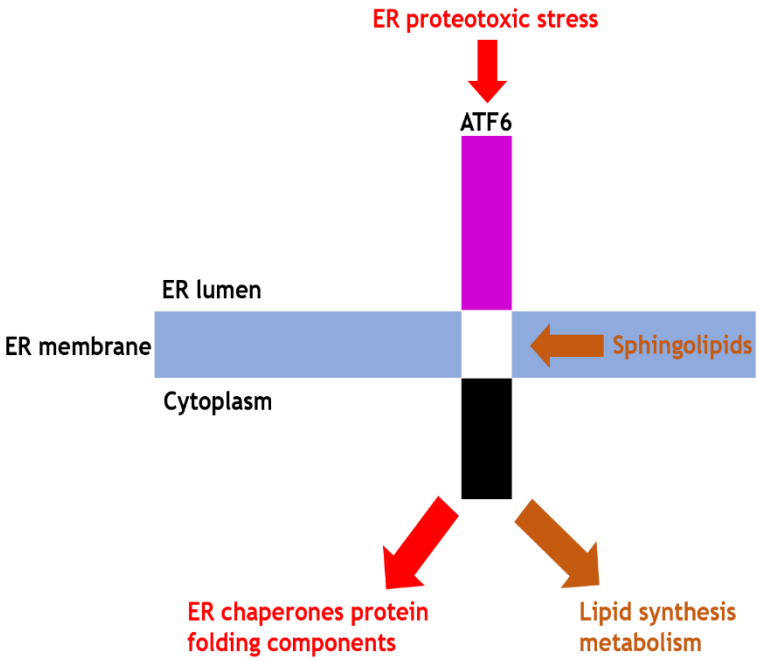

Fig. 1.6. Proteotoxicity and lipotoxicity mediated ER stress response. The mechanism of lipotoxic stress induced UPR is still not fully investigated, however, recent information suggested that the UPR could upregulated by lipotoxicity via transmembrane domain of the UPR mediators like ATF6. This pathway is distinctively different from the proteotoxicity induction, and the signal will direct to upregulate the proteins responded to lipid synthesis metabolism like ACOX1. (Tam et al., 2019).

In addition, proteotoxic stress is known to activate the UPR by the accumulation of the unfolded/misfolded protein, which is occurring in the ER lumen due to the disruption of the folding process or post-translational modification. However, lipotoxic stress activates the UPR because of the disruption of the lipid synthesis processes, as well as the disruption of the lipid bilayer of ER membrane, causing disruption of ER function (Fig. 1.7). The disruption of lipid synthesis could drive the imbalance of ER homeostasis as same as the disruption of protein synthesis, since the majority of lipids such as sphingolipids, sterols and phospholipids, are synthesised in the ER lumen (Jacquemyn et al., 2017; Miller et al., 2017; Volmer and Ron, 2015; Fu et al., 2012; Thibault et al., 2012). There is still a lack of information and knowledge about the lipotoxicity-induced UPR pathway compared to the common proteotoxicity pathway, however, there was a report suggesting that some specific lipids such as dihydrosphingosine (DHS) and dihydroceranmide (DHC), the intermediators of sphingolipid biosynthetic pathway, can directly activate the UPR via the ATF6 pathway to upregulate the expression of the lipid biosynthetic genes and proteins such as ACOX1, without the upregulating of genes involved with proteins folding which are specific to the proteotoxic stress response. However, there is still a lack of evidence to determine the mechanism which allows the proteotoxicity and lipotoxicity response to work independently, despite the induction of the same UPR mediator (Tam et al., 2019).

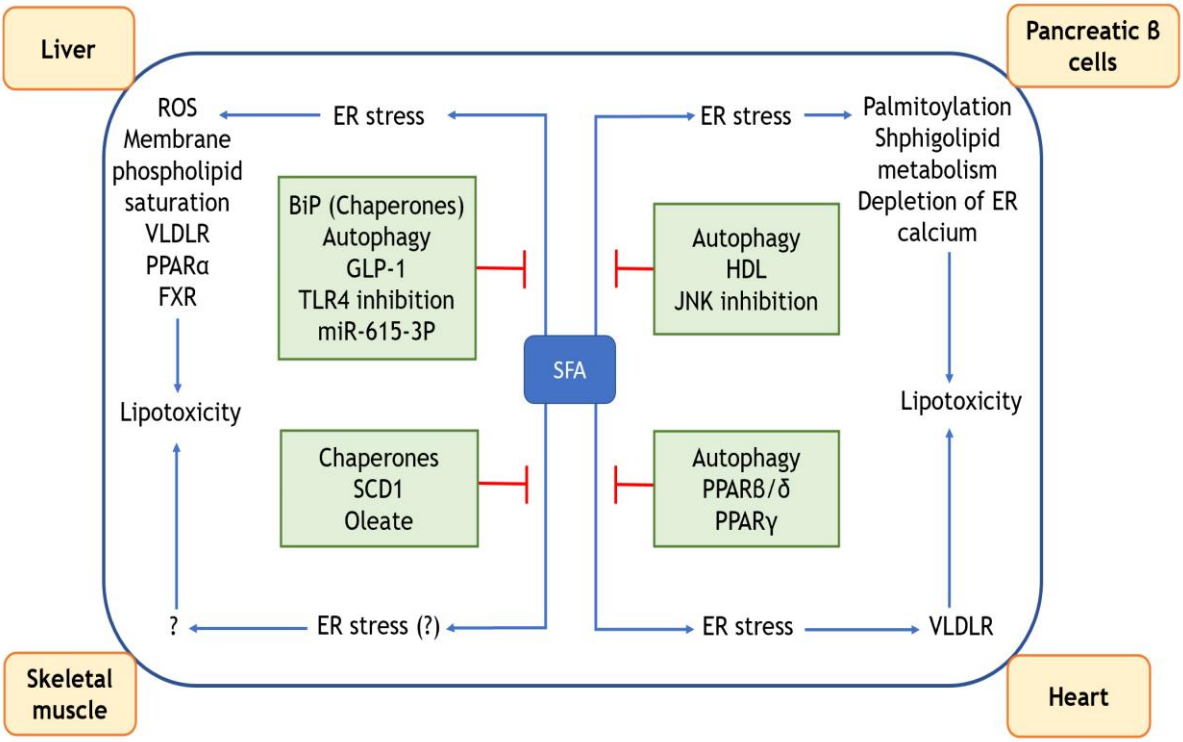

Fig. 1.7. The association of ER stress and lipotoxicity. Recent study suggested that lipotoxicity also could be induced by saturated fatty acids (SFAs) via ER stress in different cell types such as liver, pancreatic ß cells, heart, and skeletal muscle (Han and Kaufman, 2016).

1. 8. The aim of this study

Although recently our knowledge of the UPR and ATF6 activation pathway has increased, the process of translocation of ATF6 from the ER to the Golgi apparatus remains unclear. For instance, evidence suggests that the dissociation of BiP from ATF6 will lead to the transport of ATF6 and that process requires additional proteins such as PDI, COPII cargo protein, and Thbs4. However, it is still unknown what regulates the dissociation of BiP, and what role additional proteins play during the release of BiP and trafficking. Therefore, the aim of this project is to investigate the trafficking of ATF6 from the ER to the Golgi apparatus. The result of this study will provide a clearer idea of the regulatory mechanism of ATF6 and the role of additional proteins in the process. The findings may also provide useful insight for the activation processes of IRE1α and PERK, since they are all regulated by BiP, therefore it might be a common regulatory mechanism between them. In addition, a more understanding of the ATF6 pathway and the

UPR in general will help us to develop new therapeutic methods for several diseases involved with ER stress and the overexpression of the UPR.

As it was stated, the point of this research is to consider the questions which will expand the knowledge of this important cellular process of ATF6. To be specific, these will be directed toward three main questions which will be discussed in three different chapters:

1. To investigate the conformation of the ATF6 which is likely to affect the ATF6 performance in responding to stress. Since it is already well-known that specific conformations of protein such as the disulfide bond, could decrease or deflect protein function.

2. To investigate the complex formation of the ATF6 with others ER resident proteins in the presence and absence of ER stress. Even though there were several studies of the ATF6-proteins complex, the topic is still not fully discovered, therefore it will be worth to examine with the use of specific cell lines expressing mutants of ATF6.

3. The lipotoxic stress response of ATF6 is induced by specific inducers such as dihydrosphingosine (DHS) and dihydroceranmide (DHC). The recent studies suggested that the ER stress could be induced not only by the proteotoxic stress, but also lipotoxic stress, therefore this investigation might give us an interesting and useful information about the ATF6 trafficking regulation.

To achieve the aim of our study, we use specific mutants of ATF6 which were suggested to have a non-trafficking characteristic, the ATF6[D564G] and the ATF6[Y567N]. These point mutations of ATF6 luminal domain are a natural occurring, originated in patients with achromatopsia disease. It is an ideal type of mutation suitable for our ATF6 trafficking study, therefore, we created stable cell lines contained these specific mutants and mainly used these lines in our research.

CHAPTER II: MATERIALS AND METHODS

2. 1. List of cell lines

	Source
HEK-239 (Human Embryonic Kidney)	ATCC
HEK-239/HA-ATF6-V5	Oka et al., 2019
HEK-239/ HA-ATF6[D564G]-V5	This study
HEK-239/ HA-ATF6[Y567N]-V5	This study
HT-1080 (human fibrosarcoma cell)	ATCC
HT-1080/ATF6-KO	Marie Anne Pringle (University of Glasgow)
CHO (Chinese hamster ovary cells)	ATCC
CHO/ERdj3-KO	David Ron (Cambridge University)
***E.coli*, XL-1 cells**	Stratagene

2. 2. List of chemicals

	Source
10X GlycoBuffer 3	NEB
10X glycoprotein denaturing buffer	NEB
Acetic Acid	Fisher
Acetone	BDH
Ammonium Bicarbonate	Sigma
Ammonium Sulphate ((NH4)2SO4)	ICN
Ampicillin	Sigma
Bacto Agar	Melford
Bacto Tryptone	Melford
Bacto Yeast Extract	Melford
DABCO	Sigma
Dihydrosphingosine (DHS)	Sigma, #D3314
Dihydroceramide (DHC)	Sigma, #C7980
Dulbecco's modified Eagle's medium (DMEM)	Gibco
DMSO	Sigma

DpnI	NEB
Dithiobis(succinimidyl propionate) (DSP)	Pierce
1,4-Dithiothreitol (DTT)	Fisher
EDTA	Fisher
EGTA	Invitrogen
Endoglycosidase H (Endo H)	NEB
Ethanol	Fisher
Fetal Bovine Serum (FBS)	Gibco
Formaldehyde	Fisher
Glucose	Sigma
Glutamine	Gibco
Glycerol	Fisher
Glycine	Fisher
10X GlycoBuffer 3	NEB
10X glycoprotein denaturing buffer	NEB
Ham's F-12 Nutrient Mixture	Gibco
HEPES	Fisher
Hydrochloric acid (HCL)	Fisher
Hygromycin B	Thermo Fisher
Kanamycin	Roche
Lipofectamine CRISPRMAX transfection reagent	Thermo Fisher
MegaTran transfection kit	Origene
Mercaptoethanol	Sigma
Methanol	Fisher
MOWIOL	Sigma
N-Ethylmaleimide (NEM)	Sigma
Pen-Strep	Gibco
Phenol: chloroform: isoamyl alcohol	Sigma
PMSF	Sigma
Potassium Acetate	BDH
Protease inhibitor cocktail tablets	Roche
Protein A Sepharose	Zymed
QuickExtract DNA Extraction Solution	Lucigen
QuikChange II site-directed mutagenesis kit	Stratagene

Sodium Carbonate (Na2CO3)	BDH
Sodium Chloride (NaCl)	Fisher
Sodium Dodecyl sulphate (SDS)	Fisher
Sodium hydroxide (NaOH)	BDH
Sodium Phosphate (NaH2PO4)	Fisher
T7 endonuclease	New England Biolabs
Thapsigargin (TG)	Tocris
TBST	Sigma
TEMED	Sigma
Tris	Fisher
TritonX-100	Sigma
Trypsin	DIFCO
Tween	Sigma

2. 3. List of antibodies

	Source
1st antibodies	
ATF6 (mouse)	Abcam, cat. ab122897
Bip (mouse)	Biosciences, cat. #610979
HA (mouse)	Sigma, cat. H3663
HA (rabbit)	Proteintech, cat. 51064-2-AP
V5 (mouse)	Invitrogen, cat. R960-25
V5 (rabbit)	Cohesion (cat. CPA9009) or Proteintech (cat. 14440-1-AP)
Neudesin (mouse)	R&D systems, cat. MAB6714
TFG (mouse)	Invitrogen, cat. MA5-25759
ERdj3 (mouse)	Santa Cruz, cat. sc-271240
14-3-3E (mouse)	Bio-Rad, cat. VMA00525
P5 (to C-terminal peptide) (rabbit)	Bulleid's Lab
Actin (rabbit)	Sigma, cat. A2103
PERK (Rabbit)	Cell Signaling, cat. #3192
ACOX1 (Rabbit)	Abcam, cat. ab184032

HDAC2 (Rabbit)	Abcam, cat. #32117
2nd antibodies	
Goat anti-mouse IRDye 800	ThermoFisher, cat. #10751195
Goat anti-mouse IRDye 680	ThermoFisher, cat. A32729
Goat anti-rabbit IRDye 800	ThermoFisher, cat. #13477187
Goat anti-rabbit IRDye 680	ThermoFisher, cat. #35568
Immunofluorescence	
V5 (Rabbit)	Cohesion, cat. CPA9009
V5 (Mouse)	Invitrogen, cat. R960-25
CNX (Rabbit)	Abcam, cat. ab22595
GM130 (Rabbit)	Martin Lowe (University of Manchester)
Anti-mouse-FITC	Sigma, cat. F0257
Anti-rabbit-FITC	Sigma, cat. F7512
Immunoprecipitation	
V5 (Rabbit)	Cohesion or Proteintech
V5 agarose conjugate (Mouse)	Sigma, cat. A7345
ATF6 (Mouse)	Abcam, cat. ab122897
BiP (Mouse)	Biosciences, cat. #610979

2. 4. List of primers

	Primer Sequences (5'→ 3')
ATF6_D564G_FW	CATCCGCAGAAGGGGAGGCACATTTTATGTTGTG
ATF6_D564G_RV	CACAACATAAAATGTGCCTCCCCTTCTGCGGATG
ATF6_Y567N_FW	AGGGGAGACACATTTAATGTTGTGTCATTTCGAAGG
ATF6_Y567N_RV	CCTTCGAAATGACACAACATTAAATGTGTCTCCCCTTC

2. 5. Recombinant DNA

	Source
HA-ATF6α-V5 (WT)	Ron Prywes's lab
HA-ATF6α[D564G]-V5	This study
HA-ATF6α[Y567N]-V5	This study

2. 6. Cloning

Wild type ATF6. The pCGN-ATF6 plasmid containing a HA-epitope at the N-terminal, was obtained from Adam Benham (Durham University), originally a gift from Ron Prywes (Zhu et al., Mol Cell Bio 1997). This original construct was used as template to generate an ATF6α fragment containing a HA-tag at the N-terminal and a V5-tag at the C-terminal by my colleague in our lab (Oka et al., 2019). This DNA fragment was cloned into the NheI and NotI sites of pCDNA 3.1. Therefore, the construct expressed full-length ATF6 tagged with HA- and V5- epitope at the N- and C-terminal respectively. Then the plasmid construct was stably expressed in HEK-239 cell line with Hygromycin B as a selective reagent, and the cells were used as the wild ATF6 (ATF6-WT) in this study. Furthermore, this plasmid construct also was used as a template to generate the mutant ATF6 plasmid constructs.

Mutants ATF6. The point mutations on the luminal domain of ATF6, pcDNA-HA-ATF6(D564G)-V5 and pcDNA-HA-ATF6(Y567N)-V5, were made with QuikChange II site-directed mutagenesis kit. The mutant plasmid constructs were generated by standard PCR using the wild type pcDNA-HA-ATF6-V5 as a template with the appropriate primer pairs (See list of primers). Then, the *DpnI* was added to the PCR product to digest the DNA template and after that the product was transformed into *E.coli*, XL1 competent cells, by heat-shock at 42 ºC for 45 s. The transformed cells were plated on agar plate contained 100 µg/ml Ampicillin as a selective antibiotic and were incubated 24-48 h at 37 ºC. After that *E.coli* colonies were picked individually and grown in 3 ml Luria Bertani (LB) broth contained 100 µg/ml Ampicillin on shaker at 37 ºC overnight. Then the plasmid DNA was extracted from bacterial cells by using mini prep purification method with alkaline lysis for sequencing or QIAGEN plasmid midi kit for transfection. The obtained plasmid construct was confirmed by agarose gel electrophoresis and sequencing analyses (GATC-Biotech) respectively. The plasmid DNA construct that contained the point mutation of our interest, was then stably expressed in HEK-239 cell line by using MegaTrans kit for transfection with the use of Hygromycin B as a selective reagent. Then the cells carried the mutant ATF6 plasmids, HA-ATF6[D564G]-V5 or HA-ATF6[D564G]-V5, were identified by immunoblotting with mouse anti-HA or mouse anti-V5 antibody (Bulleid's Lab).

ATF6-Knockout. This is the Alt-R CRISPR/Cas9-based Knockout, the knockout ATF6 cell line was generated in our lab by Marie Anne Pringle. The single guide RNA (gRNA) matching the ATF6 genomic targets was designed using the CRISPR Design Tool - nickase analysis (crispr.mit.edu). The ATF6-KO was performed in HT-1080 cell line by using Lipofectamine CRISPRMAX transfection reagent to transfect CRISPR/Cas9-Ribonucleoprotein (RNP) complex. Then T7 endonuclease was used to digest the DNA hybrid. The positive ATF6α knockout (ATF6-KO) cells were identified by immunoblotting with mouse anti-ATF6 antibody and the deletion was verified by sequencing (Bulleid's Lab).

ERdj3-Knockout. The ERdj3-KO was performed in the CHO cells and this cell type was gifted by David Ron (Cambridge University).

2. 7. Cell culture

HEK-239 cell line. HEK-239 cell line, a human embryonic kidney cells, was grown in Dulbecco's modified Eagle's medium (DMEM), supplemented with 10% fetal bovine serum (FBS), 2mM glutamine, 100 Units/ml penicillin and 100 µg/ml streptomycin (Pen-Strep) at 37 ºC in a 5% CO_2 incubator. For AT6 transfected cell line, 200 µg/ml Hygromycin B was added to maintain the expression of transfected gene (Bulleid's Lab).

HT-1080 cell line. HT-1080 cell line, a human fibrosarcoma cells, was maintained in the same way with HEK-239 cell line by growing in DMEM supplemented with 10% FBS, 2mM glutamine and Pen-Strep antibiotics at 37 ºC in a 5% CO_2 incubator (Bulleid's Lab).

CHO cell line. CHO cell line, a Chinese hamster ovary cells, was grown in Ham's F-12 Nutrient Mixture media supplemented with 10% FBS and Pen-Strep antibiotics at 37 ºC in a 5% CO_2 incubator (Bulleid's Lab).

2. 8. Transfection

Mutant ATF6 stable cell line. HEK-293 cells at 80 % – 90% confluence were transfected with the mutant ATF6 plasmid DNAs, ATF6(D564G) or ATF6(Y567N), using MegaTran transfection kit according to the manufacturer's instructions. For stable transfections, 24 h post-transfection cells were passaged (at 1.5:10 dilution) into fresh growth medium containing Hygromycin B as a selective reagent. After 2-3 weeks, a great number of cells will die and the cells which still remain growing in selective medium are likely to retain the transfected plasmids. Then the positive cells were identified by western blotting analysis with anti-HA or anti-V5 antibody, since the constructs of the mutant ATF6 plasmid were conjugated with HA and V5 at the N- and C-terminal respectively (Bulleid's Lab).

Transient transfection. CHO-cells were transfected by using NovaCHOice® Transfection Kit (Sigma) according to the manufacturer's instructions. Cells were seeded 24 h prior to transfection. Plasmid DNA for transfection was prepared in serum free media with NovaCHOice® transfection reagent and booster reagent, the working ratio is 1 μg plasmid DNA: 1 μl transfection reagent : 0.5 μl booster reagent. The mixture was incubated for 30 minutes at room temperature, then transferred to culture cells. After 24 hours of transfection, cells can be used for experiments.

2. 9. Cells treatment

Cells were specifically treated for each experiment, therefore it was separately described in the result chapters.

2. 10. Agarose gel electrophoresis

1% agarose gel was prepared in TAE buffer (40 mM Tris-acetate, 1 mM EDTA), then into the warm gel, SYBR@ dye was added for DNA staining (1:10000). The gel solution had to be well mixed with dye and allow it to set at room temperature. DNA samples were mixed with 6X loading dye (0.25% bromphenol

blue, 0.25% xylene cyanol, 30% glycerol) before loading into the gel, then it was running at ~150V for 2 h. Gel needed to be in the dark for all of the processes (Bulleid's Lab).

2. 11. Western blotting (immunoblotting) and antibodies

Cells were washed once with ice-cold phosphate-buffered saline (PBS) contained 20 mM N-ethylmalemide (NEM) and then lysed in lysis buffer (1% Tritol X-100, 150 mM NaCl, 50 mM Tris at pH 7.5, 2 mM EDTA, and a protease inhibitor cocktail) containing 20 mM NEM. Protein concentrations of the total cell lysates were measured by Bio-Rad protein assay (Bio-Rad). Thereafter, protein sample was mixed with 4X sodium dodecyl sulfate-polyacrylamide gel electrophoresis (SDS-PAGE) loading buffer (1 M Tris at pH 6.8, 8% SDS, 40% Glyceral, and a few crystals of Bromophenol blue) and with 100 mM 1,4-Dithiothreitol (DTT) for reducing and without DTT for non-reducing condition, then the mixed sample was loaded onto 7.5%, 10%, or 12.5% acrylamide gel and running with 20 mA in 1X running buffer (25 mM Tris at pH 8.3, 192 mM Glycine, 0.1% SDS). After electrophoresis, the proteins were transferred from acrylamide gels to nitrocellulose membranes by using wet transfer technique in 1X transfer buffer (25 mM Tris, 192 mM Glycine, and 20% Methanol) at 250 mA for 1 h, after transferred the membrane was blocked with 5% skimmed milk for 1 h on shaker. Then the membrane was probed with primary antibody containing 1.5% skimmed milk for 1 h on rocker, followed by 5 min 3 times washing with 1X TBS (0.1% Tween20, 100 mM Tris pH 7.5, and 0.9% NaCl). After that, the membrane was probed with secondary antibody for 1 h on rocker, then washed again with 1x TBS for 5 min, 3 times. Finally, the signal was detected by Odyssey Sa (Oka et al., 2019).

The primary antibodies dilutions were mouse anti-HA (1: 3000), rabbit anti-HA (1: 500), rabbit anti-P5 (1:500), mouse anti-V5 (1:5000), rabbit anti-V5 (1:5000), mouse anti-ATF6 (1:500), rabbit anti-ACOX1 (1:500), rabbit anti-actin (1: 500), mouse anti-14-3-3E (1: 1000), mouse anti-ERdj3 (1: 300), mouse anti-Neudesin (1: 1000), mouse anti-TFG (1: 1000), or mouse anti-BiP (1: 250).

The secondary antibodies dilutions were anti-mouse 800 (1: 5000), anti-mouse 680 (1:5000), anti-rabbit 800 (1:5000), anti-rabbit 680 (1:5000).

2. 12. Immunoprecipitation

Cells were washed once with ice-cold PBS containing 20 mM NEM and then lysed in lysis buffer which also contained 20 mM NEM. The total protein lysate was measured by Bio-Rad protein assay. Thereafter, the protein sample was pre-cleared by adding 10% protein A-sepharose (PAS) beads prepared in immunoprecipitation (IP) buffer (1% Triton X-100, 10% glycerol, 20 mM HEPES at pH 7.5, 150 mM NaCl, 1 mM EDTA, and a complete mini EDTA-free protease inhibitor cocktail tablet) and rocked for 1 hour at 4 ºC. Then the mixture was centrifuged, and the supernatant was incubated with 10% PAS beads and specific antibody for the protein target, such as mouse anti-BiP (1:200), in IP buffer contained 1% bovine serum albumin (BSA) at 4 ºC on rocker overnight to precipitate the target protein. Subsequently, the beads were washed 3 times with IP buffer and the precipitated protein was eluted by SDS-PAGE loading buffer. The eluted protein sample was analyzed by western blot analysis (Oka et al., 2019).

2. 13. Immunofluorescence

Cells were grown on coverslips and then either left untreated or treated with 10 mM DTT for 30 minutes. Cells were washed with ice-cold PBS twice and fixed with cold methanol for 10 minutes. Then, the fixed-cells were washed again with ice-cold PBS, followed by blocking with 0.2% BSA in PBS for 30 minutes. After that, cells were incubated with primary antibody (1:200); rabbit anti-calnexin (ER), rabbit anti-GM130 (Golgi), mouse anti-V5 (ATF6), or rabbit anti-V5 (ATF6), for 1 h. Cells again were washed with ice-cold PBS and then incubated with secondary antibody (1:200); anti-rabbit FITC or anti-mouse FITC, for 45 min. After incubation cells were washed with ice-cold PBS and H_2O respectively, then mounted on slides with 6 µl anti-fade reagent (4 µl MOWIOL and 25 mg/ml DABCO). The fluorescence cells images were collected with confocal microscope (Axiocam;

Carl Zeiss MicroImaging) and analyzed using Zen software (Carl Zeiss Microimaging) (Bulleid's Lab).

2. 14. Endoglycosidase H digestion

According to the Endo H protocol from NEB, to the whole cell lysate was added 10X glycoprotein denaturing buffer (5% SDS, 400 mM DTT) and the samples heated at 105 ºC for 10 min. 10X GlycoBuffer 3 (500 mM CH_3COONa pH 6) as then added along with 500,000 units/ml Endoglycosidase H (Endo H) (Endo H:sample ratio = 1:20). The mixture was incubated at 37 ºC overnight, subsequently, adding SDS-PAGE loading buffer contained 100 mM DTT. The mixed sample was boiled at 105 ºC for 5 min prior to electrophoresis and immunoblotting analysis.

2. 15. Sucrose gradient fractionation

Cells were lysed with NP40 lysis buffer (50 mM Tris at pH 7.5, 20 mM NaCl, 20 mM NEM, 1% NP40, and a complete mini EDTA-free protease inhibitor cocktail tablet). Total cell lysate was layered on top of 5-50% sucrose gradient (top to bottom) in SW40 tube, then centrifuged at 140,000 xg, at 4 ºC for 16 h in a swing-bucket rotor. After centrifugation, the gradient was fractionated and collected by using BioComp Fractionator. Protein in the fraction was precipitated using trichloroacetic acid (TCA) precipitation method (see below). Thereafter, protein pellets were resolved in SDS-PAGE loading buffer and boiled at 105 ºC for 10 min. Protein samples were analysed by electrophoresis, followed by immunoblotting (Bulleid's Lab).

2. 16. Protein crosslinking

Cells were either treated with 5 µg thapsigargin for 1 h to induce ER stress or left untreated. Then the cells were washed from the dish and collected by centrifugation at 1500 rpm for 5 min, followed by washing with PBS buffer twice.

After that, cells were treated with 2 mM dithiobis(succinimidyl propionate) (DSP) and incubated on rocker for 30 min at room temperature to form protein cross-linking. The reaction was stopped by adding 20 mM Tris pH 7.5 for 15 minutes by rocking in a room temperature. Then cells were collected by centrifugation at 1500 rpm for 5 minutes and rinsed with ice-cold PBS supplemented with 20 mM NEM. Cells were lysis with lysis buffer, then the supernatant was pre-incubated with 10% protein A-Sepharose (PAS) beads for 30 min at 4 °C, before immunoprecipitated with mouse anti-V5 conjugated agarose beads, or rabbit anti-V5 with 10% PAS beads at 4 °C for approximately 16 h to precipitate the ATF6 complex. The beads were washed with lysis buffer containing 0.1% SDS three times, then washed with PBS three times to remove detergent. The ATF6 cross-linked complexes were eluted from the beads by adding 10 mM DTT supplemented with 25 mM ammonium bicarbonate for 10 minutes at room temperature. Supernatant was collected and send to be analyzed by mass spectrometry or analysed by immunoblotting (Oka et al., 2019).

For mass spectrometry (MS) analysis, trypsin (0.3 µl, 0.2 ng/µl, Promega, sequencing grade) was added to the eluted protein samples which were prepared from the previous section and then the mixed solution incubated at 37°C overnight, to allow complete digestion of protein samples. After the incubation, a portion of the resultant peptides were then injected on an Acclaim PepMap 100 C18 trap and an Acclaim PepMap RSLC C18 column (ThermoFisher Scientific), using a NanoLC Ultra 2D Plus loading pump and a NanoLC AS-2 autosampler (Eksigent). The peptides were held on the trap and washed for 20 min and were eluted with a gradient of increasing acetonitrile, containing 0.1% formic acid (2–20% acetonitrile in 90 min, 20–40% in a further 30 min, followed by 98% acetonitrile to clean the column, before re-equilibration to 2% acetonitrile). The eluate was sprayed into a TripleTOF 5600 + electrospray tandem mass spectrometer (AB Sciex, Foster City, CA) and analyzed in Information Dependent Acquisition (IDA) mode, performing 250 ms of MS followed by 100 ms of MS/MS analyses on the 20 most intense peaks seen by MS. The MS/MS data file generated via the “Create mgf file” script in PeakView (Sciex) was analyzed using the Mascot search algorithm (Matrix Science), against the NCBInr database considering both all species (93482448 sequences) and restricting the search to Homo sapiens (331464 sequences), trypsin as the cleavage enzyme and N-ethylmaleimide, hydrolyzed N-

ethylmaleimide modifications of cysteine, thioacyl modification of lysines and N-termini, and methionine oxidation all as variable modifications. The peptide mass tolerance was set to 20 ppm and the MS/MS mass tolerance to ±0.05 Da. A protein was accepted as identified if it had 2 or more peptides with Mascot Ion Scores above the identity threshold ($P < 0.05$), and for those proteins identified by only two peptides, the MS/MS spectral assignments match most of the peaks in the MS/MS spectra (Oka et al., 2019).

In addition, there were some modifications in the immunoprecipitation step for this method and we used this modification for most of our experiments followed by western blotting analysis. Here the cells lysate was immunoprecipitated with mouse anti-V5 conjugated agarose beads, or rabbit anti-V5 with 10% PAS beads at 4 °C for approximately 16 hours to precipitate ATF6 complex. Then the beads were washed with IP buffer three times, followed by washing with PBS three times to remove detergent. The cross-linked complexes were eluted from the beads by adding 10 mM DTT supplemented with 25 mM ammonium bicarbonate for 10 minutes at room temperature. Subsequently, centrifugation to collect supernatant, which was analysed by immunoblotting (Bulleid's Lab).

2. 17. Trichloroacetic acid (TCA) precipitation

4 parts of sample were added by 1 part of 12.5% TCA and centrifuged at 16,200xg at 4 ºC for 30 minutes. Removing TCA, then washing the protein pellet with 200 µl of 70% chilled acetone by spinning at 15,000 rpm at 4 ºC for 5 minutes, two times. After acetone was removed, the protein pellet was left to dry at room temperature about 15-20 minutes. Subsequently, the dried pellet was dissolved in SDS loading buffer (Bulleid's Lab).

2. 18. Protein precipitated from the culture media

500 µl culture media was taking after cell treatment and 50 µl 0.1% BSA, then 110 µl 50% TCA was added. The sample was incubated on ice for 10 min,

before centrifuged at 10,000xg for 15 min at 4 ºC. TCA was removed from the protein pellet with 200 µl 100% chilled ethanol and by centrifuging at 10,000xg at 4 ºC for 5 min, repeated two times. Then the pellet was air-dried for 10 min at room temperature. The pellet was dissolved in SDS loading buffer and analysed by western blotting. If the protein sample turned yellowish after dissolved, the pH was adjusted with 1M Tris pH 7.5 (Bulleid's Lab).

2. 19. Cell fraction

Cells were collected and washed with ice-cold PBS supplemented with EDTA-free protease inhibitor tablet. Then cells were resuspended with 1 ml ice-cold buffer A (10 mM HEPES pH 7.4, 250 mM Sucrose, 10 mM KCl, 1.5 mM $MgCl_2$, 1 mM EDTA, and 1 mM EGTA) and incubated 10 min on ice. The cells were lysed by passing through a 23-gauge needle, 30 times. Cell lysates were centrifuged at 1,000xg at 4 ºC for 7 min, pellet is a nuclear fraction, meanwhile supernatant is cytosolic and membrane fraction.

Nuclear fraction. The pellet was washed once with 500 µl buffer A contained protease inhibitor by centrifuge at 1,000xg at 4 ºC for 7 min. Then the pellet was discarded from supernatant and resuspended in 100 µl buffer B (10 mM HEPES pH 7.6, 2.5% Glycerol, 420 mM NaCl, 1.5 mM $MgCl_2$, 1 mM EDTA, and 1 mM EGTA). The sample was incubated on the rocker at 4 ºC for 60 min. After that, the sample was centrifuged again at 100,000xg at 4 ºC for 30 min and supernatant was collected as a nuclear extract.

Cytosolic and membrane fraction. Supernatant was centrifuged at 100,000xg at 4 ºC for 30 min, consequently, the pellet contained membrane, meanwhile the cytosol was in the supernatant. Then the membrane pellet was resuspended in 100 µl buffer B contained protease inhibitor, while the cytosol in the supernatant was precipitated by using 5x volume of 100% ice-cold acetone and centrifuge at 16,200xg at 4 ºC for 15 min. Then the cytosol was found in the pellet and resuspended in 100 µl buffer B contained protease inhibitor as well (Bulleid's Lab).

CHAPTER III: RESULTS SECTION 1 - The mutation types of ATF6 and their characterization

3. 1. The variants of ATF6 mutants

Human ATF6 is a 670 amino acids transcription factor found on the endoplasmic reticulum (ER) membrane and has a key role in the unfolded protein response (UPR) during ER stress along with PERK and IRE1. The accumulation of unfolded or misfolded protein upon ER stress, which is induced by internal or external stimulators, will lead to the downstream response of ATF6 causing its dissociation from BiP, an ER chaperone protein, and packaging into transport vesicles. These CopII-coated vesicles deliver the ATF6 to the Golgi apparatus, where it is cleaved by the site 1 protease (S1P) and site 2 protease (S2P) respectively (Shen et al., 2002; Haze et al., 1999). After the luminal and transmembrane domains are removed, the liberated cytosolic domain, containing a transcription factor of the basic leucine zipper (bZIP) family, migrates to the nucleus and upregulates target genes such as ER protein folding enzymes and chaperones protein (Wu et al., 2007; Yamamoto et al., 2007; Ye et al. 2000). By this mechanism, ATF6 can help to restore protein folding homeostasis and suppress ER stress, resulting in the prevention of cells death (Wu et al., 2007; Nadanaka et al., 2004; Haze et al., 1999).

Similar to other proteins, mutation and the non-native structure or modification can affect the function of ATF6 in several ways. Recent studies have shown that the natural ATF6 mutations found in Achromatopsia patients such as splice site, nucleotide deletion, missense, nonsense, or nucleotide duplication, can significantly attenuate ATF6 activity (Chiang et al., 2017; Kohl et al., 2015). The Achromatopsia-associated ATF6 mutations study suggested that mutations could be divided into 3 groups based on their pathomechanisms. Group 1, the luminal domain mutations show impaired trafficking of ATF6 from the ER to the Golgi, therefore, leading to a reduction or blocking of the downstream processes (Chiang et al., 2017). Group 2, the transmembrane domain mutations can upregulate the target genes even in the absence of ER stress (Chiang et al., 2017; Bommiasamy et al., 2009). Group 3, the cytosolic domain mutations still can transport to the Golgi during ER stress, however, the mutants cannot induce the transcription process of the target genes because of the lost or deficient bZIP

domain (Chiang et al., 2017). In addition, group 1 and group 3 mutants show that cell death increases in the presence of ER stress, while group 2 did not show a significant effect to cell death. According to the research on Achromatopsia mutations, the mutants in group 2 caught our attention the most because of the impaired trafficking characteristic. As it was mentioned before, the main focus of this project is to investigate the regulation ATF6 trafficking from the ER to the Golgi, thus, if we can identify the regulation factors which suppress the trafficking of the mutants in group 2, we might also find the factors that control the migration process of ATF6 as well. Consequently, we chose 2 mutants from group 2, ATF6(D564G) and ATF6(Y567N), for our research.

In addition to the natural occurring ATF6 mutations found in Achromatopsia patients, there are also several studies on deletion constructs of ATF6. The constructs were artificially created in the laboratory and used for several approaches. Here we analysed the data from several studies to identify common characteristics of the constructs and their phenotype. For instance, in table 3.1.A., are the constructs studied by Shen and his colleagues in 2002. They reported several types of the ATF6 constructs which show interesting phenotypes related to the trafficking of ATF6, such as ATF6(1-475) and ATF6(1-500), despite the amino acid sequence not being complete, the constructs still show the common function as found in the wild type ATF6. Meanwhile, the constructs with a shorter amino acid sequence like ATF6(1-430) and ATF6(1-467), lose their translocation property. Simultaneously, in table 3.1.B. (Shen and Prywes, 2004), another study shows that S2P cleavage depends on the length of the ATF6 protein sequence, not by detecting or binding to specific regions of the ATF6 sequence. For instance, short sequence constructs like ATF6(1-418) and ATF6(1-430) can still be cleaved by S2P without the prior cleaved of the S1P. On the other hand, the long sequence constructs such as ATF6(1-500) or the short construct of ATF6(1-430) fused with another protein sequence like ATF6(1-430)-HC and ATF6(1-430)-IRE1, are unable to be cleaved by S2P without the prior cleaved of the S1P. In conclusion, the data here show that amino acid sequence from 431 to 475 is likely to be a BiP binding region and amino acid at 475 is potentially a Golgi localisation-control region. Moreover, the S2P cleavage is controlled by the length of the ATF6 protein sequence, not a specific binding site.

A.

Mutation types	BiP binding	ER stress sensing	BiP releasing	Translocation	S1P cleavage
ATF6(1-430)	X	-	X	X	-
ATF6(1-475)	/	/	/	/	-
LZIP(1-280)*	X	X	X	X	-
LZIP-ATF6(431-475=LD2)**	/	/	/	/	-
3xFLAG-ATF6(S1P-)	/	/	/	/	X
LZIP-ATF6(476-550=LD3)	/	-	-	-	-
LZIP-ATF6(551-670=LD4)	/	-	-	-	-
ATF6(1-467)	-	-	-	X	X
ATF6(Δ468-475)***	-	/	-	/	/
ATF6(Δ468-500)	/	/	/	X	X
ATF6(Δ476-500)	-	/	-	/	/
ATF6(1-500)	/	/	/	/	/
ATF6(1-500Δ431-467)	<<</	/	/	/	<<</
ATF6(1-500Δ431-475)	X	-	X	/	/

B.

Mutation types	BiP binding	ER stress sensing	BiP releasing	ER localization	Translocation	S1P cleavaged	S2P cleavaged (With out S1P cleavaged)
ATF6(1-418)	-	-	-	/ (Not properly)	/	X	/
ATF6(1-430)*	-	X	-	/	X	X	/
ATF6(1-550)	-	-	-	/	-	/	X
ATF6(1-500)	-	-	-	/	-	/	X
ATF6(1-475)	-	-	-	/	-	/	/
ATF6(1-450)	-	-	-	/	-	/	/
ATF6(Δ476-500)	-	-	-	/	-	/	X
ATF6(1-430)-HC	-	-	-	/	-	/	X
ATF6(1-430)-IRE1	-	-	-	/	-	/	X
ATF6-LD-3xFLAG	-	-	-	/	-	/	X

Table. 3.1. Analysis of laboratory constructs of the mutants ATF6 to identify the characteristics of the constructs and their phenotype. The summary of the data from the study of Shen's group in 2002 (Shen et al., 2002) **(A)** and from the study of Shen and Prywes in 2004 (Shen and Prywes, 2004) **(B)**. / = Yes, X = No, - = N/A.

3. 2. Stable cell lines expressing the ATF6 mutants, ATF6(D564G) and ATF6(Y567N)

The first aim of our study was to generate stable cell lines expressing ATF6 point mutations which suppress trafficking ability of ATF6, so that we could analyse interacting partners following ER stress. As it was already mentioned before, the mechanism of ATF6 trafficking from the ER to the Golgi is unclear, until now we only know that ATF6, following ER stress, dissociates from BiP before being packaged into the CopII vesicles and transported to the Golgi. However, BiP dissociation is not likely to be the only factor to regulate ATF6 trafficking, therefore, determining the ATF6 interactome became a focus of our studies. To begin the ATF6 trafficking investigation, non-trafficking ATF6 stable cell lines were created. Our approach was based on information in a prior study, which suggested that the point mutation on the luminal domain of ATF6, such as D564G mutant where the amino acid at position 564 was changed from aspartic acid (D) to glycine (G), and Y567N mutant where the amino acid at position 567 was changed from tyrosine (Y) to asparagine (N), can suppress the transport of ATF6 from the ER to the Golgi (Chianga et al., 2017). First, the pcDNA3.1(+) vector containing the DNA fragment of wild type ATF6, was constructed by attaching HA- and V5-epitopes to the N- and C-termini respectively (Fig. 3.1.A). This plasmid construct was used as a template to produce the mutants of ATF6 by using the QuikChange II site-directed mutagenesis kit with the appropriate primer pairs for D564G and Y567N mutant (see list of primers in chapter II). The encoding protein generated from these constructs could be detected by anti-HA or V5 antibody as well as by anti-ATF6 antibody itself. In addition, using the epitope tags, we can also distinguish the expression of exogenous from endogenous ATF6. Then the mutant constructs were transformed into *E.coli*, XL1-Blue supercompetent cells, and the successfully transformed cells were selected by Ampicillin antibiotic. The ATF6 mutant plasmids DNA were extracted from cells and the mutation points were confirmed by DNA sequencing analyses (Fig. 3.1.B).

Then the mutant plasmids DNA, ATF6(D564G) and ATF6(Y567N), were transfected into HEK-293 cells to generate stable cell lines by using MegaTran 1.0 and the transfected cells were selected by placing on Hygromycin B antibiotic for several weeks until colonies appeared. The colonies were then screened by

western blot analysis with anti-HA antibody to see whether they expressed the mutant ATF6 or not. The results show that some colonies did not express the mutant ATF6 after transfection, some colonies expressed it in a low level, however there were also colonies which expressed the mutant ATF6 well and can be used for future experiments (Fig. 3.1.C). Specifically, on figure 1B, on lane 1 and 2 of the ATF6(D564G) clones, the expression of the mutants is very low, while in lanes 3 to 8 the expression is high. Meanwhile, for the ATF6(Y567N) clones, there was no expression in lanes 1-4 and 6, low expression in lane 5, and good expression in lanes 7 and 8. Therefore, the ATF6(D564G) clone from lane 3 and the ATF6(Y567N) clone from lane 7 were selected for future experiments. In addition, for the ATF6(Y567N) clones, in the lanes that expressed the mutant there was also an intense unidentified band (present with an asterisk), however the band appeared only this one time and never been detected again in the following experiments.

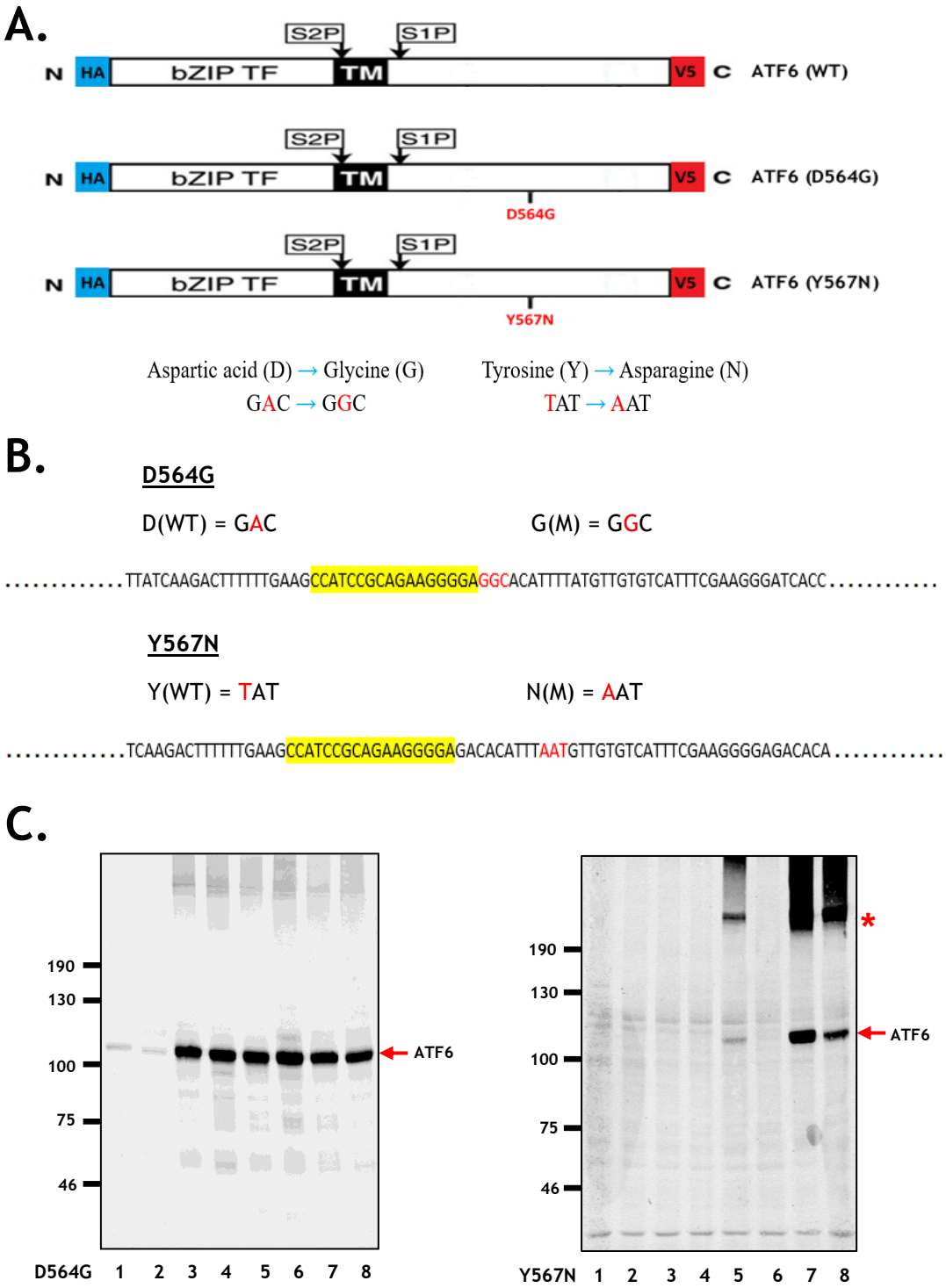

Fig. 3.1. Creating stable cell-lines expressing the ATF6 mutants, D564G and Y567N. (A) Diagram of the ATF6 constructs used in this study. **(B)** The sequences of the DNA constructs were generated by sequencing analysis. **(C)** The expression of ATF6 after transfection HEK-293 cells with plasmids contained specific point mutation in ATF6 luminal domain. HEK-293 cells transfected with a plasmid to express HA-ATF6-V5 (D564G) or HA-ATF6-V5 (Y567N), were lysed in 20 mM NEM-containing lysis buffer and then boiled for 5 minutes at 105 ºC in SDS-PAGE loading buffer with the presence of 100 mM DTT for analysis under reducing condition. The resulting protein was analyzed by immunoblotting using mouse anti-HA antibody (1: 3000). TM = Transmembrane domain, N = N-terminal/cytosolic domain, C = C-terminal/luminal domain, * = Unknown band.

3. 3. The expression of monomer (M), dimer (D), and oligomer (O) form of the ATF6 mutants

It is already well known that without any stress, ATF6 can be found in 3 different forms, the monomer, the dimer and the oligomer, because of the interaction of the disulfide bond at amino acid number 467 and 618 (Oka et al., 2019; Nadanaka et al., 2007). Recent study suggested that the oligomer is only a different form of the dimer, therefore sometimes it will be identified as C618 dimer (618D) for the dimer and C467 dimer (467D) for oligomer (Oka et al., 2019). However, in this study we will still continue to use the term of monomer, dimer and oligomer to describe different forms of ATF6 since these terms are more familiar and well known. These cysteine residues cannot only form intra- or inter-molecular disulfide bond between ATF6 molecules, but may form a disulfide bond with other molecules which were still not fully identified (Nadanaka et al., 2007). Thus, after stable ATF6 mutant cell lines, ATF6(D564G) and ATF6(Y567N) were created, cells were used to study the expression of the mutants ATF6 since the previously report of ATF6(Y567N) mutation only shows the monomeric form, but the non-reduced forms, oligomer and dimer, were not mentioned (Chiang et al., 2017). Meanwhile, the ATF6(D564G) mutant does not have a report about its disulfide formation. Therefore, we were interested in the disulfide status of the different types of ATF6, since the redox forms of ATF6 could also be important for retention and transport.

Consequently, the wild type ATF6, and the ATF6(D564G) and ATF6(Y567N) mutant cells were used to examine the difference of the disulfide formations. Cells were treated with or without 10 mM DTT, a reducing agent, for 30 minutes to induce ER stress and ATF6 trafficking. Then cells were collected, and the cell lysates were analyzed by immunoblotting with anti-HA antibody (Fig. 3.2). The results demonstrate that in the non-reduced condition, the untreated wild type ATF6 cells lane show all 3 redox forms of ATF6 with monomer, dimer and oligomer. The untreated ATF6(D564G) mutant also shows a similar result with the wild type, but with more expression of the dimer instead of oligomer. Simultaneously, the untreated ATF6(Y567N) shows a significantly different result compared to the wild type and the ATF6(D564G) mutant, since the untreated non-reduced ATF6(Y567N) only shows a single band of ATF6 monomer which was similar to the form of ATF6

when it was completely reduced. This result demonstrates that these point mutants, especially ATF6(Y567N) mutant, somehow affected the formation of the interchain disulfide bond within the ATF6 luminal domain and suggests that this mutation may result in the misfolding of this domain. Moreover, the early studies suggested that the reduced monomer of ATF6 is likely to be the only form of ATF6 which could be packed into the COP II vesicle and traffics from the ER to the Golgi during ER stress. Hence, the reduced monomer form of ATF6 is required and plays an important role in trafficking (Schindler and Schekman, 2009; Nadanaka et al., 2007). However, our results here suggested that the reduction of ATF6 is insufficient to drive the trafficking process of ATF6 during ER stress, since the ATF6(Y567N) mutant which only presents the reduced monomer form was still retained in the ER and was not transported to the Golgi upon ER stress.

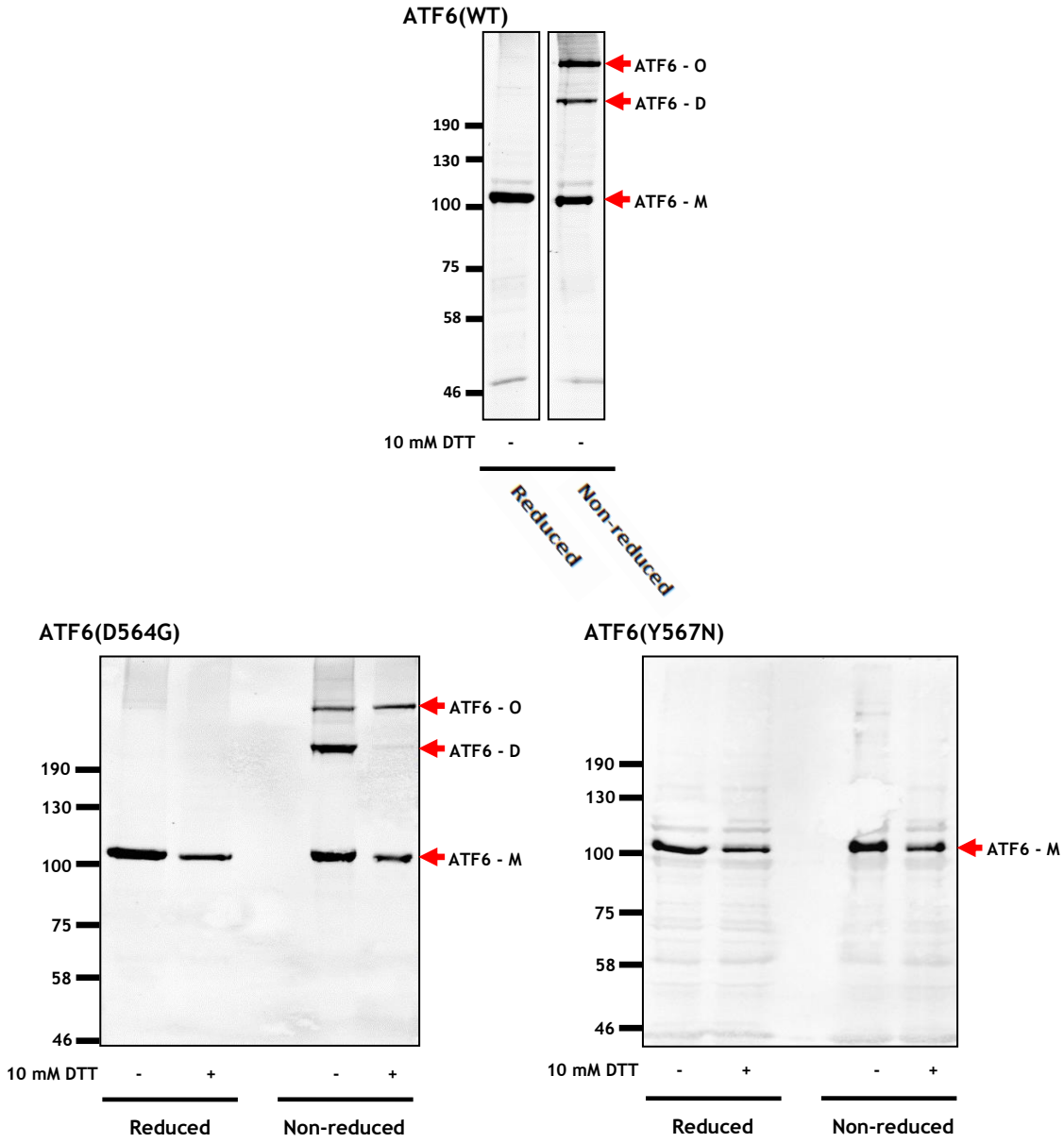

Fig. 3.2. The expression of different forms of ATF6 in the presence of ER stress. The recombinant HA- and V5-tagged wild-type ATF6 was expressed in HEK-293 cells and then the expressed ATF6 protein in the untreated cells was analysed by immunoblotting with mouse anti-HA (1:3000) in reducing and non-reducing conditions. Recombinant HA- and V5-tagged ATF6 mutants, D564G and Y567N were expressed in HEK-293 cells and then treated with or without 10 mM DTT for 30 minutes to induce ER stress. The ATF6 protein was analysed with the same condition as the wild type. O = Oligomer, D = Dimer, M = Monomer.

3. 4. The mutants ATF6 do not traffic from the ER to the Golgi

As we already mentioned earlier, the ATF6(D564G) and ATF6(Y567N) mutants are a naturally occurring mutant found in Achromatopsia disease and were reported as a member of the non-trafficking group of ATF6 mutants (Chiang

et al., 2017). Therefore, after we generated the mutant cells lines, we evaluated the consequence of mutated ATF6 on ER-to-Golgi trafficking. According to previous studies, it was shown that after trafficking from the ER to the Golgi upon ER stress, ATF6 is modified to an O-linked glycosylation form by glycosyltransferases, within the trans-Golgi compartment. The result of the O-linked glycan modification is to generate a slower migrating full-length ATF6, also known as the Golgi form of ATF6 (Shen et al., 2002; Hanisch, 2001; Ye et al., 2000). This modification specifically occurred only in the Golgi apparatus, thus it is a trustable indicator that we can use to examine the Golgi localisation of ATF6. Therefore, we verified the non-trafficking character of our mutants ATF6, ATF6(D564G) and ATF6(Y567N), by detecting its Golgi form. In this experiment, the wild type ATF6 and the mutants ATF6 stable cells lines were treated with 30 μM S1P inhibitor for 1 hour to prevent cleavage of any Golgi localised protein before being treated with or without 10 mM DTT for 45 minutes to induce ER stress and the UPR. After that, cells were collected and lysed, then the cells lysates were analysed by immunoblotting with anti-HA antibody in the reduced and non-reduced condition (Fig. 3.3). The results show that the Golgi form of ATF6 is only present in the wild type ATF6 cells, while it is absent in the mutant ATF6 for both ATF6(D564G) and ATF6(Y567N). This evidence suggests that these ATF6 mutants are impaired in trafficking from the ER to the Golgi during ER stress as reported previously, compared with the wild type ATF6 (Chianga et al., 2017).

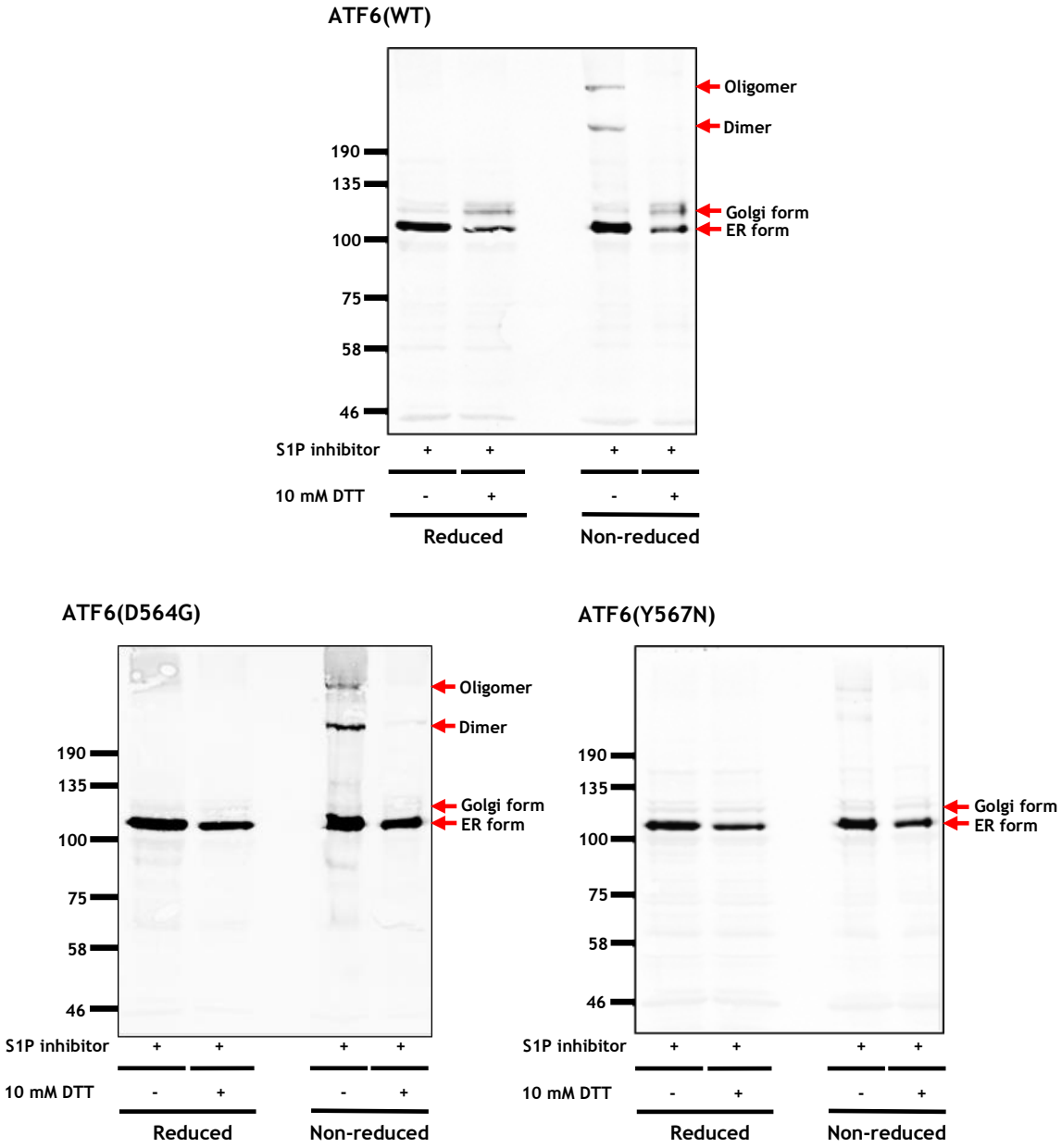

Fig. 3.3. Impaired trafficking of ATF6 from ER to Golgi in the presence of ER stress. Recombinant HA- and V5-tagged ATF6, wild-type, D564G mutant and Y567N mutant, were expressed in HEK-293 cells and then treated with 30 μM S1P inhibitor for 1 hour before challenged with or without 10 mM DTT for 45 minutes to induce ER-to-Golgi trafficking. Then cells were collected, and the cells lysates were analyzed by immunoblotting with mouse anti-HA antibody (1:3000) in the reduced and non-reduced condition.

3. 5. The ATF6 mutants' localisation in the presence of ER stress

Following the trafficking of ATF6 mutants' experiments, the location of the created-mutants ATF6, ATF6(D564G) and ATF6(Y567N), before and after stressed,

were confirmed by immunofluorescence. Since the results of our previous experiment already shown that the generated mutants of ATF6 were not trafficking during ER stress, this experiment was carried out to confirm this specific character of our ATF6 mutants. Therefore, the advantage of the non-trafficking property of the mutants ATF6 was used as a key focus for this experiment. HEK-293T cells that stably expressed either wild type or mutants ATF6, both ATF6(D564G) and ATF6(Y567N), were treated with or without 10 mM DTT for 30 minutes to induce ER stress and ATF6 trafficking. Then cells were immunostained with anti-calnexin, anti-GM130 or anti-V5 antibody. Calnexin and GM130 are specific protein markers for ER and Golgi apparatus, respectively, then the location of the ER and the Golgi can visualised by staining cells with these antibodies. Meanwhile, the ATF6, both wild type and mutants, was visualised by using anti-V5 antibody. After staining, cells were imaged with confocal microscope and analysed using AxioVision4 software. Even though, after the immunostaining by using all of these antibodies, the cells staining will be visualised in green under confocal microscope, we still can indicate the location of ER, Golgi and ATF6 by the difference of the fluorescent pattern. Therefore, if the fluorescent pattern of V5 staining is similar to the pattern of calnexin staining, it means ATF6 is located in the ER. Meanwhile, if the fluorescent pattern of V5 staining is similar to the pattern of GM130 staining, it means ATF6 is located in the Golgi. The images generated from the immunofluorescence test (Fig. 3.4) show that without stress, both wild type and mutants ATF6 were localised in the ER since the pattern of the V5 staining which represents the ATF6 protein is similar to the pattern of calnexin staining which represents ER location.

However, only the wild type ATF6 was re-localised into the Golgi in the presence of ER stress, while the mutants ATF6 are still retained in the ER after cells were treated with DTT to induce ER stress since the pattern of V5 staining of the wild type ATF6 is now more similar to the pattern of GM130 which represents the Golgi location. Meanwhile, the patterns of V5 staining of the mutants ATF6 are still resembled with the pattern of calnexin staining which means the mutants ATF6 are still in the ER. This confirms that our created-mutants ATF6, both ATF6(D564G) and ATF6(Y567N), are poorly trafficking from ER to Golgi during ER stress.

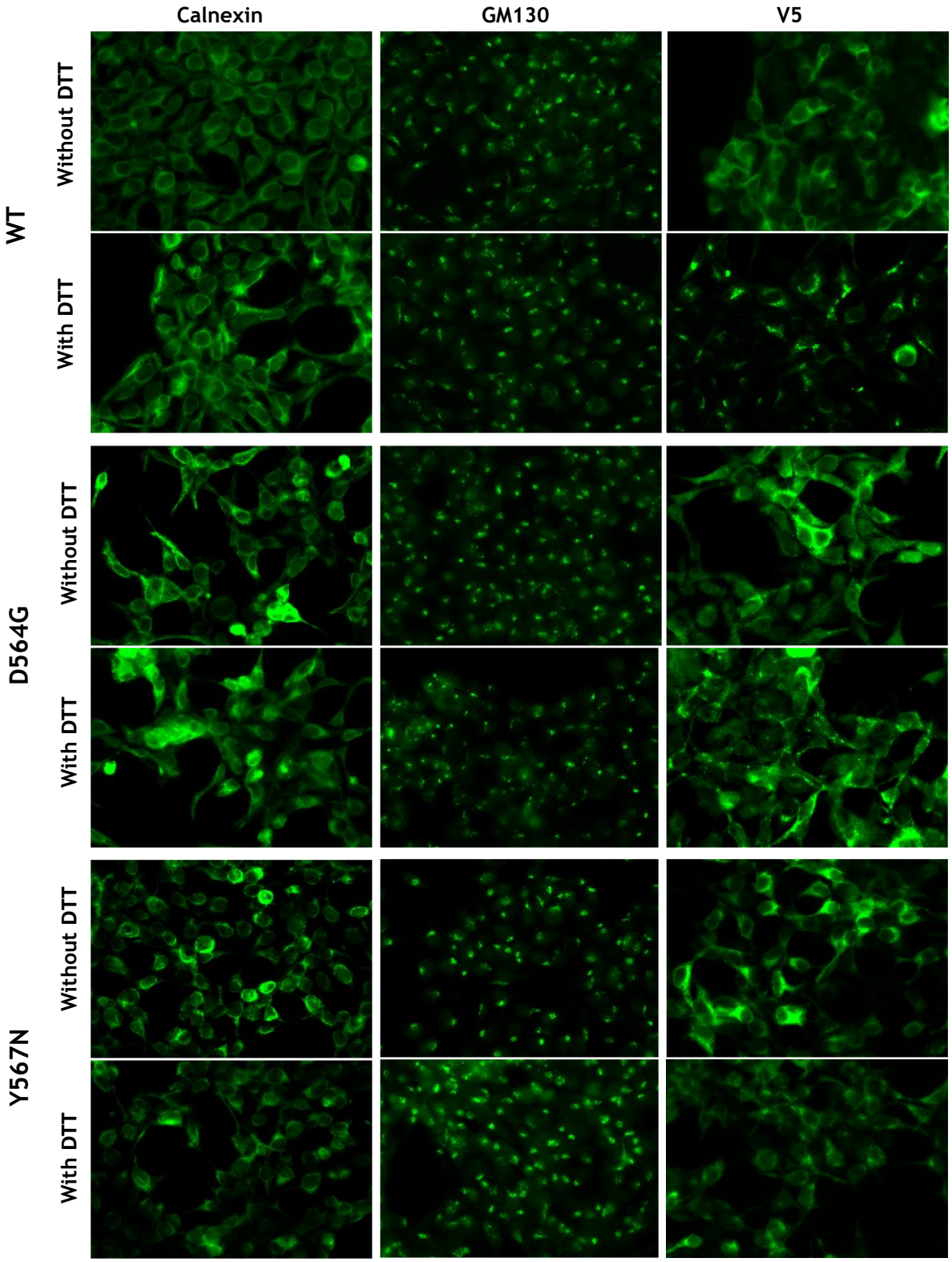

Fig. 3.4. Impaired trafficking of mutants ATF6, D564G and Y567N, during ER stress. Recombinant HA- and V5-tagged ATF6, wild-type, D564G mutant, and Y567N mutant were stably expressed in HEK-293 cells, and then were treated either with or without 10 mM DTT for 30 minutes to induce ER stress and the trafficking of ATF6. The location of ATF6 was visualised by immunofluorescence labeling and confocal microscopy by using anti-V5 antibody. Anti-calnexin antibody was used to visualise ER localisation, meanwhile, the Golgi was visualised by GM130 immunostaining.

3. 6. The dissociation of ATF6 from BiP in the present of ER stress is insufficient to drive the trafficking processes of ATF6 from the ER to the Golgi apparatus

It is already well known that BiP is one of the important proteins in UPR regulation. This ER chaperone protein was reported to be a repressor of the UPR sensors, ATF6, PERK and IRE1, activation (Shen et al., 2005; Ma et al., 2002; Shen et al., 2002; Bertolotti et al., 2000). Without ER stress, BiP binds with the luminal domain of the UPR mediators, including ATF6, and inactivates it until the presence of ER stress. The dissociation of BiP upon ER stress is counted as an initiation of the UPR response, since only after the release of BiP, could ATF6 and other UPR mediators upregulate the downstream processes (Shen et al., 2002). Previous studies suggested that the dissociation of BiP leads to the formation of ATF6 monomer, a form of ATF6 that could exit the ER and be cleavage in the Golgi by S1P and S2P (Nadanaka et al., 2007). In addition, the overexpression of BiP dramatically affects the activation of ATF6 by delaying ATF6 trafficking, and the translocation will completely abolish, if BiP is not released (Shen et al., 2002). In this experiment, we aimed to investigate whether the ER stress induced BiP dissociation is sufficient enough to allow trafficking of ATF6 from the ER to the Golgi, or it still requires other additional factors to fulfill the processes after the release of BiP. Therefore, the advantage of the non-trafficking property of the mutants ATF6, ATF6(D564G) and ATF6(Y567N), stable cells line was used to determine the dissociation of BiP and subsequent ATF6 trafficking.

The wild type ATF6 cell line and the mutated ATF6 cell lines, both ATF6(D564G) and ATF6(Y567N), were treated with or without 10 mM DTT for 30 minutes to induce ER stress and ATF6 trafficking, followed by immunoprecipitation using anti-BiP antibody and then immunoblotting with anti-HA antibody to detect ATF6 bands. It is clear that the amount of ATF6 co-immunoisolated with BiP is significantly decreased after the treatment with DTT in both wild type and mutants ATF6 cells (Fig. 3.5). The results demonstrate that BiP dissociates from ATF6 during ER stress, even though, ER-to-Golgi trafficking of mutated ATF6, both ATF6(D564G) and ATF6(Y567N), did not occur. Meanwhile, the results of ATF6(Y567N) mutant show that the amount of ATF6 that we obtained after immunoprecipitation varied. This suggests that the interaction of BiP with ATF6(Y567N) mutant is very weak and unstable compared with the wild type ATF6

and the ATF6(D564G) mutant. However, despite the unstable interaction, the ATF6(Y567N) mutant was still retained in the ER and could not traffic to the Golgi upon ER stress. This is an unexpected result, since it has been suggested for quite a long time that the association of BiP plays an important role in the retention of ATF6 in the ER and preventing trafficking (Shen and Prywes, 2005; Shen et al., 2002). Thus, the fact that the ATF6(D564G) and ATF6(Y567N) mutants has impaired trafficking despite the dissociation of BiP demonstrates that there may be other specific factors or co-factors which play a crucial role in the trafficking process of ATF6 after the dissociation of BiP, and without those unknown factors ATF6 will continuously remain in the ER in the presence of ER stress.

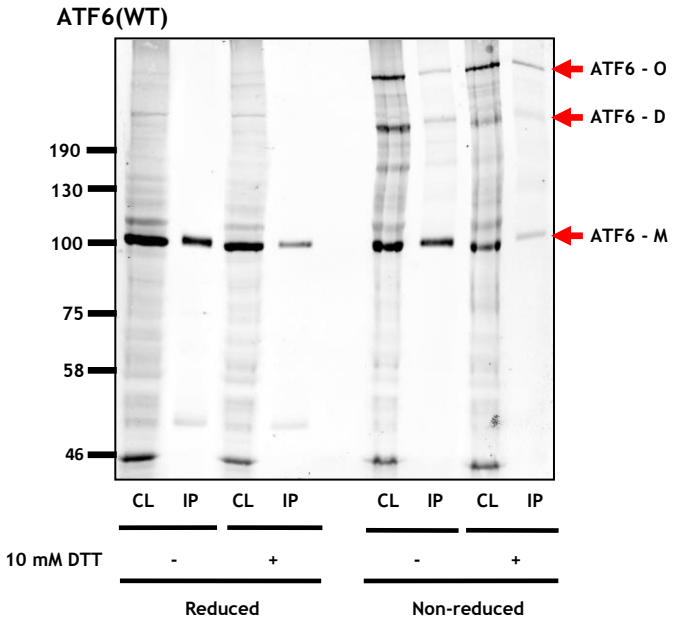

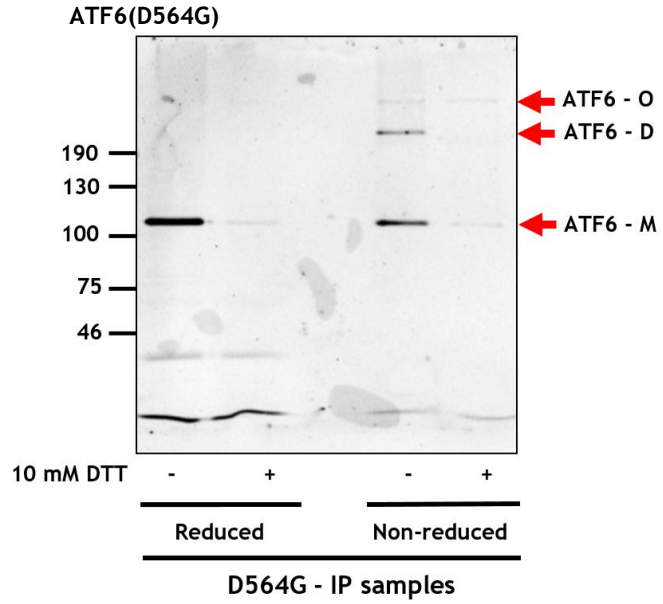

D564G - IP samples

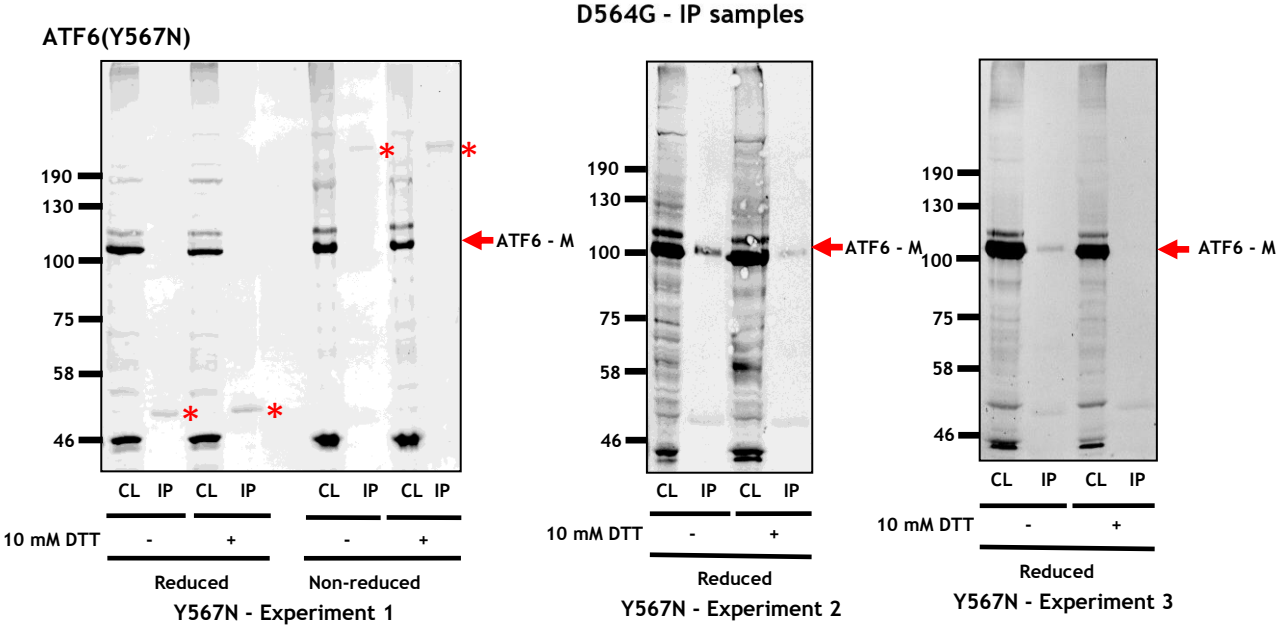

Fig. 3.5. The association of BiP and ATF6 with and without the presence of ER stress. Recombinant HA- and V5-tagged ATF6; wild-type, D564G, and Y567N, were stable expressed in HEK-293 cells and then the cells were treated with or without 10 mM DTT for 30 min to induce ER stress. The presence of BiP-ATF6 complex was analysed by immunoprecipitation with mouse anti-BiP antibody (1: 200) followed by immunoblotting with rabbit anti-HA antibody (1: 1000) in the reduced and non-reduced condition. The figures here show the result of both the total cells lysate samples and the immunoprecipitation samples for WT and Y567N. For the D564G mutant the figure here only presents the result of the immunoprecipitation samples, meanwhile, the result of the total cells lysate sample of D564G was already presented in figure 3.2. CL = Total cells lysate sample, IP = Immunoprecipitation sample, * = Nonspecific band, O = Oligomer, D = Dimer, M = Monomer.

3. 7. The cleaved form of ATF6 produced by the Golgi proteases, S1P and S2P, in the presence of ER stress

Another experiment that we performed to characterise the mutants ATF6, ATF6(D564G) and ATF6(Y567N), was to identify the cleavage form of ATF6 following activation by ER stress. Generally, when ATF6 senses ER stress, it traffics from the ER to the Golgi by dissociating from BIP and packaging into COPII vesicle (Vishnu et al., 2014; Schindler and Schekman, 2009; Adachi et al., 2008; Nadanaka et al., 2007). In the Golgi, ATF6 is cleaved by the Golgi proteases, S1P and S2P respectively and generates the cleavage forms. 50 KDa cleaved form of the ATF6 cytosolic domain with the conserved basic leucine zipper (bZIP) protein, N-terminal, is continuously moving to the nucleus and upregulates the ER stress response genes by binding to ER stress-responsive cis-acting elements (Okada et al., 2003; Shen et al., 2002; Ye et al., 2000; Yoshida et al., 2000). Meanwhile, the cleaved form of the ATF6 luminal domain, C-terminal, is degraded by lysosomal proteolytic mechanism (Hong et al., 2004). First, we investigated the cleaved forms of ATF6 under the normal condition of ER stress by using DTT or thapsigargin (TG) as stress inducers. If ATF6 can migrate from the ER to the Golgi and become cleaved by S1P and S2P proteases, the cleaved form of ATF6 will be generated. Meanwhile, if ATF6 cannot traffic from the ER to the Golgi, the cleaved form will simply not be produced. For this experiment, the HEK-293 cell-line stably expressed the recombinant HA- and V5-tagged ATF6, the wild-type, the ATF6(D564G) mutant or ATF6(Y567N) mutant, were used again. Cells were treated

with 20 mM NH_4Cl for 45 minutes to prevent the cleaved form of ATF6 from degradation, and then followed with 10 mM DTT for 30 minutes to induce ER stress (Fig. 3.6.A) or with 5 μM TG for 1 hour (Fig. 3.6.B). Then cells were lysed and analysed by immunoblotting with mouse anti-V5 antibody (1: 5000) to detect the cleaved form of the ATF6 luminal domain, a C-terminal (ATF6-C), under non-reduced condition. The results of DTT treatment (Fig. 3.6.A) show that the wild type ATF6 was cleaved by S1P and S2P and generated the approximately 40 KDa monomer of the cleaved form of the ATF6-C, while ATF6(Y567N) mutant is clearly not showing the C-domain cleaved form. However, the ATF6(D564G) mutant is giving a band with similar size of the cleaved form, ATF6-C, with a bit faster mobility on the gel. It remains unclear whether the band that we obtained with DTT treatment is the cleaved form of ATF6 or not. However, it might be the cleaved form of ATF6 since the previous study showed that the natural mutant of ATF6 obtained from Achromatopsia patient does not fully lose the ability to traffic from the ER to the Golgi during ER stress (Chiang et al., 2017). Therefore, the strong ER stress inducer like DTT might still drive a small amount of our ATF6(D564G) mutant to move to the Golgi. This requires future experiments to prove and clarify.

The results of TG treatment (Fig. 3.6.B) show that in the non-reducing condition the wild type ATF6 was cleaved by S1P and S2P and produced the approximately 90 KDa dimer of the ATF6-C instead of the monomer form since TG induces ER stress without disrupting disulfide formation in the ER, while DTT induces ER stress with some disruption in the disulfides in the ER. For ATF6(Y567N) mutants, the result is clearly not showing the cleaved form of ATF6, either monomer or dimer. However, the result of ATF6(D564G) still shows the same unidentified band, which was seen in the DTT result previously, but no sign of the dimer of the ATF6-C as it found with wild type ATF6.

In addition, there is another interesting information obtained from the result of TG treatment. For the wild type ATF6, after cells were treated with TG to induce stress, there appeared two additional bands, migrating faster and slower than the dimeric form of ATF6 (Fig. 3.6.B, lane 2). The slower migration band, which found above the ATF6 dimer band, is likely to be another disulfide-bonded form of ATF6 since it can be seen in the result of the stressed ATF6(Y567N) mutant

too. However, the faster migrated band, which is found below the ATF6 dimer band, is only seen with the stressed wild type ATF6. Nevertheless, there is a possibility that this band might be another disulfide-bonded form of ATF6 as well. In addition, if the bands are in fact represent the disulfide-bonded forms of ATF6, the forms are likely to be a mixed disulfide complex between the ATF6 and catalytic enzymes in PDI or PDIR families such as ERp72, ERp57 and ERp18. To identified this, future study is required.

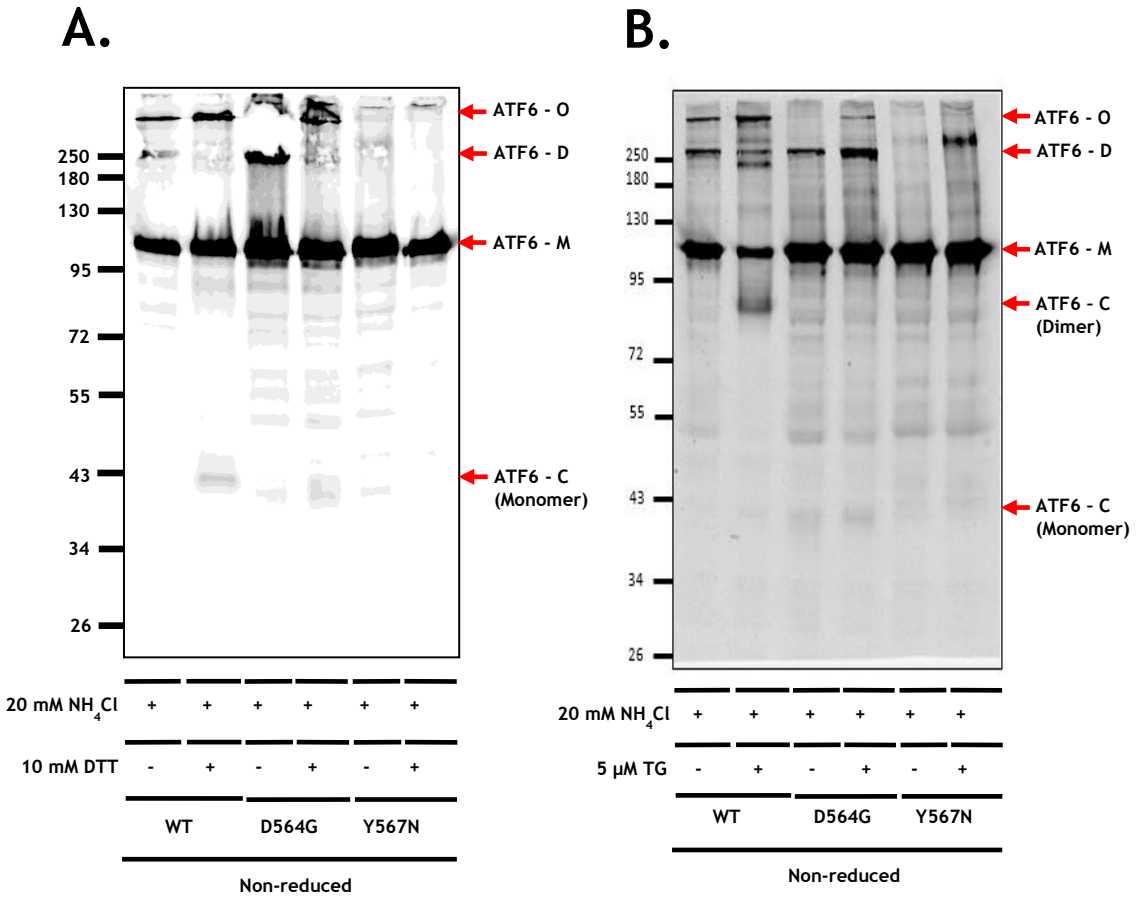

Fig. 3.6. The cleaved form of ATF6 generated by S1P and S2P proteases after ATF6 has migrated to the Golgi in the presence of ER stress. Recombinant HA- and V5-tagged ATF6; wild-type, D564G, and Y567N, were stable expressed in HEK-293 cells and then the cells were treated with 20 mM NH4Cl for 45 minutes and followed with 10 mM DTT for 30 minutes to induce ER stress **(A)** or with 5 µM TG for 1 hour **(B)**. Then cells were lysed and analysed by immunoblotting with mouse anti-V5 antibody (1: 5000) in the non-reduced condition. O = Oligomer, D = Dimer, M = Monomer, C = C-terminal/luminal domain.

To continue the investigation into the cleaved forms of ATF6 we needed to confirm whether the S1P and S2P proteases are able to cleave these mutants or not. We first measured the appearance of the cleaved form of the ATF6 cytosolic

domain, the N-terminal (ATF6-N), in a time-course (Fig. 3.7.A). The recombinant HA- and V5-tagged ATF6, wild-type, was stable expressed in HEK-293 cells and then the cells were treated with 100 µg/ml cycloheximide for 2 hours to inhibit protein synthesis so we can observe the cleaved form of ATF6 without confounding contributions from transcription or translation. Then, cells were treated with 5 µg/ml Brefeldin A for 0, 30, 60, 90, or 120 minutes to merge the Golgi to the ER so that S1P and S2P proteases can cleave ATF6 without trafficking or ER stress inducing. Cell lysates were precipitated by mouse anti-ATF6 antibody and analysed by immunoblotting with rabbit anti-HA antibody (1: 1000) in the non-reduced condition. The result shows that the cleaved form of the ATF6 cytosolic domain is produced after cells were treated with Brefeldin A for 60 minutes, so this specific time of Brefeldin A treatment will be used for following experiments. Second, we measured the cleaved form of the ATF6 luminal domain, the C-terminal (ATF6-C) (Fig. 3.7.B). The same cell-line expressed the recombinant HA- and V5-tagged ATF6, wild-type, which we used in the previous experiment, were used in this experiment again. Cells were treated with 100 µg/ml cycloheximide for 2 hours and followed with 5 µg/ml Brefeldin A for 0 and 60 minutes. Then the treated cells were collected and lysed. The protein lysate was precipitated by mouse anti-V5 agarose beads and analysed by immunoblotting with rabbit anti-V5 antibody (1: 5000) in the non-reduced condition. The data here (Fig. 3.7.B) shows similar pattern as seen in the result of TG treatment (Fig. 3.6.B) with the additional unknown bands at upper and lower position than the band of ATF6 dimer, however in this experiment the slower migration band, which was found above the ATF6 dimer band, is very faint and almost not detected. The dimer of the cleaved form of the ATF6 luminal domain is clearly detected after 60 minutes of Brefeldin A treatment too. Therefore, Brefeldin A treatment resulted in the same cleaved forms of ATF6, for both cytosolic and luminal domains.

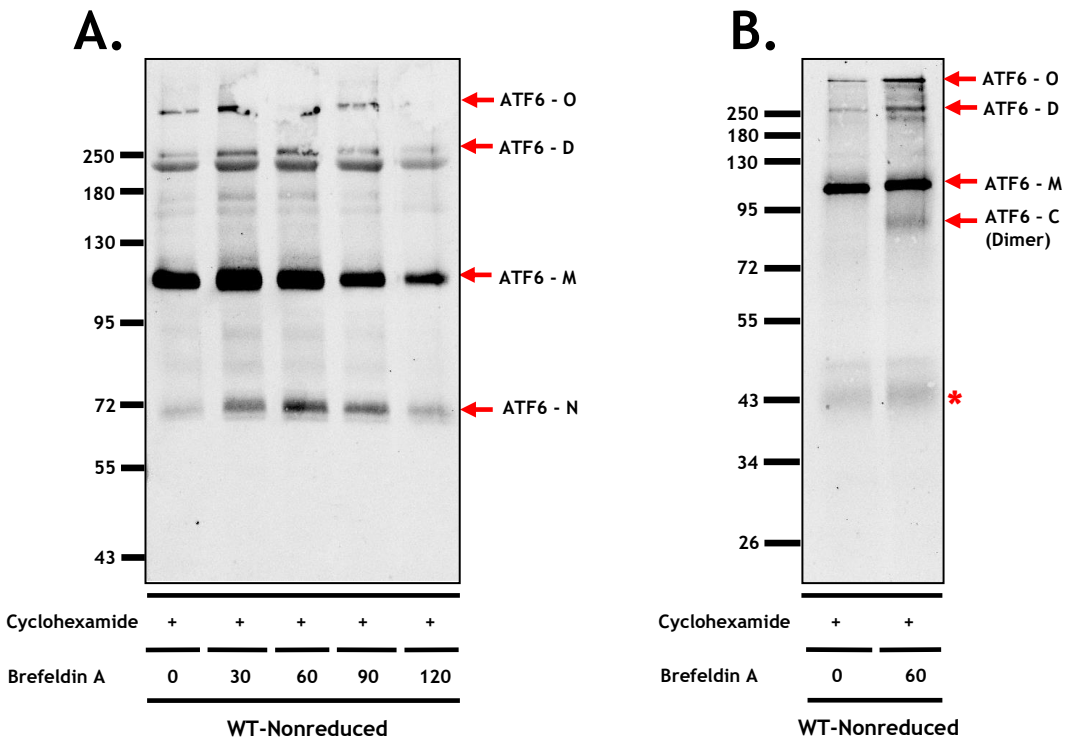

Fig. 3.7. The cleaved form of ATF6 generated by S1P and S2P proteases when the Golgi was merged with the ER by the inducing of Brefeldin A. **(A.)** The cleaved form of the ATF6 cytosolic domain, the N-terminal (ATF6-N). Recombinant HA- and V5-tagged ATF6, wild-type, was stable expressed in HEK-293 cells and then the cells were treated with 100 µg/ml cycloheximide for 2 hours and followed with 5 µg/ml Brefeldin A for 0, 30, 60, 90, or 120 minutes. The lysed cells were precipitated by mouse anti-ATF6 antibody and analysed by immunoblotting with rabbit anti-HA antibody (1: 1000) in the non-reduced condition. **(B.)** The cleaved form of the ATF6 luminal domain, the C-terminal (ATF6-C). Recombinant HA- and V5-tagged ATF6, wild-type, was stable expressed in HEK-293 cells and then the cells were treated with 100 µg/ml cycloheximide for 2 hours and followed with 5 µg/ml Brefeldin A for 0 and 60 minutes. The lysate cells were precipitated by mouse anti-V5 agarose beads and analyzed by immunoblotting with rabbit anti-V5 antibody (1: 5000) in the non-reduced condition. O = Oligomer, D = Dimer, M = Monomer, N = N-terminal/cytosolic domain, C = C-terminal/luminal domain, * = Background band.

We then carried out a similar experiment with the mutant forms of ATF6, for both ATF6(D564G) and ATF6(Y567N), to determine whether relocalisation of the S1P to the ER would result in cleavage (Fig. 3.8). The recombinant HA- and V5-tagged ATF6; wild-type, D564G, and Y567N, were stable expressed in HEK-293 cells. The cells were treated with or without? 30 µM S1P inhibitor for 60 mins, then treated with 5 µg/ml Brefeldin A for 0 and 60 minutes. The treated cells were lysed and immunoprecipitated with mouse anti-V5 agarose beads. Therefore,

the precipitated samples were analyzed by immunoblotting with rabbit anti-V5 antibody (1: 5000) under non-reducing conditions, as it was done in the previous experiment. The results showed that only the wild type ATF6 can form dimer after being cleaved by S1P protease when the Golgi was merged to the ER. Meanwhile, the ATF6(D564G) and ATF6(Y567N) mutants were cleaved, but only generated the monomeric form. When cells were treated with the S1P inhibitor prior to Brefeldin A, the cleaved bands of ATF6, both dimer and monomer, were not formed demonstrating that they were a result of S1P activity. To sum up, the mutants ATF6 still can be cleaved by S1P when the Golgi was merged to the ER by Brefeldin A, so the non-trafficking function of the mutants can be confirmed now, however the mutations appear to strongly effect the ATF6 disulfide formation which could be one reason preventing the mutant ATF6 from trafficking.

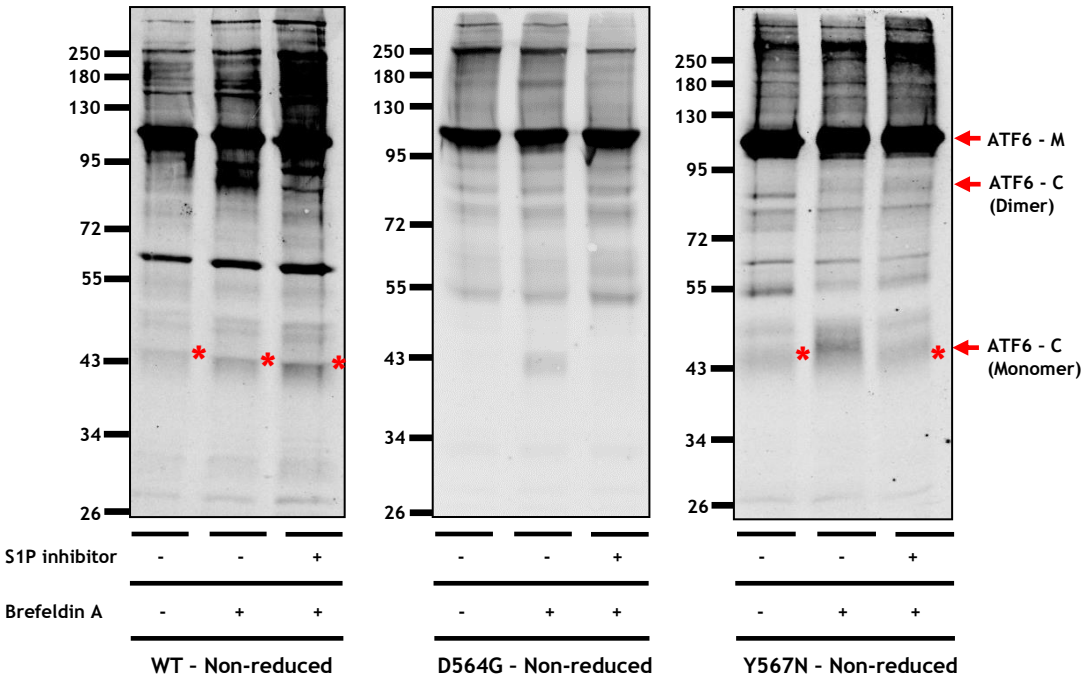

Fig. 3.8. The cleaved form of the ATF6 luminal domain generated by S1P and S2P proteases when the Golgi was merged with the ER by treatment with Brefeldin A. Recombinant HA- and V5-tagged ATF6; wild-type, D564G, and Y567N, were stable expressed in HEK-293 cells and then the cells were treated with or without 30 μM S1P inhibitor for 60 mins, then treated with 5 μg/ml Brefeldin A for 0 and 60 minutes. The lysate cells were precipitated by mouse anti-V5 agarose beads and analyzed by immunoblotting with rabbit anti-V5 body (1: 5000) in the non-reduced condition. M = Monomer, C = C-terminal/luminal domain. * = Background band.

3. 8. Chapter Discussion

Several ATF6 mutants have been studied and reported upon, both naturally originated and laboratory-synthetically generated. Several mutants also reportedly carried significant effects on the normal function of ATF6, mostly inhibiting or suppressing the ER stress response of ATF6 (Table. 3.1). The malfunction or non-function of ATF6 causes several diseases such as Achromatopsia, stroke, myocardial infarction, diabetes, inflammatory bowel disease, neurodegenerative diseases (Ranjan et al., 2021; Ghemrawi and Khair, 2020; Glembotski, Rosarda and Wiseman, 2020; Lee et al., 2020; Yang et al., 2019; Chianga et al., 2017). Related to the aim of our study, the phenotype of two specific point mutations of ATF6 luminal domain, which were found naturally occurring in the patients who suffer from Achromatopsia disease and have been reported to prevent the ATF6 migration from ER to Golgi (Chianga et al., 2017), were regenerated for our experiments. The first mutant is the point mutation of ATF6 at amino acid 564, which was changed from aspartic acid (D) to glycine (G), also known as ATF6(D564G). The second mutant is the mutant of amino acid 567 from tyrosine (Y) to asparagine (N), this mutant also known as ATF6(Y567N). Using these specific mutants in our study, we can confirm that ATF6(D564G) and ATF6(Y567N) mutants can suppress the trafficking of ATF6 in the presence of ER stress (Fig. 3.3 and 3.4), as it was reported (Chianga et al., 2017). Moreover, despite the mutation point of ATF6(D564G) and ATF6(Y567N) mutant are located only a few amino acids apart, our study found that the expression of these two mutants is significantly different, since the ATF6(Y567N) only appeared as a monomer without the disulfide-bonded dimer or oligomer formation. Meanwhile, the ATF6(D564G) shown all of redox forms, monomer, dimer and oligomer, however in the non-stressed condition the dimer form of ATF6(D564G) is significantly increasing compared to the wild type ATF6 (Fig. 3.2). These mutations are obviously disrupted in their formation of the disulfide bond on the luminal domain of ATF6. It still remains unclear how these point mutations affect disulfide formation, however it might have disrupted the conformation of ATF6 protein and made ATF6 to become misfolded. Hence, the misfolded ATF6 is losing the ER stress response function as a result. This might be one of the reasons that we still found the interaction between BiP and the mutants ATF6, since a common

function of BiP is binding with the misfolded proteins which appear in the ER lumen.

BiP is well known as an initiation of UPR process, the releasing of BiP upon ER stress will lead to the downstream responses of the UPR mediators like ATF6. The mechanism of BiP dissociation from ATF6 remains unclear, however, some studies suggested that the presence of the unfolded/misfolded protein upon ER stress or the presence of ATP alone, are insufficient to drive the departer of BiP from ATF6 (Schindler and Schekman, 2009; Shen et al., 2005). In addition, BiP can be modified to a disulfide form or sulfenylated by some ER oxidoreductase such as PDIR. This thiol modification of BiP had reported to strongly affect the stability of BiP-ATF6 complex (Wang and Sevier, 2016; Higa et al., 2014; Wei et al., 2012). However, according to the recent report of Oka in 2019, they found that upon the released of BiP, ATF6 still remains in the ER by binding to a member of the PDI family like ERp18. Since ERp18 is also an ER oxidoreductase and has function as a disulfide exchange (Jeong et al., 2008), therefore, ERp18 is likely to form mixed disulfides with ATF6 and change the disulfide formation within the luminal domain of ATF6 to the appropriated form which could be packed into COP II vesicle and moved to the Golgi (Oka et al., 2019). Thereby, the presence of ERp18 here might play an important role in the retention of the ATF6 mutants in the ER after the releasing of BiP during stress, since our study clearly shows the dissociation of BiP from the ATF6 mutants, however, the mutants still remained non-trafficking (Fig. 3.5). This result underlines that the departure of BIP is not sufficient enough to drive the trafficking process of ATF6 or the downstream response of ATF6 branch upon ER stress because we did not detect the Golgi form of the ATF6 mutants or the cleaved forms that would have been generated by S1P and S2P proteases in the Golgi apparatus (Fig. 3.3 and 3.6). Accordingly, additional factors like ERp18 are required after the releasing of BiP, so the ATF6 could be packaged into COP II vesicle. Moreover, the different conformation of ATF6 mutants from the wild type might also affect the interaction between the mutants and other proteins such as ERp18, hence the mutants cannot be modified and exit the ER in the presence of ER stress.

The reduced monomer of ATF6 is reported as a required form to exit the ER and to move to the Golgi during the UPR, and also the most preferable form

for the S1P cleavage (Sato et al., 2011; Nadanaka et al., 2007). In the absence of ER stress, the wild type ATF6 is found as monomer, dimer, and oligomer by forming intra- and/or inter-molecular disulfide bonds, between the two cysteine residues in the luminal domain. All of these redox forms of ATF6 are retained in the ER lumen by binding with BiP. Meanwhile, in the presence of ER stress, after the releasing of BiP, it was assumed that the different forms of ATF6 will be reduced to monomers by the ER oxidoreductase enzymes before trafficking to the Golgi to continue the UPR process (Oka et al., 2019; Nadanaka et al., 2007; Shen et al., 2002). However, in contrast to the previous knowledge, the results of our study suggested that the monomeric form of ATF6 is not the most preferable form for S1P and S2P cleavage, since we detected the dimeric form of the wild type ATF6 luminal domain as a result of S1P and S2P cleavage rather than seeing the monomeric form when we treated cells with TG to induce stress or merged the Golgi to the ER by Brefeldin A (Fig. 3.6.B and 3.7). Meanwhile, the non-trafficking mutants ATF6 only generated the monomeric form after the cleavage by S1P and S2P, when we merged the Golgi to the ER, despite that fact that the ATF6(D564G) mutant can form the dimer and oligomer like the wild type ATF6 (Fig. 3.8). We do not know why the ATF6(D564G) mutant only generated the monomeric ATF6 luminal domain after the cleavage by S1P and S2P. Nevertheless, it is clear that the S1P could recognize and cleave both dimeric and monomeric forms of ATF6. In addition, according to this result, the monomer is also not likely to be the form of ATF6 that could exit the ER during the time of the UPR as previously thought (Nadanaka et al., 2007). Our results suggested that the dimeric form of the wild type ATF6 is more likely to be the form that exits the ER during stress activation rather than the monomer, since the wild type ATF6 only produced the dimeric form of the luminal domain after S1P and S2P cleavage when cells were treated with TG (Fig. 3.6.B).

It is already reported for quite long time that the luminal domain of ATF6 has two conserved cysteine residues at amino acid 467 and 618 involved in disulfide formation. However, only recent studies demonstrated that the oligomeric and the dimeric form of ATF6 are in fact both dimers with the differentiated by electrophoretic mobility. The band that we previously considered as oligomeric form of ATF6, is in fact a dimer stabilised by an interchain disulfide between C467 residues, meanwhile, the dimer is stabilized by

a C618 interchain disulfide (Koba et al., 2020; Oka et al., 2019; Nadanaka et al., 2007). Moreover, the dimer (C618-dimer) of ATF6 is a minor form compared to the oligomer (C467-dimer) (Koba et al., 2020; Oka et al., 2019). According to this information, the unknown bands that appeared upper and lower the dimeric (C618-dimer) band of wild type ATF6 when cells were induced ER stress by TG (Fig. 3.6.B), could be the result of a mixed disulfide formed between C618 and C467 residues of ATF6 or between the ATF6 molecule and the disulfide exchange protein(s).

According to the information from other studies and from our investigation, BiP releases prior to redox modification of ATF6, with the luminal domain of ATF6 forming a dimer catalysed by ER oxidoreductase enzymes in the PDI family. This change seems to be a critical stage of the ATF6 stress response and trafficking. The disruption of this process by the mutation of ATF6 may be one of the causes of the defective trafficking of these ATF6 mutants.

CHAPTER IV: RESULTS SECTION 2 - The identification of proteins in complex with ATF6

4. 1. Isolation of ATF6 protein complex

The trafficking of ATF6 following ER stress from the ER to the Golgi is a complex process that potentially requires a number of additional factors, for instance, ATP, COPII cargo receptor, protein disulfide isomerases (PDI), and thrombospondin (Thbs). ATP has been identified to be required for protein quality-control by BiP, therefore a lack of ATP inhibits the dissociation of BiP from ATF6 under stress conditions (Vishnu et al., 2014; Mirazimi and Svensson, 2000; Dorner and Kaufman, 1994; Braakman, Helenius, and Helenius, 1992). However, our studies in the previous chapter suggested that the dissociation of BiP-ATF6 complex does not mean that ATF6 will translocate to the Golgi or undergo proteolysis. These results are supported by previous studies (Nadanaka et al., 2004; Antonny and Schekman, 2001). Moreover, to package into COP II vesicle, the rearrangement of ATF6 disulfide bonds is likely to be an important requirement and maybe facilitated by proteins in PDI family such as the protein disulfide isomerase A5 (PDIA5 or PDIR) and ERp18 (Oka et al.,2019; Higa et al., 2014; Schindler and Schekman, 2009; Nadanaka et al., 2007; Nadanaka et al., 2004). Specifically, proteins in the PDI family participate in inter- and intra-molecular disulfide bonds rearrangement to activate ATF6 in the UPR. In addition, the vesicle packaging of ATF6 is also reported to involve proteins in the thrombospondin (Thbs) group, the common one being Thbs4 which binds to the luminal domain of ATF6 and promotes vesicle formation, and the migration of ATF6 to the Golgi (Brodya et al., 2016; Lynch et al., 2012). Despite the identification of some components, the mechanisms underlying these processes remain elusive, and it is likely that additional proteins participate in this process. Therefore, our next series of experiments were aimed at identifying the protein complex of ATF6 in the resting condition and during stress. Here we use our non-trafficking mutants of ATF6, D564G and Y567N. The result of this study should provide a clearer idea of the identity of proteins which participate in ATF6 retention and trafficking. The promising proteins found in this analysis will also form the basis for future experiments to verify their interaction with core proteins namely ATF6 and BiP.

First, to study the ATF6 protein complex we carried out sucrose gradient centrifugation of cell lysates to separate the complexes with different molecular weights, containing different proteins. Analysing the protein complexes could help us determine the composition of ATF6 protein complexes in different cell types and conditions and indicate possible changes to protein components in the ATF6 complex, despite this, surprisingly there was no report based on the sucrose gradient separation up until now. According to the knowledge of the interaction and dissociation of ATF6 with different proteins before and after the presence of ER stress, we expected that there might be some specific pattern of ATF6 proteins complexes, when cells expressed wild type or mutants ATF6, are treated with and without ER stress inducer such as DTT. Therefore, we can use the complex distribution from this experiment as a reference for other experiments to identify specific proteins which are interacting with ATF6. Thus, the recombinant HA- and V5-tagged wild-type ATF6 and ATF6(D564G) plasmid were expressed in HEK-293 cells and then the cells were treated with 10 mM DTT for 30 minutes to induce ER stress. The treated cells were lysed, and total cell lysates were separated by sucrose gradient centrifugation with sucrose density from 5% to 45%. After centrifugation, the protein fractions were collected and precipitated with acetone. Thereafter, protein was analyzed by immunoblotting with mouse anti-V5 and mouse anti-BiP antibody (Fig. 4.1) or with mouse anti-HA antibody under reducing conditions (data not shown). Results show that there was a lot of variation between each experiment, so it was hard to define a common pattern with an acceptable accuracy. The results that are shown here are only one example from several experiments we have done. Hence, sucrose gradient centrifugation with a lot of different separated fractions might not be an ideal method to identify the complex of ATF6, but the results still show a distinctive difference between wild type and mutant ATF6(D564G). Accordingly, in figure 4.1. for the wild type, the density of ATF6 band was significantly decreased after fraction 8 and then reappeared in fraction 13. Meanwhile, in the mutant cells the density of ATF6 band was significantly decreased only after fraction 12. In addition, BiP band also appeared differently between wild type and mutant. For the wild type, BiP quickly disappeared after fraction 6, when the band in mutant cells was shown until fraction 12-13. Therefor it is clearly suggested that the wild type ATF6 and the mutant ATF6 are formed the protein complex differently and this could be affected an ability of trafficking and non-trafficking of the wild type

and mutant ATF6. However, when compared the stress induced to the noninduced, it shown only a little shifting of the protein bands, specifically in the wild type cells.

Hence, we can conclude that the wild type and the mutant ATF6 are likely to form a complex with distinct proteins and for the wild type there are also slight shifts of the protein members in the complex when cells are exposed to stress. The shifting of the protein members in the complex was also seen between the cells at steady state and the cells exposed with stress. Therefore, the dissociation and/or the association of specific proteins in the ATF6 complex are important for the downstream response of ATF6 towards stress. Moreover, for the wild type ATF6, there seems to be two complexes centered on fractions 7 and 13. Meanwhile, the mutant has a broader separation centered around fraction 8. In addition, BiP seems to be associated with the mutant ATF6 complex throughout the gradient but prominently with more dense fractions than the wild type ATF6 complex.

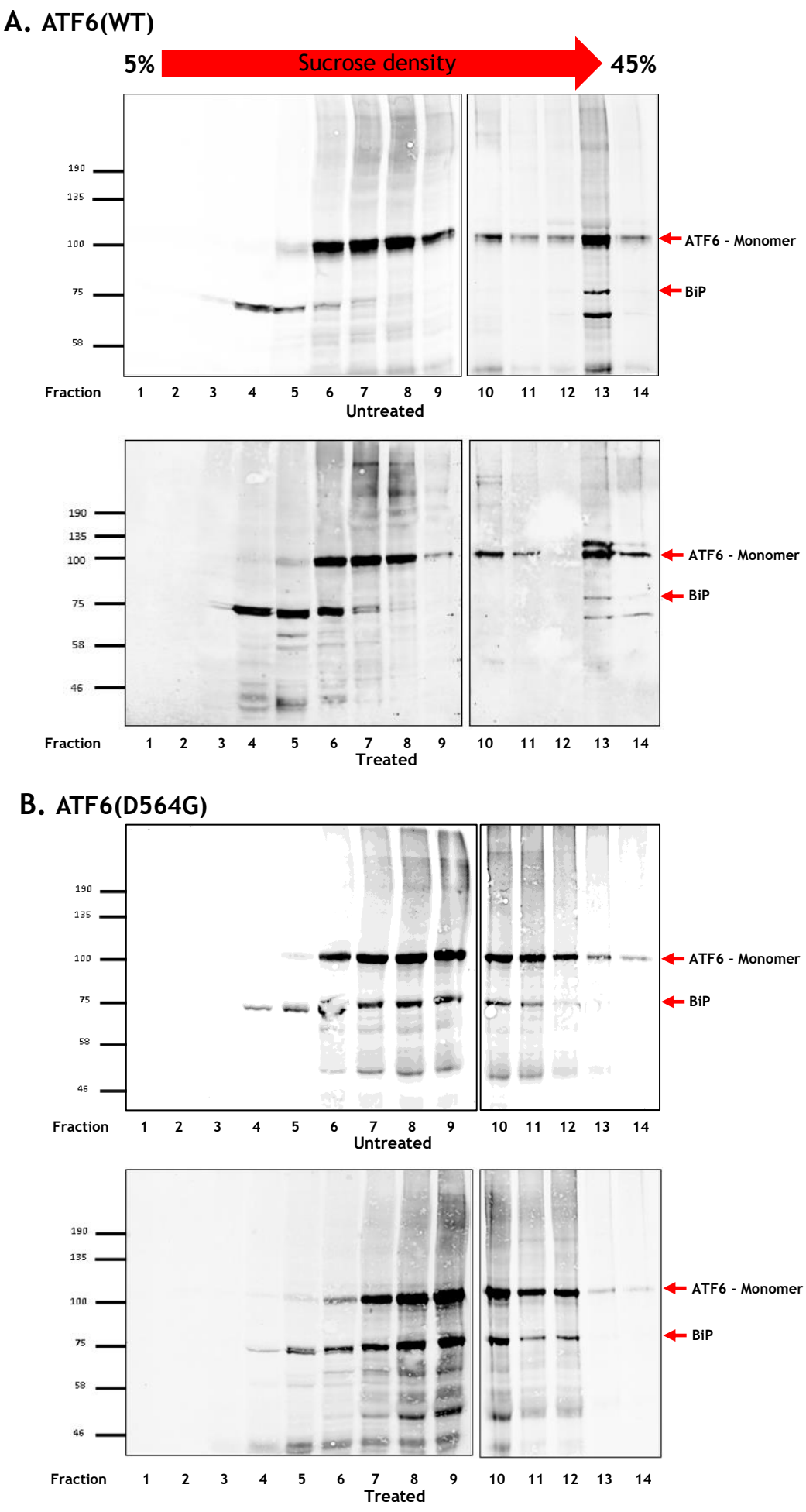
A. ATF6(WT)
5%
Sucrose density
45%
190
135
100
75
58
ATF6 - Monomer
BiP
Fraction 1 2 3 4 5 6 7 8 9 10 11 12 13 14
Untreated
190
135
100
75
58
46
ATF6 - Monomer
BiP
Fraction 1 2 3 4 5 6 7 8 9 10 11 12 13 14
Treated
B. ATF6(D564G)
190
135
100
75
58
46
ATF6 - Monomer
BiP
Fraction 1 2 3 4 5 6 7 8 9 10 11 12 13 14
Untreated
190
135
100
75
58
46
ATF6 - Monomer
BiP
Fraction 1 2 3 4 5 6 7 8 9 10 11 12 13 14
Treated

Fig. 4.1. The isolated protein complex of ATF6 in the presence of ER stress. Recombinant HA- and V5-tagged wild-type ATF6 (**A.**) and ATF6(D564G) (**B.)** were expressed in HEK-293 cells and then treated with 10 mM DTT for 30 minutes to induce ER stress. The treated cells were lysed, and total cell lysates were separated by sucrose gradient centrifugation protocol with sucrose density from 5% to 45%. After centrifugation, the protein fractions were collected and precipitated with acetone. Thereafter, protein complexes were analyzed by immunoblotting with mouse anti-V5 (1:5000) and mouse anti-BiP (1:250) under reducing conditions.

4. 2. Identifying-protein partners which associate with ATF6 during ER stress

The sucrose gradient method in the previous experiment might be not a suitable method to separate the protein complex of ATF6, however it still gives us a broad range idea about the possibility of the complex formation of ATF6 with the other proteins before and after stress. Now we known that ATF6 is likely to form a complex differently with and without stress, and also forming it differently between the wild type and the mutant ATF6. The different complex formation of the mutant ATF6 from the wild type might be the result of the unusual conformation of the mutant which we already saw from the experiments in the previous chapter. Here we continued to investigate the complex of ATF6 by using the more sensitive method for proteins detection and identification, a mass spectrometry analysis. For these experiments un-transfected HEK-239 cells, as well as stable cell-lines expressing the non-trafficking mutants ATF6, ATF6(D564G) and ATF6(Y567N), were used to identify the partner proteins of ATF6 in non-stressed and stressed conditions. Cells were treated with or without thapsigargin for 1 hour to induce ER stress before performing crosslinking with Dithiobis(succinimidyl propionate) (DSP), an amine-specific thiol-cleavable crosslinking reagent, to ensure that even weak interacting proteins were captured together with the ATF6. Subsequently, the ATF6 complexes were immunoisolated with anti-V5 agarose beads from the whole cell lysate. We used anti-V5 agarose beads in this step, so we capture only the exogenous ATF6 with the V5 tag on the C-terminus and not the endogenous ATF6. The interacting proteins were eluted from the beads by using the reducing reagent DTT that cleaves the crosslinker. Finally, the eluted proteins were sent for analysis by mass spectrometry. Raw data file of mass spectrometry analysis shown list of proteins contained in a sample along with other information such as number of sequences of each protein in a

sample, data base used to analyse protein sequences, and emPAI (Table. 4.1.A). The experiment was carried out three times and the proteins consistently observed. Only the proteins were present in ATF6(D564G) and ATF6(Y567N) samples, and not in the control samples from untransfected HEK293 cells, will be listed.

Proteins, that were identified specifically interacting with the mutants ATF6 after comparison with the untransfected HEK-239 cells, are listed along with emPAI and the % coverage (Table. 4.1.C). The data shows that there are several proteins which have a potential to control ATF6 trafficking, most of them are ER proteins with a role in protein folding and modification processes, such as BiP, Grp94, the protein disulfide isomerases in the PDI family, glycoprotein quality control proteins, and calcium binding proteins in the CREC family (Oka et al., 2018; Higa et al., 2014; Honore, 2009; Jeong et al., 2008). When we compared the data that we obtained (Table. 4.1.C) to the data of the wild type ATF6 obtained from a previous study of my colleague in our laboratory (Table. 4.1.B) (Oka et al., 2018), 14-3-3 protein epsilon (14-3-3E), TRK-fused gene protein (protein TFG), Neudesin and the DnaJ homolog subfamily B member 11 (DNAJB11 or ERdj3) were chosen as the identified proteins with the most potential role as ATF6 trafficking control factors (Hanafusa, Wada, and Hosokawa, 2019; Romine and Wiseman, 2019; Pennington et al., 2018; Kanadome et al., 2017; Genereux et al., 2015; Johnson et al., 2015; Beetz et al., 2013). Therefore, these proteins were analysed further to confirm their interaction with ATF6 and to determine their role in ATF6 trafficking.

A.

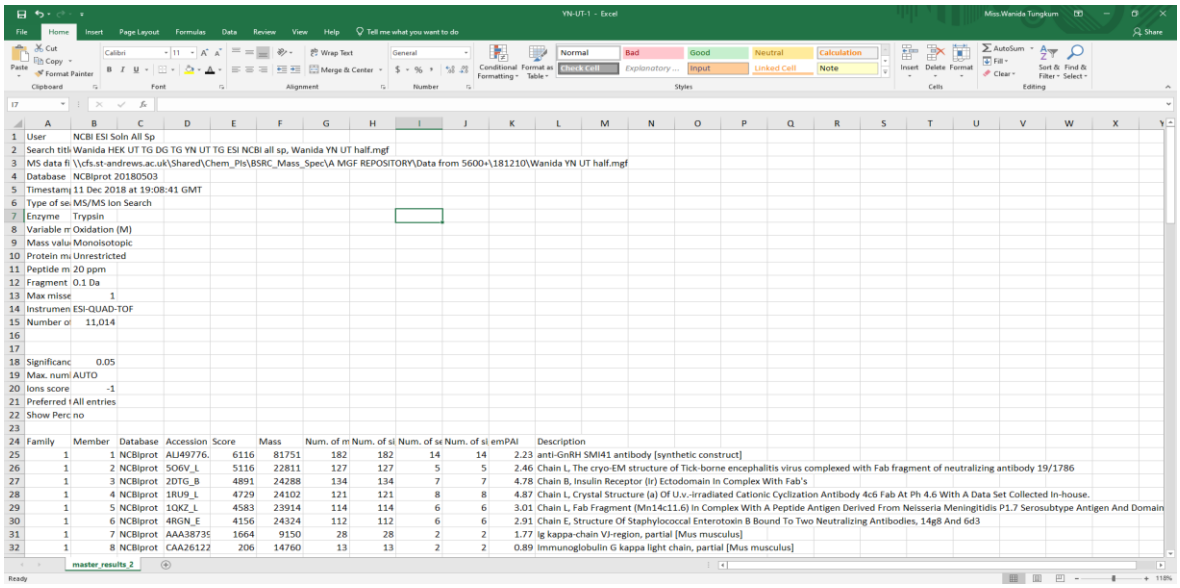

Family	Member	Database	Accession	Score	Mass	Num. of m	Num. of si	Num. of se	Num. of si	emPAI	Description
1	1	NCBIprot	AU49776.	6116	81751	182	182	14	14	2.23	anti-GnRH SMI41 antibody [synthetic construct]
1	2	NCBIprot	5O6V_L	5116	22811	127	127	5	5	2.46	Chain L, The cryo-EM structure of Tick-borne encephalitis virus complexed with Fab fragment of neutralizing antibody 19/1786
1	3	NCBIprot	2DTG_B	4891	24288	134	134	7	7	4.78	Chain B, Insulin Receptor (Ir) Ectodomain In Complex With Fab's
1	4	NCBIprot	1RU9_L	4729	24102	121	121	8	8	4.87	Chain L, Crystal Structure (a) Of U.v.-irradiated Cationic Cyclization Antibody 4c6 Fab At Ph 4.6 With A Data Set Collected In-house.
1	5	NCBIprot	1QKZ_L	4583	23914	114	114	6	6	3.01	Chain L, Fab Fragment (Mn14c11.6) In Complex With A Peptide Antigen Derived From Neisseria Meningitidis P1.7 Serosubtype Antigen And Domain
1	6	NCBIprot	4RGN_E	4156	24324	112	112	6	6	2.91	Chain E, Structure Of Staphylococcal Enterotoxin B Bound To Two Neutralizing Antibodies, 14g8 And 6d3
1	7	NCBIprot	AAA38735	1664	9150	28	28	2	2	1.77	Ig kappa-chain VJ-region, partial [Mus musculus]
1	8	NCBIprot	CAA26122	206	14760	13	13	2	2	0.89	Immunoglobulin G kappa light chain, partial [Mus musculus]

B.

	ATF6(WT)		ATF6(WT) +Thapsigargin	
Protein	**%coverage**	**emPAI**	**%coverage**	**emPAI**
BiP	41	2.94	42	4.12
Grp94	29	0.98	26	0.58
Calreticulin	17	0.1	0	0
Erp72	39	2.01	37	0.79
P5	34	1.04	36	1.26
Grp170	3	0.04	0	0
Erp57	31	1.19	26	0.69
Cyclophilin B	30	0.86	32	0.86
Reticulocalbin-1	10	0.13	0	0
Reticulocalbin-2	5	0.14	0	0
Erp29	20	0.38	11	0.38
Calumenin	10	0.14	6	0.14
Glucosidase 2 subunit beta	7	0.08	6	0
PDI	14	0.18	26	0.18
VCP	3	0.05	10	0.11
Erp18	0	0	13	0.28
Ero1	6	0.11	6	0.11
Urotensin-2 isoform b	6	0.38	6	0.38
Peroxiredoxin-4	9	0.17	16	0.17

C.

	ATF6(D564G)		ATF6(D564G) +Thapsigargin		ATF6(Y567N)		ATF6(Y567N) +Thapsigargin	
Protein	**%coverage**	**emPAI**	**%coverage**	**emPAI**	**%coverage**	**emPAI**	**%coverage**	**emPAI**
BiP	44	3.57	28	1.87	47	4.97	33	2.32
Grp96	30	2.21	23	1.46	16	0.79	7	0.31
Calreticulin	39	1.69	2	0.1	24	1.21	0	0
Erp72	49	4.49	20	1.05	31	1.86	7	0.39
P5	30	1.41	16	0.64	35	2.97	23	1.2
Peroxiredoxin-1	0	0	36	4.5	31	5.78	34	5.78
Erp57	28	1.98	0	0	13	1.32	0	0
Cyclophilin B	22	2.3	25	1.7	41	5.02	25	1.73
14-3-3E	41	3.32	11	0.63	47	4.99	8	0.39

Protein canopy homolog 2	31	1.5	5	0.26	5	0.26	0	0
Erp29	12	0.63	4	0.18	12	0.64	0	0
ERdj3	11	0.42	5	0.26	18	0.8	7	0.43
Glucosidase 2 subunit beta	9	0.49	5	0.27	9	0.5	1	0.08
PDI	9	0.52	8	0.4	0	0	5	0.28
Calnexin	8	0.42	0	0	7	0.33	0	0
Erp18	7	0.28	0	0	8	0.28	0	0
Ero1	6	0.24	4	0.24	8	0.3	0	0
Protein TFG	0	0	4	0.24	14	0.39	4	0.12
Neudesin	0	0	5	0.28	0	0	5	0.28
PDIR	9	0.52	8	0.4	32	1.53	33	2.32
Peroxiredoxin-4	14	1.16	0	0	7	0.37	0	0
ARMET	3	0.97	0	0	4	0.98	0	0
Grp170	2	0.09	0	0	3	0.16	0	0

Table. 4.1. The crosslinked proteins which interacted with ATF6 during thapsigargin-induced ER stress. The table demonstrates percent coverage and emPAI values of the proteins from Mass Spectrometry analysis. ATF6(WT) + Thapsigargin, ATF6(D564G) + Thapsigargin and ATF6(Y567N) + Thapsigargin indicate that cells were treated with 5 μM Thapsigargin for 1 hour before crosslinking. **(A.)** An Excel table, example of raw data of mass spectrometry analysis with list of proteins contained in the sample. **(B.)** Data obtained by my colleague Dr. Ojore Oka (Oka et al., 2019). **(C.)** Data obtained by myself.

4. 3. The interaction of specific proteins in the ATF6 protein complex

Based on the information that we obtained from the mass spectrometry analysis, we were able to establish a list of proteins which were identified as members of an ATF6 protein complex that maybe involved with the regulation of ATF6 trafficking and/or retention. The list of the proteins which we investigated further included 14-3-3E, protein TFG, Neudesin, and ERdj3. These protein candidates were chosen because ERdj3 and protein TFG are already shown some recognition role involved with the ER stress response, meanwhile, 14-3-3E and Neudesin were a high possibility candidate with a broad range of unidentified roles in cells (Hanafusa, Wada, and Hosokawa, 2019; Romine and Wiseman, 2019; Pennington et al., 2018; Kanadome et al., 2017; Genereux et al., 2015; Johnson et al., 2015; Beetz et al., 2013). For this experiment, the wild type ATF6 and the non-trafficking mutants ATF6; ATF6(D564G) and ATF6(Y567N), which were stably

expressed in HEK-239 cells, were used to examine the interaction of the interested proteins with ATF6 during ER stress. Cells were treated with or without 5 μM TG for 1 hour to induce ER stress before performing the crosslinking with DSP to ensure that even the weak interacting proteins were captured. The whole cells lysate was pre-cleared with 10% protein-A sepharose (PAS) beads and the ATF6 complexes were immunoisolated from the whole cell lysate by using mouse anti-V5 conjugated agarose beads. Subsequently, a lysis buffer containing 0.1% SDS was used in the washing step, then the interacting proteins were eluted by using the reducing reagent DTT. The eluted proteins were analysed by western blot with anti-14-3-3E, anti-ERdj3, anti-neudesin, or anti- protein TFG antibody. Unfortunately, the first attempt at our investigation showed no promising results. For 14-3-3E and ERdj3, we obtained positive results, but 14-3-3E antibody has very high background, meanwhile ERdj3 band was very faint to almost not be able to recognize. Thus, it is hard to conclusively interpret this initial experiment. Simultaneously, the results of neudesin and TFG did not indicate their presence in complex with ATF6 (Fig. 4.2.A).

To make sure the results we obtained here are not due to the approach taken, the same membrane that we were used to blot with anti-14-3-3E, anti-TFG, anti-neudesin, or anti-ERdj3 were re-blotted with anti-BiP. In addition, P5 protein also was used as another positive control besides BiP since both P5 and BiP are already confirmed as members of ATF6 protein complex and was detected previously following crosslinking and immunoprecipitation (Oka et al., 2018). The results of this re-blotting experiment show the presence of both BiP and P5 in the immunoisolated ATF6 complex (Fig. 4.2.B). Hence, we are assured that the approach is working, and we can have confidence that our immunoisolated ATF6 should contain the proteins identified by mass spectrometry. Therefore, the next step is to confirm the non-detection of our interested proteins.

Next, we repeated the crosslinking and immunoprecipitation experiment with some changes in our method, and focused on only one protein, ERdj3, at this time. ERdj3 was selected as a main focus here instead of the other three proteins, since it was reported to be involved with the UPR regulation by playing a role as a BiP co-factor. Recent studies suggested that ERdj3 assisted and helped BiP to interact with unfolded proteins after BiP dissociates from the UPR reporters such

as ATF6 (Hanafusa, Wada, and Hosokawa, 2019; Romine and Wiseman, 2019; Genereux et al., 2015; Shen and Hendershot, 2005). In this experiment, first, wild type ATF6 cells were treated with TG and we performed crosslinking with DSP as the original method, then the treated cells were lysed. Thereafter the cell lysate was not precleared before immunoprecipitation and the immunoprecipitated ATF6 protein complex was washed with immunoprecipitation buffer in the absence of 0.1% SDS before elution with DTT. This time we demonstrated the presence of ERdj3 in the immunoisolated ATF6 (Fig. 4.1.C). These results indicate that the number of interacting proteins is low and can only be verified by western blotting when a less stringent approach is taken.

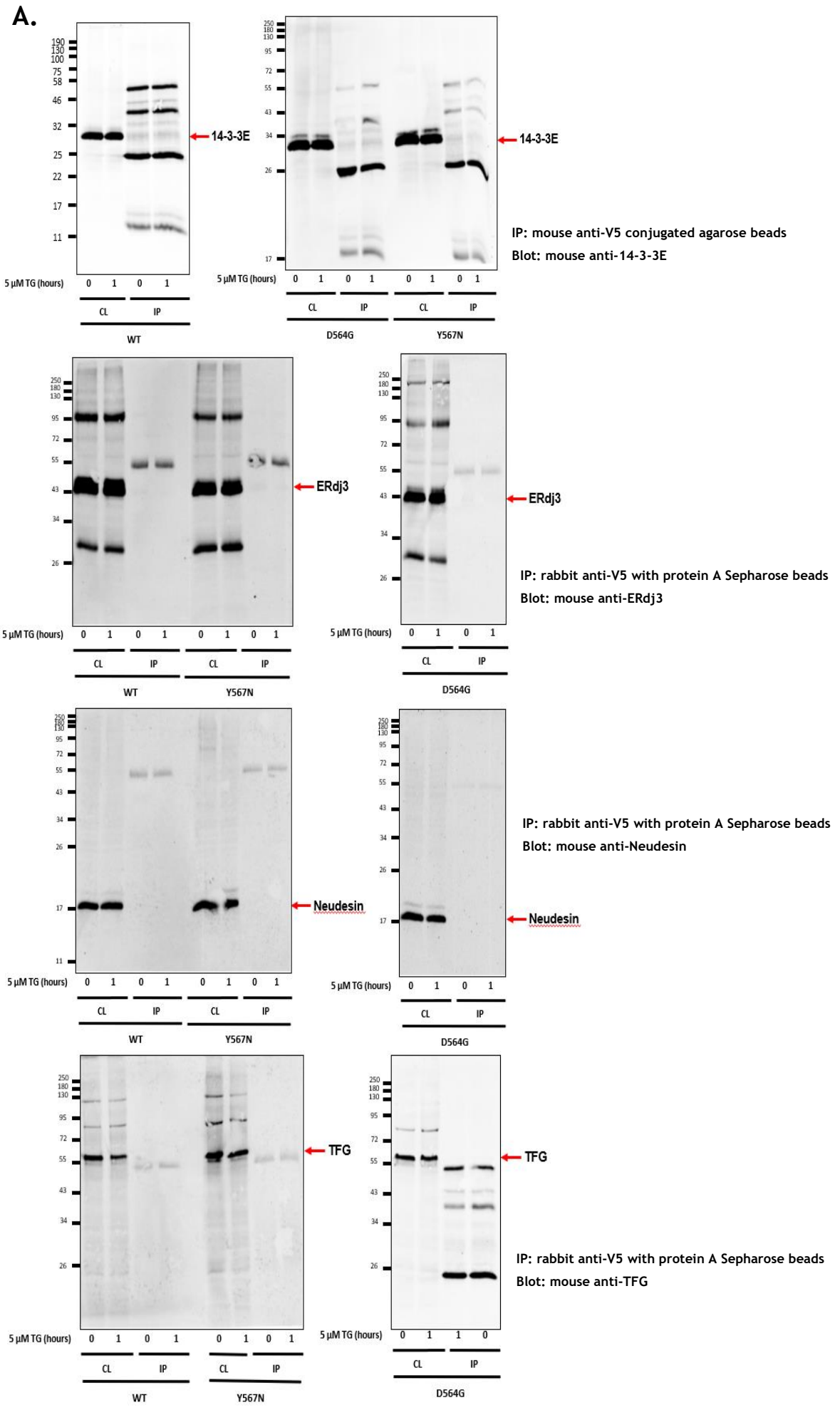
A.
14-3-3E
14-3-3E
IP: mouse anti-V5 conjugated agarose beads
Blot: mouse anti-14-3-3E
5 µM TG (hours)
CL
IP
WT
D564G
Y567N
ERdj3
ERdj3
IP: rabbit anti-V5 with protein A Sepharose beads
Blot: mouse anti-ERdj3
Neudesin
Neudesin
IP: rabbit anti-V5 with protein A Sepharose beads
Blot: mouse anti-Neudesin
TFG
TFG
IP: rabbit anti-V5 with protein A Sepharose beads
Blot: mouse anti-TFG

B.

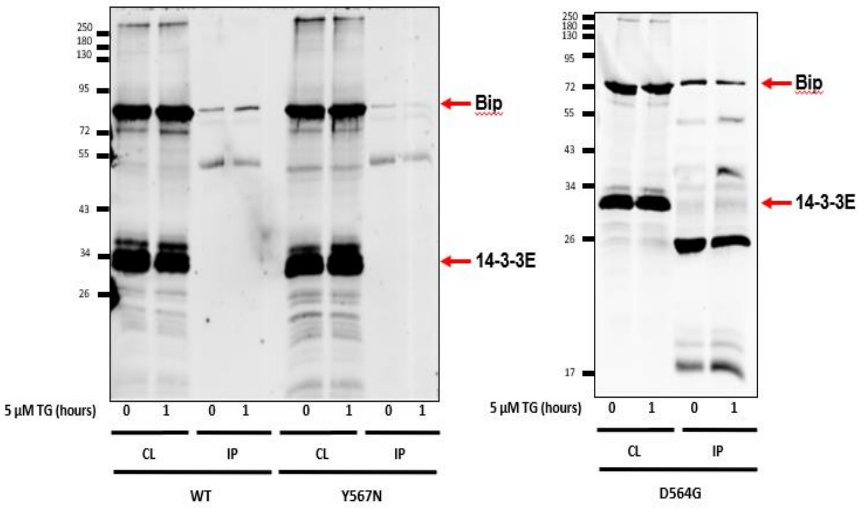

IP: mouse anti-V5 conjugated agarose beads (D564G) or rabbit anti-V5 with protein A Sepharose beads (WT and Y567N)

Blot: mouse anti-BiP

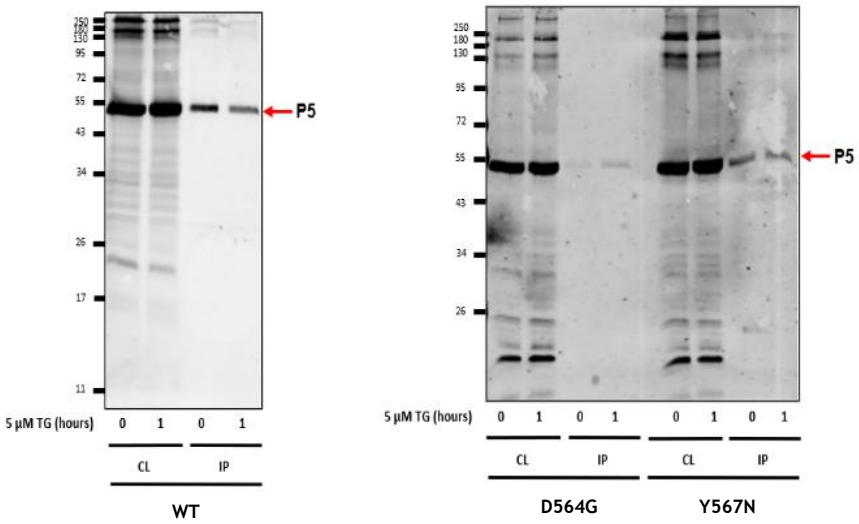

IP: rabbit anti-V5 with protein A Sepharose beads

Blot: rabbit anti-P5

C.

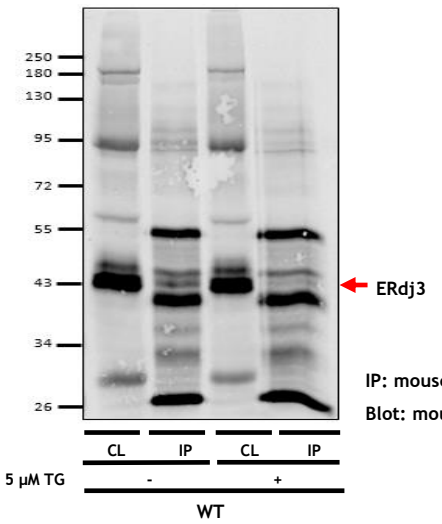

IP: mouse anti-V5 conjugated agarose beads

Blot: mouse anti-ERdj3

Fig. 4.2. The association of 14-3-3E, ERdj3, Neudesin, and TFG with ATF6 during the presence of ER stress. Recombinant HA- and V5-tagged wild-type ATF6, ATF6(D564G), and ATF6(Y567N) were stably expressed in HEK-293 cells, and then were treated either with or without 5 μM thapsigargin for 1 hour before crosslinking. After that, the whole cell lysates were immunoprecipitated by using standard protocol with pre-clear step and using lysis buffer with 0.1% SDS in the washing step **(A.)** and **(B.)**, or immunoprecipitated by using modified protocol without pre-clear step and using IP buffer instead of lysis buffer with 0.1% SDS in the washing step **(C.)**, followed by immunoblotting with mouse anti-14-3-3E (1:1000), mouse anti-ERdj3 (1:250), mouse anti-Neudesin (1:1000), mouse anti-TFG (1:1000), mouse anti-BiP (1:250), or rabbit anti-P5 (1:500) antibodies in the reduced condition. CL = Total cells lysate sample, IP = Immunoprecipitation sample.

4. 4. The interaction of ERdj3 with ATF6

Following the previous experiment, we decided to focus on ERdj3 rather than all four proteins at the same time. Several proteins in the ERdj family were reported as BiP co-factors which stimulate the interaction of BiP and the unfolded proteins, and some of ERdjs even binding directly to the unfolded protein clients (Pobre, Poet, and Hendershot, 2018). However, only Erdj3 is found in the results of our mass spectrometry analysis. Therefore, the protein has a high potential for a role in regulating the ATF6 trafficking process as well. In this experiment, the HA and V5 conjugated wild type ATF6 and the non-trafficking mutants ATF6; ATF6(D564G) and ATF6(Y567N), which were stably expressed in HEK-239 cells were used to investigate the interaction of ERdj3 with ATF6 during ER stress. Cells were treated with or without 5 μM TG for 1 hour to induce ER stress before performing the crosslinking with DSP to ensure that even the weak interacting proteins in the ATF6 complex were captured. The ATF6-proteins complex was immunoisolated from whole cell lysate by using the new modified protocol, which we were adapted in the previous experiment, with mouse anti-V5 conjugated agarose beads. Then the interacting proteins were eluted using reducing reagent DTT and were analysed by western blot in reduced conditions with mouse anti-ERdj3 antibody. However, the result with the wild type ATF6 cell-line has a high background and a lot of non-specific bands even though one of the proteins is convincing to be ERdj3 (Fig. 4.2.C). Therefore, we decided to modify this method again to reduce the background and non-specific bands. To prevent the high background that appeared when using antibodies raised in the same species for immunoisolation

and western blotting, we used a rabbit anti-V5 antibody with 10% PAS beads instead of anti-V5 conjugated agarose beads for immunoisolation and used mouse anti-ERdj3 antibody for western blotting. The resulting blot had less background and provided clearer evidence for an interaction between ATF6 and ERdj3 before and after thapsigargin treatment (Fig. 4.3). Thus, the rabbit anti-V5 antibody was used for immunoprecipitation in ERdj3 cross-linking method subsequently.

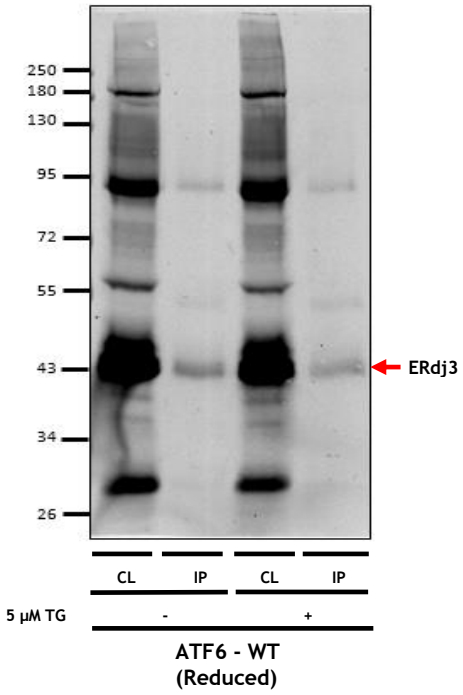

Fig. 4.3. The association of ERdj3 with ATF6 during the presence of ER stress. Recombinant HA- and V5-tagged wild-type ATF6 were stable expressed in HEK293 cells, and then were treated either with or without 5 μM thapsigargin for 1 hour before crosslinking. After that, the whole cell lysates were immunoprecipitated by using the modified protocol with rabbit anti-V5 antibody with 10% PAS beads, followed by immunoblotting with mouse anti-ERdj3 antibody (1:250) in the reduced condition. CL = Total cells lysate sample, IP = Immunoprecipitation sample.

Given the less stringent conditions for the verification experiments, it was important to determine whether the presence of ERdj3 in the immunoisolates was due to specific or non-specific binding. As a negative control we carried out an immunoisolation with an antibody to actin. If the presence of ERdj3 was due to binding to the beads, we would expect to find ERdj3 in the negative control. For this experiment, the HA- and V5-conjugated wild type ATF6 and the non-trafficking mutants ATF6; ATF6(D564G) and ATF6(Y567N), which were stably expressed in HEK-239 cells were treated to induce ER stress before performing the

crosslinking with DSP. Then, the treated cells were lysed and immunoisolated by using the rabbit anti-V5 or anti actin antibody. The interacting proteins were eluted by using the reducing reagent DTT and were analysed by western blot in reduced condition with mouse anti-ERdj3 antibody. The results showed that ATF6-ERdj3 complex was isolated only when anti-V5 antibody was used to precipitate the complex, while the negative control did not co-purify ERdj3 (Fig. 4.4.A). Thus, we can conclude that the cross-linking and immunoprecipitation method allows the specific identification of proteins interacting with ATF6. The results also demonstrated that ERdj3 interacted with ATF6 in the resting state and partially dissociates during ER stress in both wild type and mutant cells-lines since the intensity of ERdj3 decreased after cells were treated with the ER stress inducer in every cell type (Fig. 4.4.A, B, and C). In conclusion, it shows that ERdj3 interacts with ATF6 and may play some specific role in ATF6 retention in the ER during the absence of ER stress. In addition, ERdj3 dissociation might not necessarily lead to ATF6 trafficking since ERdj3 dissociated from the mutant ATF6 in the present of ER stress, but the mutants are not transported from the ER to the Golgi unlike the wild type ATF6 which traffics after ERdj3 dissociated. However, we have to confirm this hypothesis with other experiments.

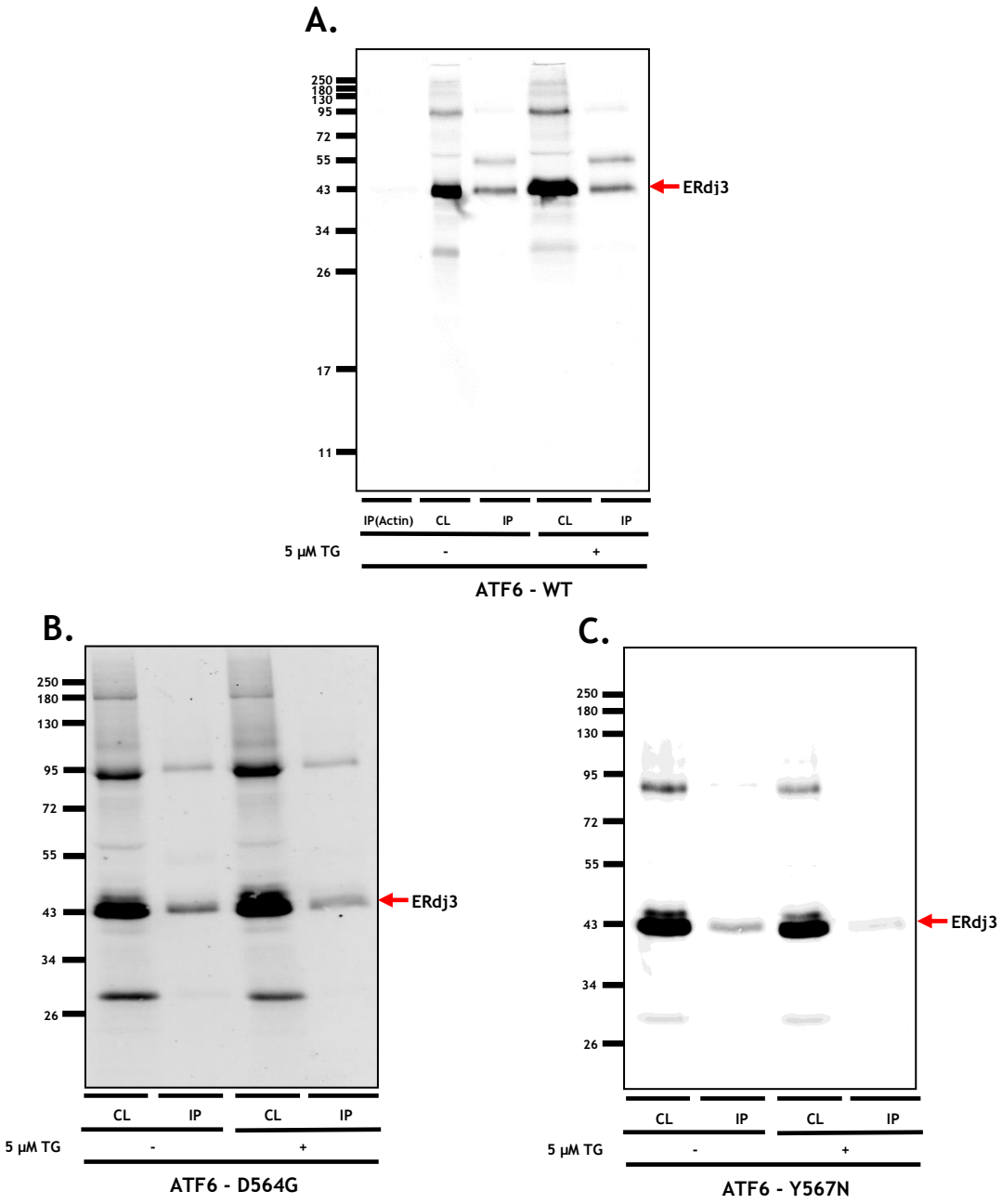

Fig. 4.4. The association of ERdj3 with ATF6 during the presence of ER stress. Recombinant HA- and V5-tagged wild-type ATF6, ATF6(D564G), and ATF6(Y567N) were stable expressed in HEK293 cells, and then were treated either with or without 5 μM TG for 1 hour before crosslinking. After that, the whole cell lysates were immunoprecipitated by using the modified protocol with rabbit anti-V5 antibody, followed by immunoblotting with mouse anti-ERdj3 antibody (1:250) in the reduced condition. **(A.)** the result of wild type ATF6 cells-line. **(B.)** the result of ATF6(D564G) cells-line. **(C.)** the result of ATF6(Y567N) cells-line. CL = Total cells lysate sample, IP = Immunoprecipitation sample.

4. 5. The expression of ERdj3 in ATF6-KO cells

According to the previous experiment we can verify the interaction of ERdj3 with ATF6, thus in this experiment the role of ERdj3 will be examined deeper. As it was mentioned before there is a report stating about the role of ERdj3 in regulating BiP activity in the presence of ER stress, mainly being a co-factor of BiP in protein folding process after the dissociation of BiP from the UPR mediators like ATF6, PERK, and IRE1 (Hanafusa, Wada, and Hosokawa, 2019; Romine and Wiseman, 2019; Genereux et al., 2015; Shen and Hendershot, 2005). However, there is no report on the role of ERdj3 in the function of ATF6 in response to ER stress conditions. Therefore, a knockout-ATF6 cell line will be used to investigate the role of ERdj3 in regulating ATF6. First, the HT-1080 cell-line expressing endogenous ATF6 (ATF6-WT) or the knockout ATF6 (ATF6-KO) cell line were treated with or without 1 μM thapsigargin for 24 hours in serum free media, then the culture media were collected, and the proteins were precipitated from the media by using Trichloroacetic acid (TCA) precipitation. Meanwhile, the treated cells were lysed by using the normal lysis conditions. After that, both proteins from the culture media and the cells lysate were examined by western blotting with mouse anti-ERdj3 antibody under reducing condition. The results indicated that after both cell types, WT and KO, were treated with ER stress inducer for 24 hours, ERdj3 was secreted from the cells into the culture media (Fig. 4.5.A). However, the level of ERdj3 in the cell extract only increased in the ATF6-WT cells after they were induced by ER stress, meanwhile the expression of ERdj3 in ATF6-KO cells remained unchanged (Fig. 4.5.B). To summarise, the expression of ERdj3 is firmly correlated with ATF6, first ATF6 is likely to be the only UPR sensor that can directly upregulate ERdj3 during ER stress since depleting ATF6 could attenuate the induction of expression of ERdj3 following stress. Second, ERdj3 was still released from cells in the presence of ER stress despite the lack of ATF6 expression, so ERdj3 and ATF6 are associated, but this interaction is not related to the retention of ATF6 or ERdj3 in the ER. Recent studies have not elucidated the mechanism of ERdj3 retention, despite the lack of an ER retrieval signal (Pobre, Poet, and Hendershot, 2019). The data of our experiments indicate that the secretion of ERdj3 is not constitutive because even in the ATF6-KO cells, ERdj3 is located in the ER until the presence of ER stress without any release to the extracellular space. Moreover, the ERdj3 secreted during ER stress may be by

binding to misfolded protein and being co-secreted with it, rather than being overexpressed as was suggested previously, since the secretion of ERdj3 is increasing when the misfolded protein is increasing during ER stress, while the actual level of ERdj3 expression in the cells is stable.

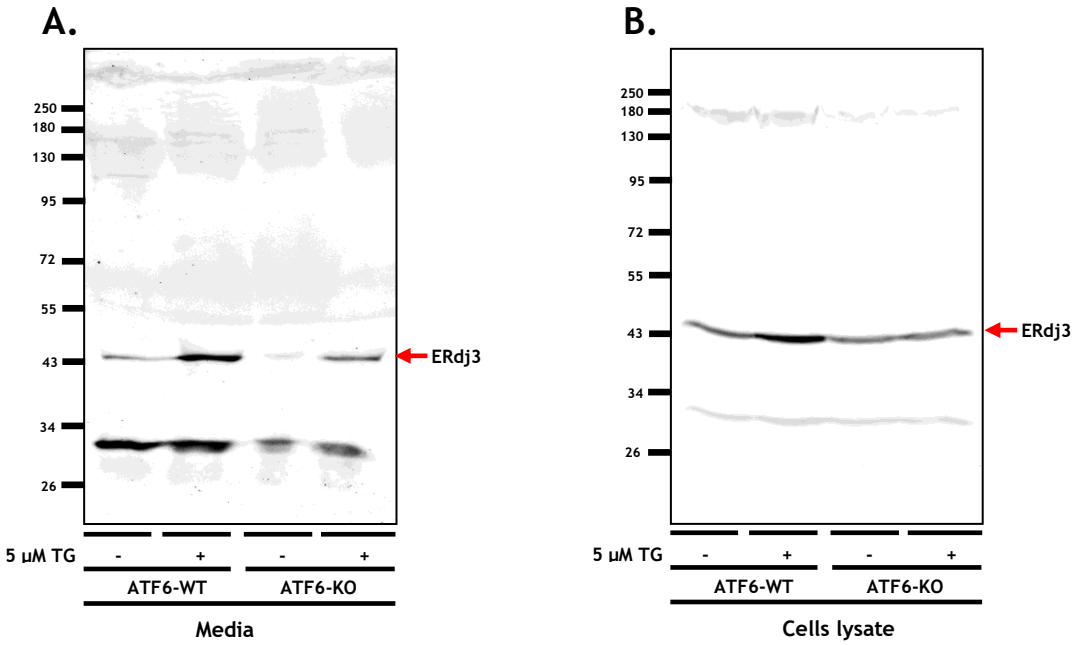

Fig. 4.5. The association of ERdj3 with ATF6 during the presence of ER stress. HT1080 cell-line with the knock-out (KO) ATF6 or the wild type (WT) ATF6 were treated either with or without 1 µM thapsigargin for 24 hours in the serum free media, then the culture media was collected, and the contained proteins were precipitated from the media **(A.)**, meanwhile, the treated cells were lysed **(B.)**. After that, both proteins from the culture media and the cells lysate were examined by immunoblotting with mouse anti-ERdj3 antibody (1:250) in the reduced condition.

4. 6. The expression of BiP and PERK in the ERdj3-KO cells

Next, we studied the role of ERdj3 in the ER stress response. As it was mentioned before, our understanding of the role of ERdj3 in the ER stress response is limited and researchers still debate whether ERdj3 is serving as a pro-folding or pro-degradation factor in the ER. However, recent studies have shown that ERdj3 binds to misfolded protein transferring it to the ER chaperone, BiP, during ER stress (Jin et al., 2008; Shen, and Hendershot, 2005). Moreover, ERdj3 is likely to be regulated by ATF6 (Genereux et al., 2015), rather than being a regulator of ATF6 trafficking as we found in the previous experiments. Therefore, the association of BiP and PERK with ERdj3 will be investigated here to observe the

role of ERdj3 in the UPR by using the ERdj3 wild type (ERdj3-WT) and knockout (ERdj3-KO) cell-lines. First, the correlation between ERdj3 and PERK activation will be evaluated, in this experiment the CHO cells expressing endogenous ERdj3 were treated with 1 μM TG for 0, 3, 6, 9, 12, and 24 hours before lysis. Then, the whole cell lysates were analysed by immunoblotting with rabbit anti-PERK antibody. The result shows that in the wild type ERdj3 cell-line, PERK was activated to phosphorylated PERK (P-PERK) after 3 h treatment with ER stress inducer and the P-PERK form decreases after 24 h of treatment (Fig. 4.6.A). Hence, we used the 3 hours of TG treatment to induce ER stress and activate PERK for subsequent experiments. In the following experiment, ERdj3-WT or ERdj3-KO CHO cells were treated with 1 μM TG for 0 or 3 hours before lysis (Fig. 4.6.B). Then, the whole cell lysates were analysed by immunoblotting with rabbit anti-PERK antibody as described before. The results show no difference between the wild type and the knockout ERdj3, both expressed the P-PERK after ER stress was induced by TG treatment for 3 hours. These results suggest that ERdj3 is not required for PERK activation. Even though ERdj3 is required to assist BiP in the proteins folding process upon ER stress, the ERdj3 is not likely to be involved with the releasing of BiP from the UPR reporters like PERK. Our result agrees with the previous study which suggested the interaction of free-BiP with the complex of ERdj3 and misfolded proteins (Genereux et al., 2015).

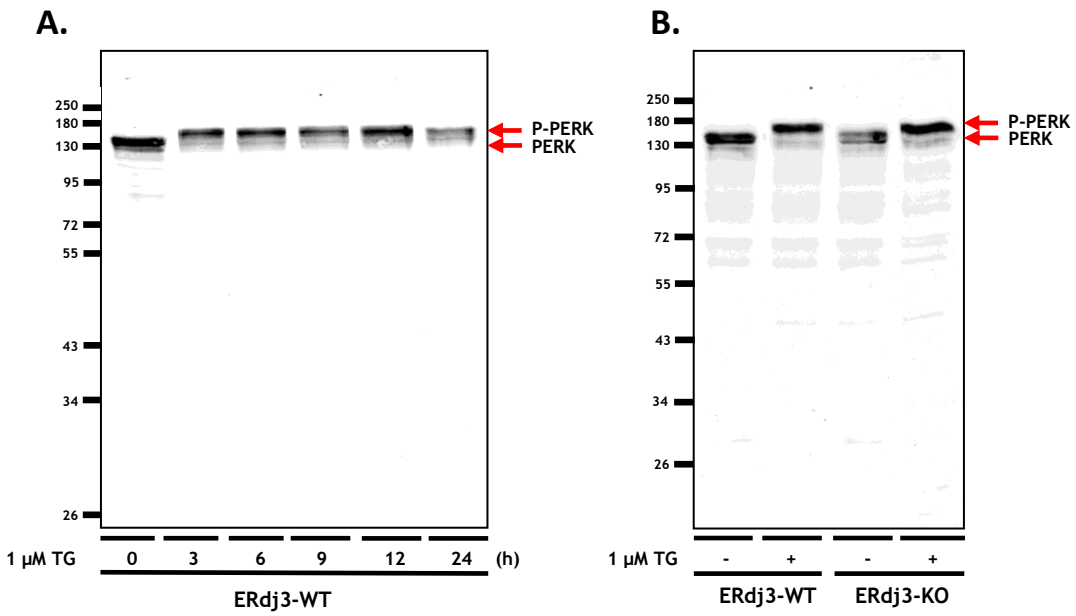

Fig. 4.6. The expression of PERK in ERdj3 cells line in the presence of ER stress. (A.) CHO cells expressed endogenous ERdj3 were treated with 1 μM TG for 0, 3, 6, 9, 12, and 24 hours before lysis. After that, the whole cell lysates were analyzed by immunoblotting with rabbit anti-PERK antibody (1:250). **(B.)** CHO cells expressed the wild type ERdj3 or CHO cells with the knockout ERdj3 were treated with 1 μM TG for 0 or 3 hours before lysis. After that, the whole cell lysates were analysed as described in **(A.)**.

The induction of BiP is used as a readout of ATF6 activation, since it has been reported for long time that BiP is a downstream target of ATF6. Therefore, any attenuation of BiP induction might also suggest a disruption of the ATF6 pathway indicating a role for ERdj3. In this experiment we considered the role of ERdj3 upon BiP induction using the ERdj3-WT and KO cell-lines. The experiment was carried the same way as for PERK. The CHO cells expressed endogenous ERdj3-WT were treated with 1 μM TG for 0, 3, 6, 9, 12, and 24 hours before lysis. Then, the whole cell lysates were analysed by immunoblotting with mouse anti-BiP antibody under reducing conditions. The experiment was carried out three times, meanwhile the density of the protein bands was analysed by ImageJ program and the data were shown in bar graph for better distinguish (Fig. 4.7.A). In the wild type ERdj3 cell-line, BiP was induced with expression increasing after 3 hours treatment with ER stress inducer. Then it started to decrease at 12 hours treatment and dropped dramatically at 24 hours treatment. Hence, we will use the 3 hours of TG treatment to induce ER stress and activate BiP for the next

experiment. After that, CHO cells expressed ERdj3-WT or ERdj3-KO were treated with 1 μM TG for 0 or 3 hours before lysis. Then, the whole cell lysates were analysed by immunoblotting with mouse anti-BiP antibody as was described previously (Fig. 4.7.B). The results of this experiment show no qualitative difference between the wild type and the knockout ERdj3, both increased the expression of BiP after 3 hours incubation with TG to induce ER stress. However, BiP induction was attenuated in the ERdj3-KO cells if the fold induction of BiP is compared between the ERdj3-WT and the ERdj3-KO cells. Therefore, without ERdj3, the increase in BiP expression is muted. To summarize, the effect of ERdj3 towards ATF6 might be not too significant despite ERdj3 being one of the protein members of the ATF6 complex and also involved in BiP-misfolded proteins interaction in the UPR (Genereux et al., 2015; Jin et al., 2008; Shen, and Hendershot, 2005).

In addition, despite it being reported that ERdj3 has a role in promoting BiP function in the ATPase cycle by transferring the misfolded protein to BiP, our results show that ERdj3 does not contribute to the releasing of BiP from ER stress sensors such as PERK in the presence of ER stress, since the lack of ERdj3 in the KO cells does not disrupt the downstream activity of the UPR. Nevertheless, we still cannot confirm whether without ERdj3, the ATPase cycle of BiP after releasing from UPR sensors is disrupted.

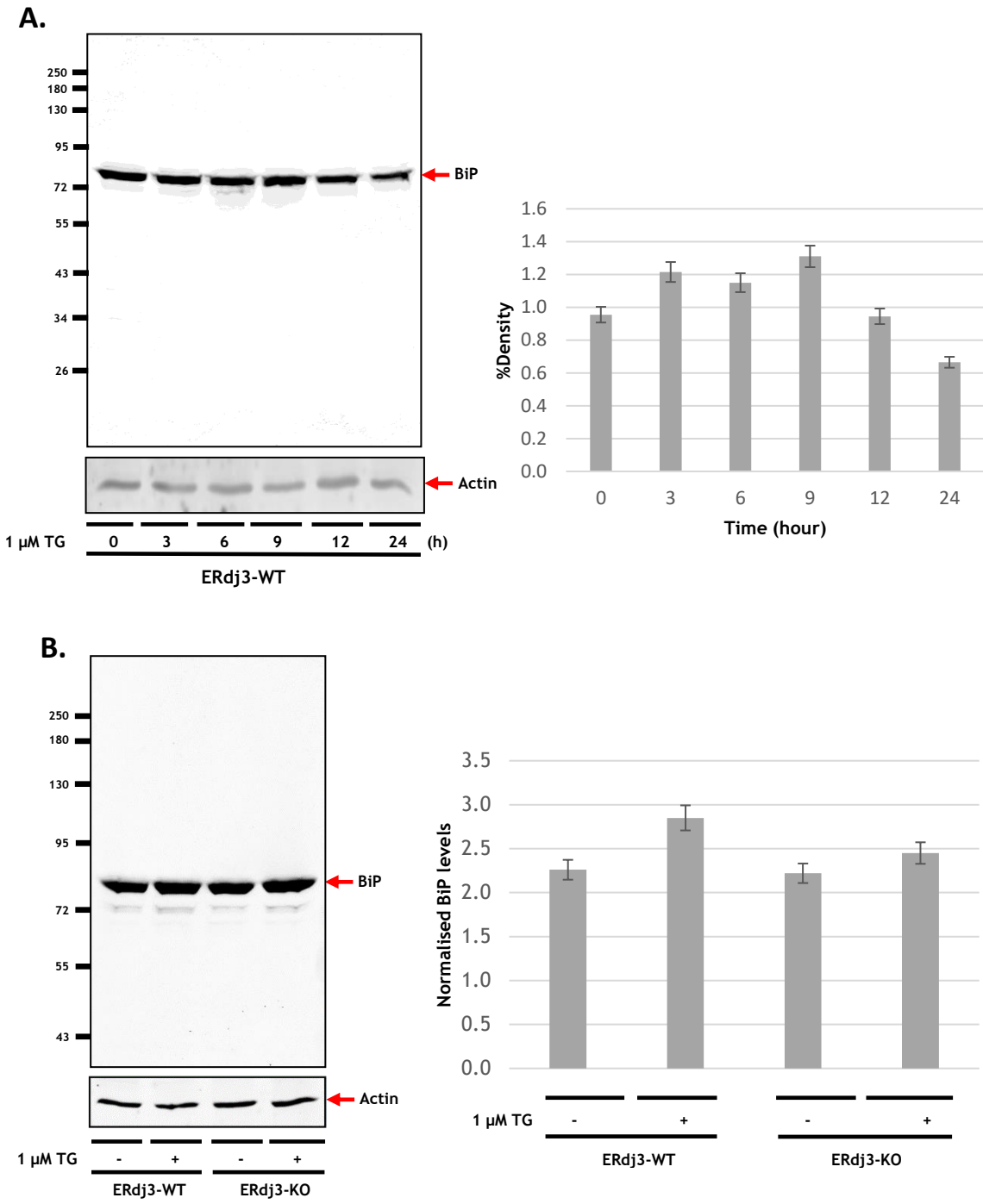

Fig. 4.7. The expression of BiP in ERdj3 cells line in the presence of ER stress. (A.) CHO cells expressed endogenous ERdj3 were treated with 1 μM TG for 0, 3, 6, 9, 12, and 24 hours before lysis. After that, the whole cell lysates were analyzed by immunoblotting with mouse anti-BiP antibody (1:250) in the reduced condition. **(B.)** CHO cells expressed the ERdj3-WT or CHO cells with the ERdj3-KO were treated with 1 μM TG for 0 or 24 hours before lysis. After that, the whole cell lysates were analysed as described in **(A.)**. The experiment was carried out three times and the density of the protein bands were analysed by ImageJ to generate the bar graphs.

4. 7. The expression of the ATF6 Golgi form in the ERdj3-KO cells

In this experiment, we explored the consequence of ERdj3 depletion on ATF6 trafficking to the Golgi by observing the expression of the Golgi form of ATF6. Previous studies suggested that upon ER stress ATF6 became activated and transported from the ER to the Golgi after dissociation from BiP and packed into COP II vesicles. In the Golgi apparatus, ATF6 underwent modification to an O-linked glycosylation form by the work of glycosyltransferases, within the trans-Golgi compartment. The result of the O-linked glycan modification in the Golgi apparatus is to generate a slower migrating form of the full-length ATF6, which is also known as the Golgi form of ATF6 (Shen et al., 2002; Hanisch, 2001; Ye et al., 2000). This specific modification only appeared with ATF6 in the Golgi apparatus after the trafficking from the ER upon the stress response, thus it is a trustable indicator that we can use to investigate the Golgi localisation of the ATF6 before and after stress exposure. Therefore, ERdj3-WT and KO cells were used to examine the expression of the Golgi form of ATF6. CHO cells, which stably expressed the ERdj3-WT and KO, were transiently transfected with recombinant HA- and V5-tagged wild-type ATF6. Then the transfected cells were treated with 30 μM S1P inhibitor for 1 hour to inhibit cleavage by S1P protease, followed by treated with 10 mM DTT for 45 minutes to induce stress before the cells were lysed. Subsequently, the whole cell lysates were analysed by immunoblotting with mouse anti-ATF6 antibody in the reduced condition. The results that we obtained show no differences between ERdj3-WT and KO cells, both cell types which were transiently transfected with ATF6-WT can generate the Golgi form of ATF6, when ER stress was caused by DTT after 45 minutes of treatment (Fig. 4.8). According to the fact that the Golgi form of ATF6 could be generated in both cell types, we can assume that the ERdj3 depletion in cells has no direct effect on ATF6 trafficking when cells exposed with stress.

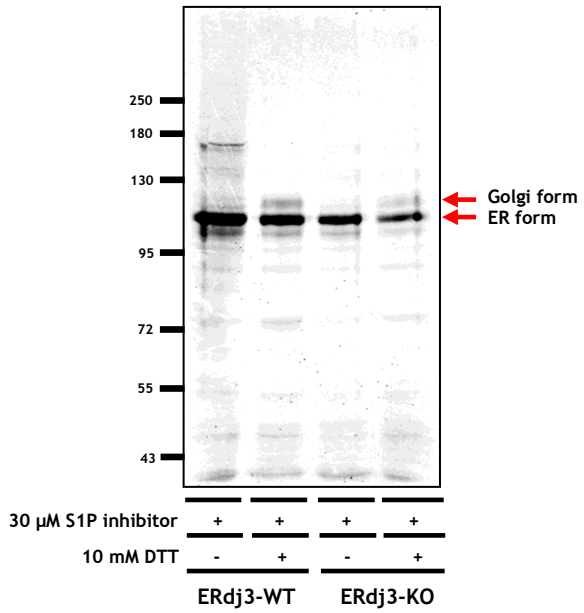

Fig. 4.8. The expression of the Golgi form of ATF6 in the ERdj3 wild type (WT) and knockout (KO) cell-lines in the presence of ER stress. CHO cells expressed ERdj3-WT or ERdj3-KO were transiently transfected with the recombinant HA- and V5-tagged wild-type ATF6. Transfected cells were treated with 30 μM S1P inhibitor for 1 hour, and then treated whit 10 mM DTT for 45 minutes before lysis. Subsequently, the whole cell lysates were analysed by immunoblotting with mouse anti-ATF6 antibody (1:250) in the reduced condition.

However, even though the Golgi form of ATF6 could be produced in both ERdj3-WT and KO cells, the generating time after exposure to ER stress might vary in the different cell types. The faster or slower trafficking of ATF6 upon ER stress will make our understanding about ERdj3 toward ATF6 trafficking clearer. Therefore, in order to analyse the kinetics of trafficking, the CHO cells expressing ERdj3-WT or ERdj3-KO were used again. Both cell types were transiently transfected with recombinant HA- and V5-tagged wild-type ATF6. Then transfected cells were pre-treated with S1P inhibitor for 1 hour prior to treatment with DTT for varied time point, 0, 15, 30, 45, and 60 minutes before lysis. Furthermore, the whole cell lysates were analysed by immunoblotting with mouse anti-ATF6 antibody under reducing conditions (Fig. 4.9). The result again showed no significant differences between the ERdj3-WT and KO cells, the time course of the Golgi form appearance in both cell types is very similar after cells were stressed with DTT. Nevertheless, closer inspection of the Golgi form of ATF6 which was generated by both cell types indicates that the expression might be slightly less in the knockout compared with the wild type cells. The difference is not

significant so if there is an effect of ERdj3 on ATF6, the effect is very limited and does not disrupt ATF6 activation.

According to the information we obtained from these experiments, the results clearly shown no significant effect of ERdj3 toward the trafficking or the expression of ATF6. Hence, we can assume here that the interaction between the ATF6 and ERdj3 that we saw is likely to be due to the abnormal conformation of ATF6 than interacting for ATF6 retention or trafficking, since it already reported that ERdj3 assisted the refolding process of BiP by binding with the misfolded proteins and transferring it to BiP (Genereux et al., 2015). ERdj3 might recognise the mutants of ATF6 as one of the misfolded protein clients and associate with mutants ATF6 to bring it in to the refolding processes.

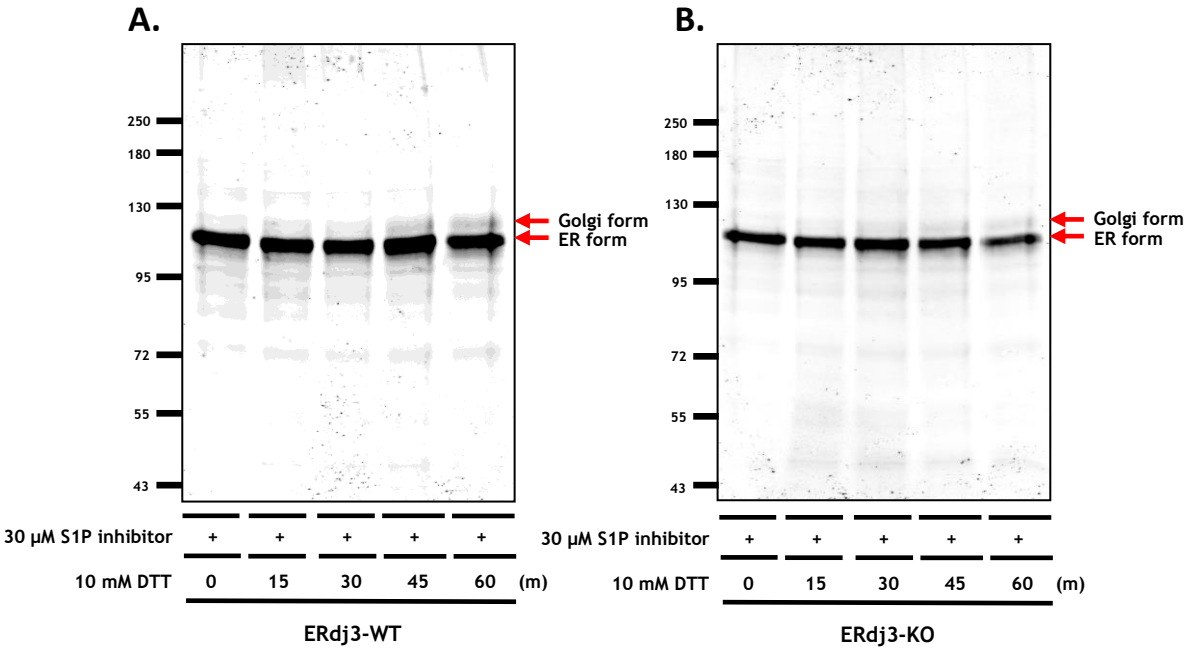

Fig. 4.9. The expression of the Golgi form of ATF6 in the ERdj3 wild type (WT) and knockout (KO) cell-lines in the presence of ER stress in a time-related manner. CHO cells expressed ERdj3-WT **(A.)** or ERdj3-KO **(B.)** were transiently transfected with the recombinant HA- and V5-tagged wild-type ATF6. Transfected cells were treated with 30 μM S1P inhibitor for 1 hour, and then treated whit 10 mM DTT for 0, 15, 30, 45, and 60 minutes before lysis. Subsequently, the whole cell lysates were analysed by immunoblotting with mouse anti-ATF6 antibody (1:250) in the reduced condition.

4. 8. Chapter Discussion

In this chapter, the aim was to identify the proteins that exist in the complex with ATF6 before and during ER stress. In addition, we investigated the role of these proteins in the UPR related to ATF6, by using our created mutant ATF6 stable cells lines. To this aim, firstly, we tried to compare differences in the ATF6-proteins complex in the wild type ATF6 cell-line, compared to the mutant ATF6 cell-line, ATF6(D564G), in the presence and absence of ER stress by fractionation based on density/size of the complex. Unfortunately, the results we obtained from sucrose gradient experiments were highly erratic. However, we were able to distinguish between the wild type and the mutant ATF6(D564G). The results were sufficient to prove our hypothesis that the wild type ATF6 and the mutant carried different protein members within the complex and those proteins affected the performance of ATF6 during the UPR (Fig. 4.1).

To identify proteins that exist in the ATF6 complex, the more sensitive method of crosslinking followed by mass spectrometry analysis was used. The results of mass spectrometry show numerous proteins which could be in the complex and have a role in ATF6 trafficking (Table. 4.1). However, as mentioned, mass spectrometry is a very sensitive method so it can also detect very small amount of protein which come from non-specific binding. Thus, only four promising proteins that we identified from mass spectrometry such as 14-3-3E, protein TFG, Neudesin, and ERdj3, were chosen and their interaction with ATF6 determined by immunoisolation and western bloting (Hanafusa, Wada, and Hosokawa, 2019; Romine and Wiseman, 2019; Pennington et al., 2018; Kanadome et al., 2017; Genereux et al., 2015; Johnson et al., 2015; Beetz et al., 2013). Unfortunately, we could not detect any of these 4 proteins from the ATF6 complex from our first attempt (Fig. 4.2). Therefore, we decided to focus on the individual protein rather than do it all at the same time. We also modified some steps of our method so it can be used more effectively, since we were concerned that the concentration of the proteins might be too low and/or the affinity between the proteins and ATF6 is too low. The first protein that we decided to investigate was ERdj3, an ER co-chaperone in DnaJ family, which has been reported to be involved with the regulation of BiP function in the UPR (Hanafusa, Wada, and Hosokawa, 2019; Romine and Wiseman, 2019; Genereux et al., 2015; Shen and Hendershot,

2005). After some modification of our method, the results of immunoprecipitation showed that the ERdj3 is part of the ATF6 complex (Fig. 4.2.C), therefore we continued to study the role of ERdj3 in the ATF6 complex to see whether or not it is involved with ATF6 activation and trafficking.

The role of Erdj3 during ATF6 activation had not previously been investigated. Recent studies only looked at the role of ERdj3 in the protein folding process by transferring proteins clients to BiP (Hanafusa, Wada, and Hosokawa, 2019; Romine and Wiseman, 2019; Genereux et al., 2015; Shen and Hendershot, 2005). Therefore, it is difficult to predict the role of ERdj3 in the ATF6 complex, it could be involved in retention or trafficking control. However, the results of our studies suggested that, first, the ERdj3 interacts with ATF6 in normal conditions, and dissociated from ATF6 in the presence of ER stress (Fig. 4.3). However, the dissociation of ERdj3 from ATF6 is insufficient to lead to the trafficking of ATF6 from the ER to the Golgi, since the dissociation of ERdj3 is also found in the mutants of ATF6, but the mutants are still retained in the ER following ER stress (Fig. 4.4). This information suggests that ERdj3 might be participating in retention rather than driving the trafficking process of ATF6.

Second, the expression of ERdj3 during the stress response is seems to be regulated by ATF6, rather than ATF6 being regulated or activated by ERdj3, since the expression of the Golgi form of ATF6 and also the ATF6 related protein such as BiP, show no noticeable difference following ATF6 activation between the wild type and the knockout ERdj3 cell-lines. Both ERdj3 cell types can generate the cleaved form of ATF6, and the Golgi form, when cells are exposed to stress. The kinetics of activation after exposure to ER stress are also similar in both ERdj3 cell types. Also, the induction of BiP shows a similar result between two cell types; the expression of BiP started to increase after 3 hours and dropped after 12 hours (Fig. 4.7). ERdj3 might assist BiP for proteins folding processes by transferring the unfolded proteins to BiP (Genereux et al., 2015; Jin, Zhuang and Hendershot., 2009), however the absence of ERdj3 in the KO cells does not significantly affect BiP performance. Hence, our results suggest that BiP has other co-factors which can cope with the absence of ERdj3 during ER stress. Moreover, the ERdj3 depletion in cells also has no significant effect on ATF6 regulation, since ATF6 still

could maintain its activity following ER stress by upregulating the downstream events (Fig. 4.8).

Third, our research suggested that ATF6 is the UPR sensor which can directly upregulate ERdj3 expression during ER stress, since the lack of ATF6 could prevent the increasing of ERdj3 level in the ATF6-KO cells following stress, even though, it still secreted from the cells (Fig. 4.5). Our result is in contrast with a previous study of PERK, another ER stress response mediator. PERK was found to regulate the secretion of an ERdj3-misfolded protein complex. The absence of PERK caused the accumulation of the complex in the ER lumen (Romine and Wiseman., 2019). Therefore, from our study the association of ATF6 is not related to the secretion of ERdj3 from the ER, since it still could secrete to the extracellular space without the presence of ATF6. According to the recent studies, the mechanism of ERdj3 retention in the ER lumen is still not elucidated, despite the lack of an ER retrieval sequence of ERdj3 itself, however some studies suggested that the secretion will only occur after the association of ERdj3 with unfolded proteins in the presence of ER stress (Pobre, Poet, and Hendershot, 2019; Genereux et al., 2015). Meanwhile, the results of our experiments demonstrate that the secretion of ERdj3 is not constitutive because ERdj3 is located in the ER until the presence of ER stress without any release to the extracellular space, even in the ATF6-KO cells which were deprived of ATF6 expression. Moreover, the secretion of ERdj3 during ER stress is likely to be by binding to unfolded protein and being co-secreted from the cells with it, rather than being overexpressed, since the secretion of ERdj3 is increasing when the unfolded protein increases during ER stress, while the actual level of ERdj3 expression in the ATF6-KO cells remains stable (Fig. 4.5.B). This result extends the previous studies which highlighted the possibility of co-secretion of ERdj3 and the misfolded protein clients (Romine and Wiseman., 2019; Genereux et al., 2015).

In addition, even though, it has been reported that the ERdj3 has a supportive role toward BiP in the ATPase cycle by transferring the unfolded protein to BiP during the UPR, the results from our research indicate that ERdj3 is not required for the release of BiP from ER stress sensors such as ATF6 and PERK, since the lack of ERdj3 in the ERDj3-KO cells does not disrupt the downstream activity of ATF6 or PERK during the UPR. For instance, in the ERdj3-KO cells PERK

could still generate P-PERK and ATF6 also could produce the Golgi form, when ER stress was induced (Fig. 4.6, 4.8 and 4.9). Therefore, according to the results we achieved from these experiments, ERdj3 has no significant effect on the trafficking or the expression of ATF6. Consequently, we can assume here that the interaction between the ATF6 and ERdj3 that we saw is likely to be due to the abnormal conformation of ATF6 rather than associated with ATF6 for its retention or trafficking, since it has already been reported that ERdj3 acts as a co-chaperone for BiP (Romine and Wiseman., 2019; Genereux et al., 2015). In this case, the ERdj3 might recognise the mutants of ATF6 as one of the unfolded protein clients which accumulated in the ER lumen in the presence of ER stress, thence ERdj3 associates with the mutant ATF6 like D564G and Y567N to bring it in to the refolding processes. However, this hypothesis still requires future study to support.

CHAPTER V: RESULTS SECTION 3 - The lipotoxic stress response of ATF6

5. 1. The role of specific sphingolipids, DHS and DHC, in the activation of the UPR sensor ATF6

Recently, a new study has suggested that ER stress could be induced not only by proteotoxicity, but also by lipotoxicity, and both pathways are distinct. Proteotoxic stress is the main pathway of the UPR that has been identified and studied for numerous years, even though, not all of the mechanisms were investigated until now. For proteotoxic stress induction of the UPR, research suggested that the UPR sensors; ATF6, PERK and IRE1, sense stress via the luminal domain following the release of the ER chaperone, BiP. Proteotoxic stress, induced by internal or external factors, was thought to be the only pathway of the UPR activation for several years, however recent studies introduced lipotoxic stress as another mechanism to induce ER stress which also can activate the UPR process. Since the majority of lipids such as sphingolipids, sterols and phospholipids, are also synthesized in the ER (Jacquemyn et al., 2017; Miller et al., 2017; Volmer and Ron, 2015; Fu et al., 2012; Thibault et al., 2012) the disruption of these lipid synthesis processes, as well as the disruption of the lipid bilayer of ER membrane, could disrupt ER function and cause stress to the ER. In addition, it was reported that the induction of lipotoxic stress is likely to be through individual pathways which work separately from the proteotoxic stress pathway (Tam et al., 2019; Volmer and Ron, 2015; Promlek et al., 2011). Various studies suggested that the UPR members, including ATF6, sense lipotoxic stress via the transmembrane domain motif, which causes an increase of membrane fluidity during stress (Tam et al., 2019; Halbleib et al., 2017; Volmer et al., 2013). Moreover, from the report of Tam et al. in 2019, the intermediators of sphingolipid biosynthetic pathway such as dihydrosphingosine (DHS) and dihydroceranmide (DHC) can directly activate the UPR via the ATF6 branch to upregulate ER lipid biosynthetic genes, instead of the upregulation of genes involved with proteins folding as we normally see in the proteotoxic stress response. The mechanism of this process is completely distinct from the regular proteotoxic stress as both pathways seem to work independently. Therefore, we want to use these two specific sphingolipids to investigate the ATF6 pathway in our created mutants, ATF6(D564G) and ATF6(Y567N), to see whether they could respond to lipotoxic stress, as they could

not respond to proteotoxic stress because of the point mutation within the luminal domain.

For this experiment, firstly, the recombinant HA- and V5-tagged wild-type ATF6 (ATF6-WT), expressed in HEK-293 cells, was used to reproduce the results of the research of Tam et al. in 2018. We studied the ER stress induced mechanism of DHS and DHC in the ATF6-WT before using these lipids to induce ER stress with our mutants. Therefore, the ATF6-WT cells were treated with 5 μM TG, or 50 μM DHS or DHC for 2 hours to induce ER stress. Here TG was used as a positive control to induce ER stress via the regular proteotoxic stress pathway. Then the treated cells were lysed and separated into membrane fraction and nuclear fraction by centrifugation. Thereafter, the protein fractions were collected and analysed by immunoblotting with mouse anti-ATF6 antibody under reducing condition to evaluate the appearance of the cleaved ATF6 upon the stress response. The results of this experiment show that, for the membrane fraction, there were no differences between TG treatment and sphingolipids, DHS and DHC, treatment. However, the results of nuclear fraction were significantly different, only cells which were treated with TG show both the ER form and the cleavage-nuclear form of ATF6. While the results of the nuclear fraction of the DHS and DHC treatment cells merely showed the single band of the ER form as with the untreated cells (Fig. 5.1.A). Our results using DHS and DHC induced ER stress are in contrast to the reported results of Tam et al. in 2019, our results shown no ER stress induction with DHS and DHC, whilst the results of Tam clearly show that these sphingolipids could induce ER stress by specifically activating the ATF6 pathway. Therefore, we continued with further experiments to determine whether DHS and DHC could induce an UPR.

Consequently, the recombinant HA- and V5-tagged wild-type ATF6 (ATF6-WT), expressed in HEK-293 cells, was used again in these experiments. Cells were treated with S1P inhibitor for 1 hour to prevent ATF6 cleavage by S1P and S2P following ATF6 transport from the ER to the Golgi after ER stress. Then cells were treated with 10 mM DTT for 30 mins, or with 50 μM DHS or DHC for 16 hours to induce ER stress. Here DTT was used as a positive control for ER stress as it causes a build-up of the O-link glycosylated Golgi form that can be distinguished by SDS-PAGE analysis. The treated cells were lysed and analysed by immunoblotting with mouse anti-HA antibody under the reducing condition. The results shown that only

DTT treatment can induce the Golgi form of the wild type ATF6, the results of DHS and DHC treatment show only a single band of ER form without Golgi form of ATF6 (Fig. 5.1.B). The results correlate with our previous experiment on the ATF6 nuclear form. However, despite the DHS and DHC results showing a similarity to the result of the untreated cells here, from this experiment we cannot conclude that the DHS and DHC lack the ability to induce ER stress since TG, one of the well-known ER stress inducers, only poorly induces the Golgi form of ATF6 during ER stress in the presence of S1P inhibitor. Hence, from this result we can only conclude that if the DHS or DHC can induce ER stress, the mechanism will not lead to detection of the Golgi form of ATF6, similar to the situation with TG induction. Therefore, other experiments are required to test the ability of DHS and DHC to induce ER stress.

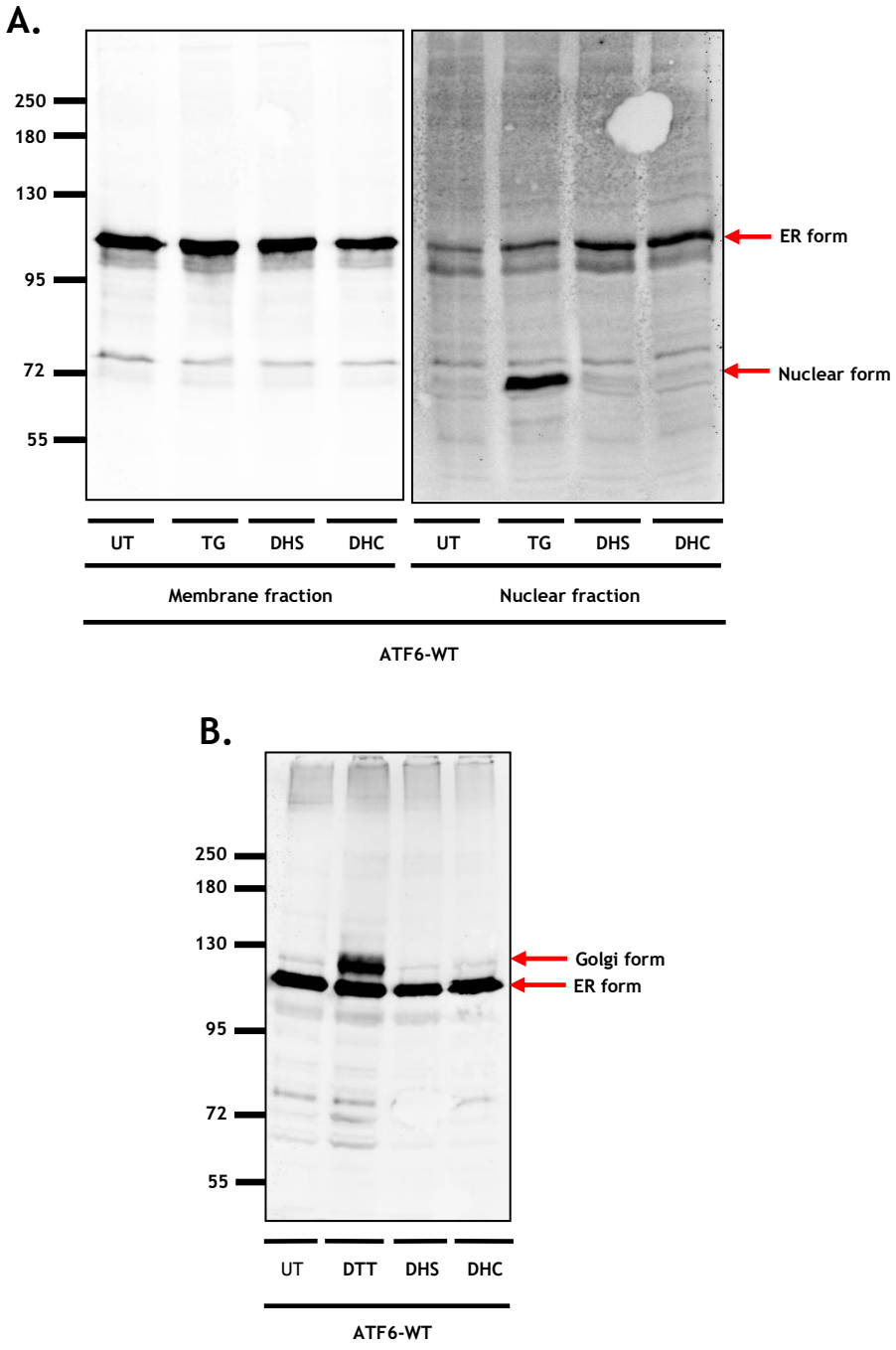

Fig. 5.1. The activation of the UPR sensor ATF6 induced by DHS and DHC. (A). Recombinant HA- and V5-tagged wild-type ATF6 (ATF6-WT) were expressed in HEK-293 cells, then treated with 5 μM TG, or 100 μM DHS or DHC for 2 hours to induce ER stress. The treated cells were lysed and separated into membrane and nuclear fractions by centrifugation. Thereafter, the protein fractions were collected and analysed by immunoblotting with mouse anti-ATF6 antibody (1:250) under reducing conditions. **(B).** WT-ATF6 cell-line was treated with S1P inhibitor for 1 h and then treated with 10 mM DTT for 30 mins or 50 μM DHS or DHC for 16 hours. Then cells were lysed and analysed by immunoblotting with mouse anti-HA antibody under reducing conditions. UT = Untreated control cells.

5. 2. The ATF6 activation output induced by lipotoxic reagents, DHS and DHC

According to our previous experiments, the ER stress-induced function of DHS and DHC still remained elusive, hence, we continued to investigate the role of DHS and DHC in induction of ER stress. In this experiment, the downstream output of DHS and DHC-induced ER stress and UPR via the ATF6 branch activation, was examined. First, induction of BiP expression was analysed, since BiP is the main protein upregulated by the UPR and is a downstream target of ATF6. Here, the HEK-293 cells stably expressed recombinant HA- and V5-tagged wild-type ATF6 (ATF6-WT), were used. Cells were treated with 1 μM TG, or 50 μM DHS or DHC for 16 hours to induce ER stress and the UPR. Here TG was used as a positive control to induce ER stress instead of DTT. Subsequently, the treated cells were lysed, and the total cell lysates were analysed by immunoblotting with mouse anti-ATF6, mouse anti-BiP, and rabbit anti-Actin antibody in the reduced gel. As it was stated in the results of the previous experiment, the TG-induced ER stress would not indicate the Golgi processed form of ATF6, therefore, we used TG as a positive control by measuring the expression of BiP, an ER stress response element in the ATF6 pathway. The result shows that DHS and DHC do not induce the expression of BiP. Meanwhile, our positive control TG did show the expected increase of BiP expression (Fig. 5.2.A). Therefore, from these results we can be more confident that DHS and DHC are not likely to be the ER stress inducers, these results are in contrast with the publication of Tam's group in 2019.

Subsequently, ACOX1, a protein involved in lipid biogenesis and metabolism that was reported to be one of the ATF6 target proteins in DHS- and DHC-activated ER stress (Tam et al., 2019), was investigated to ascertain the role of DHS and DHC in the UPR. The same HA- and V5-tagged wild-type ATF6 cell-line was treated with 1 μM TG, or 50 μM DHS or DHC for 16 hours to induce ER stress same as in the previous experiment. The TG, proteotoxic stress inducer of ER stress, was used as a positive control again here. Then, the treated cells were lysed and analysed by immunoblotting with mouse anti-ACOX1 antibody in the non-reduced condition. For ACOX1, the result shows that only TG can upregulate the expression of ACOX1, despite the TG not directly targeting lipid biogenesis and metabolism, meanwhile the expression of the protein after cells were treated with DHS and DHC remained

not significantly changed (Fig. 5.2.B). This result also indicates opposite results to Tam's research in 2019.

Accordingly, it is hard to make an assumption here since the results we got for this study, clearly shown that the DHS and DHC cannot significantly induce the expression of ER stress response proteins such as reduced-ATF6, the Golgi form of ATF6 and BiP, same as the expression of the protein involved with lipid metabolism like ACOX1. Even though, it was already reported that ACOX1 can be upregulated directly by DHS and DHC via ATF6 pathway of the UPR (Tam et al., 2019), in our study ACOX1 remains unchanging after inducing by DHS and DHC compared to the inducing of standard ER stress inducers such as DTT and TG. At first, this information convinced us to think that the DHS and DHC might not be able to induce ER stress via lipotoxicity as it was reported, even so it remained unclear why our study and the study of the other group about these sphingolipids inducing UPR, are pointing to a completely different direction. However, there is also the possibility of the DHS and DHC that we used for our experiments might be not working for some unknown reasons too, despite we purchased it from the same company with the one was used in the Tam's team experiments and the possibility of two reagents, DHS and DHC, that will be not working at the same time, might be very low. Therefore, the future study is obviously needed to clarify about this lipotoxic stress pathway of ER stress, as same as the role of DHS- and DHC-activated ATF6 in the UPR.

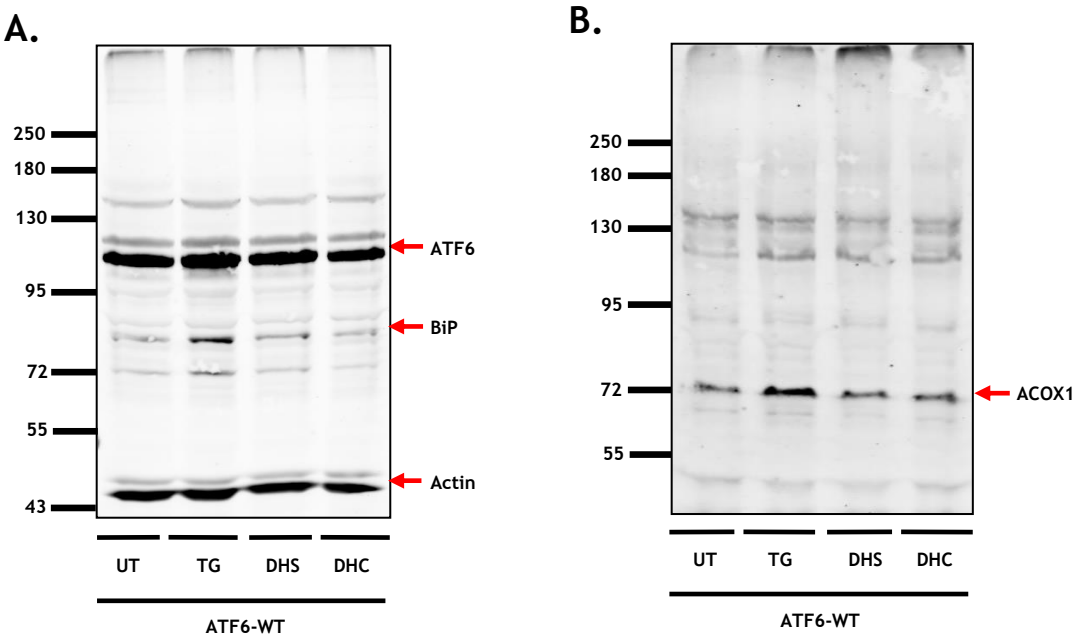

Fig. 5.2. The downstream output of the ATF6 activation induced by DHS and DHC in the UPR. (A). Recombinant HA- and V5-tagged wild-type ATF6 were expressed in HEK293 cells, was treated with 1 μM TG, or 50 μM DHS or DHC for 16 hours to induce ER stress. The treated cells were lysis and the total cell lysates were analyzed by immunoblotting with mouse anti-ATF6 (1:250), mouse anti-BiP (1:250), and rabbit anti-Actin (1:250) antibody in the reduced gel. **(B).** The same ATF6-WT cell-line was treated with 1 μM TG, or 50 μM DHS or DHC for 16 hours to induce ER stress. Then, the treated cells were lysis and analyzed by immunoblotting with mouse anti-ACOX1 (1:500) antibody in the non-reduced condition.

5. 3. Chapter Discussion

As it was stated that the aim of this chapter was to focus on lipotoxic stress, which was reported to be a mechanism for activating ER stress distinct from proteotoxic stress. Understanding of this alternative pathway of ATF6 in regulating ER homeostasis would help us to establish a clearer picture of how ATF6 trafficking is controlled in general. Even though the role of lipotoxic stress is a new topic and still lacks of understanding compared to the proteotoxic stress, some specific lipids, such as DHS and DHC, were already reported to activate the UPR via the ATF6 branch (Tam et al., 2019). Therefore, in our study we tried to reproduce the DHS- and DHC-induced ER stress result in order to study the role of sphingolipids in the activation of our luminal domain mutants of ATF6. However, the results we obtained from several experiments are pointed in a different direction to that

observed previously. Our results contradicted the original report. In our study, the ATF6 downstream events, such as reduction of ATF6, generating the Golgi form of ATF6 and BiP induction, following the UPR were not seen following treatment with DHS and DHC (Fig. 5.1). Similarly, the result of proteins regulated by lipid synthesis such as ACOX1, also showed no induction after cells were treated with DHS and DHC, compared with the expression of the proteins in the non-treated cells. Meanwhile, the expression of ACOX1 was clearly increasing in the cells that treated with the standard ER stress inducer like TG (Fig. 5.2). However, the reason why DHS and DHC cannot induce the other proteins and the other forms of ATF6 is remains to be addressed.

Even though, the results which we obtained here, are convincing there is a possibility that the DHS and DHC might not be able to upregulate the downstream processes of the ATF6 pathway in the UPR as efficiently as proteotoxic stress. As the report of DHS- and DHC-activated ATF6 is a very new study, the data or the information might be changed in the future when more experiments are performed. However, there may be factors that we used in our experiments, such as cell types that they used in their experiments are different from the cells that we used since every cell type has its own specificity and sensitivity, therefore different cell types may generate different result as well. In addition, the method that they used to treat their cells with DHS and DHC, also needed to be considered, despite our attempts to reproduce their experiments as close as possible, because sometimes only small thing could make a huge different in research experiment. Therefore, in the future study the conditions and source of reagents should be reviewed and verified again. Moreover, we also need a positive control that would allow us to know that the added lipids actually do get into the cells after treated since lipids are sometime hardly to go into the cells.

CHAPTER VI: DISCUSSION AND CONCLUSION

6. 1. The non-native conformation of the non-trafficking ATF6 mutants affects their performance in responding to stress

The aim of our study was to investigate the trafficking process of ATF6, one of the three main UPR reporters, alongside PERK and IRE1. Up until now, the understanding of ATF6 trafficking remains poor, despite the broad range studies of ER stress and ATF6 in general. Research about ATF6 roughly suggested that during the UPR, the luminal domain of ATF6 senses the stress signal and dissociates from BiP, the ER chaperone which binds with the UPR sensers like ATF6 in the resting stage (Sato et al., 2011; Chen et al., 2002). The detachment of BiP from ATF6 is well known as an initiation of ATF6 downstream processes in the UPR, since the binding of BiP with ATF6 and other UPR reporters is very stable until the presence of ER stress (Schindler and Schekman, 2009; Shen and Prywes, 2005; Shen et al., 2005). Following, ATF6 will pack into COP II vesicles and translocate to the Golgi apparatus, where the ATF6 will undergo proteolysis by S1P and S2P protease (Higa et al., 2014; Ye et al., 2000; Haze et al., 1999). Then the cleaved ATF6 moves to the nucleus and upregulates the unfolded protein response genes. It remains unclear what is regulating the packed of ATF6 into COP II and driving it to move to the Golgi during stress, some studies suggested that some specific ER proteins in the thrombospondin, and PDI family such as thrombospondin 4, PDIR, and ERp18, assist in the trafficking process of ATF6. Reports advised that those ER proteins are assisting the process by changing the disulfides within ATF6 to the monomeric form for trafficking (Oka et al., 2019; Higa et al., 2014; Lynch et al., 2012; Jeong et al., 2008). Moreover, some proteins involved in glycoprotein quality control such as glucosidase II and calreticulin are also reported to interact with the ATF6 before it traffics (Honore, 2009; Ye et al., 2000; Haze et al., 1999).

However, there is still a lot we do not know about the trafficking of ATF6 upon ER stress, such as which disulfide form of ATF6 is the form that likely to be transported during ER stress. In addition, the role of the mentioned proteins which were reported to be involved with the trafficking process of ATF6 is still not known. It is likely that additional protein(s) will also be involved in the process. Therefore, our study aimed to fill this gap in knowledge. The additional knowledge which we gained from our experiments will also build up a clearer

picture of ATF6 and the UPR for future study. Understanding more about ATF6 and the UPR could also help researchers discover therapeutic treatments for several diseases in the future too, since the malfunction or non-function of ATF6 is proving to relate to several diseases such as Achromatopsia, neurodegenerative diseases, stroke, diabetes, inflammatory bowel disease, and myocardial infarction (Ranjan et al., 2021; Ghemrawi and Khair, 2020; Glembotski, Rosarda and Wiseman, 2020; Lee et al., 2020; Yang et al., 2019; Chianga et al., 2017).

To address our aims, we decided to take advantage of previous studies into ATF6 mutants that lack the ability to be trafficked to the Golgi. After we examined several studies about ATF6 mutants, both laboratory-synthetically generated and naturally occurring (Chapter 3.1), we found interesting mutations which carried the non-trafficking property from the research of Chianga's group. This report published in 2017 identified several mutation types of ATF6 which can be found in Achromatopsia patients. The members of class one mutations, as it was identified in this paper, are mutated in the luminal domain of ATF6 and have impaired trafficking. Therefore, we were interested in using the same mutants to study the trafficking of ATF6 compared to the wild type ATF6. We aimed to identify the differences between the mutants and the wild type ATF6, since this would help us to understand more about the mechanism of ATF6 trafficking and also the factors that regulate this process.

The two ATF6 mutations occurring in Achromatopsia patients, ATF6(D564G) and ATF6(Y567N), were reproduced for our study (Chapter 3.2). The ATF6(D564G) is the point mutation of ATF6 luminal domain at amino acid 564, which was changed from aspartic acid (D) to glycine (G), meanwhile, the ATF6(Y567N) is the mutation of amino acid 567 from tyrosine (Y) to asparagine (N) (Chianga et al., 2017). After testing our regenerated ATF6 mutants, ATF6(D564G) and ATF6(Y567N), we found that these mutants could suppress ER-to-Golgi trafficking of ATF6 as reported previously (Fig. 3.3 and 3.4). However, we found more interesting information not included in the original work. From our study, even though these two point-mutations are located only a few amino acids apart and both lack trafficking, the redox forms of these two are different. In the resting state, the ATF6(D564G) appears in all disulfide forms that are also found in the wild type ATF6, oligomer, dimer and monomer, while the ATF6(Y567N) only

appears as monomer (Fig. 3.2). This result made us concerned about what redox form of ATF6 trafficked to the Golgi, since a previous study reported that the monomeric form of ATF6 is likely to be the most preferable form for trafficking and S1P cleaved (Nadanaka et al., 2007). ATF6(Y567N) which shows only monomeric form, remains in the ER without any trafficking in the presence of ER stress. Moreover, the phenotype of the mutant ATF6 is obviously showing the disruption of the interchain disulfides in the luminal domain of ATF6. It is still remains unclear how these point mutations affect the disulfide status of ATF6, however the change in conformation of ATF6 might make the other proteins in the UPR recognise it as an unfolded protein. Hence, the unfolded ATF6 could lose its trafficking function as a result. This might be one of the reasons that we still noted the interaction between BiP and the mutants ATF6, since a common function of BiP is reported to bind with the unfolded proteins which appear in the ER lumen during ER stress (Schindler and Schekman, 2009).

BiP is one of the most well-known ER chaperones, that regulates the unfolded protein in the ER lumen. However, the mechanism of the BiP dissociation from the UPR sensors like ATF6 during ER stress, is still not fully understood. Previously, researchers thought the main reason of the BiP dissociation might be simply a competitive process between the unfolded proteins that accumulate in the ER lumen upon stress, and the UPR reporters, since the unfolded proteins are a strong competitor compared with the UPR reporters, leading to the dissociation of BiP from UPR reporters (Shen et al., 2002; Bertolotti et al., 2000; Bukau and Horwich, 1998). However, recent studies suggested that the complex of ATF6-BiP is very stable and the accumulation of the unfolded proteins upon ER stress or the presence of ATP alone, cannot simply lead the dissociation of BiP from ATF6, it requires more additional factors (Schindler and Schekman, 2009; Shen et al., 2005). Other studies suggested that BiP can be modified by some ER oxidoreductase such as PDIR and this thiol modification of BiP affects the stability of the BiP-ATF6 complex, therefore this kind of modification of BiP might be regulating the association of BiP with ATF6 and other UPR reporters (Wang and Sevier, 2016; Higa et al., 2014; Wei et al., 2012). In addition, the binding of BiP results in ATF6 retention in the ER lumen since the dissociation of BiP from the ATF6 luminal domain may unmask a Golgi localisation sequence, leading to the transport of ATF6 from the ER to the Golgi. Indeed, the over expression of BiP

can slow down or inhibit the transport process of ATF6 upon ER stress (Shen et al., 2002). However, our study suggests that the dissociation of the ER retention factor like BiP from ATF6 is insufficient to induce ATF6 trafficking, since we found that BiP also dissociated from the mutants ATF6, both ATF6(D564G) and ATF6(Y567N), as occurs from the wild type ATF6. Despite the dissociation of BiP, the ATF6 mutants still remain in the ER lumen during ER stress (Chapter 3.6). Therefore, it seems like the trafficking process of ATF6 requires other additional factors to assist after BiP release. Accordingly, this retention of the ATF6 mutants might be controlled by the a redox switch or glycosylation modification of ATF6, since there were studies which suggested that the association of ER oxidoreductase like ERp18 and PDIR, and proteins involved in glycoprotein quality control such as glucosidase II and calreticulin, are important for ATF6 to package into COP II vesicles prior to transport to the Golgi (Oka et al., 2019; Higa et al., 2014; Lynch et al., 2012; Honore, 2009; Jeong et al., 2008; Ye et al., 2000; Haze et al., 1999). The mutants of our study might not bind to the mentioned proteins and/or be modified because of the altered conformation and are retained after ER stress.

ATF6 is found in three different forms during the absence of ER stress, monomeric, dimeric and oligomeric form, which are the result of intra- and/or inter-molecular disulfide formation between the two cysteine residues in the luminal domain of ATF6. The masking by BiP of the translocation region of the ATF6 luminal domain will retain all of these redox forms of ATF6 in the ER. Researchers suggested that during ER stress, after the dissociation of BiP, ATF6 will be reduced to the monomeric form before transport to the Golgi, since the reduced monomer of ATF6 is likely to be the most preferable form for trafficking and for S1P and S2P cleavage (Sato et al., 2011; Nadanaka et al., 2007; Shen et al., 2002). However, our study shows the contrasting result since we only detected the dimeric form of ATF6 luminal domain after S1P and S2P cleavage when we induced ER stress with TG or when we merged the Golgi to the ER by Brefeldin A (Fig. 3.6 and 3.7). Interestingly, when we merged the Golgi to the ER by using Brefeldin A, our non-trafficking mutants ATF6 only generated the monomeric form as a result of S1P and S2P cleavage, even though the ATF6(D564G) mutant can express all of redox form the same as the wild type ATF6 (Fig. 3.8). It seems that the redox forms of ATF6 could be produced during S1P and S2P cleavage. Nonetheless, it is clear that the S1P could recognise and cleave both dimeric and

monomeric forms of ATF6, and that the wild type ATF6 will exit the ER in dimeric form rather than the monomeric.

It has previously been reported that the luminal domain of ATF6 has two conserved cysteine residues at amino acid 467 and 618, and these cysteine residues can form the intra- and/or inter-molecular disulfide bonds between each other, hence the ATF6 could be found as monomer, dimer, and oligomer. Recently, the additional information about ATF6 disulfide formation suggested that the oligomeric and the dimeric form of ATF6, are in fact both dimers differentiated by electrophoretic mobility. The band that we used to think as an oligomeric form of ATF6 (slower mobility), appeared to be a disulfide formation between C467 residues, meanwhile, the dimer (faster mobility) appears to be a disulfide formation between C618 residues (Koba et al., 2020; Oka et al., 2019; Nadanaka et al., 2007). This information allows us to conclude that the unknown bands we found at the upper and the lower position than the dimeric (C618-dimer) band of the wild type ATF6 in the presence of ER stress induced by TG (Fig. 3.6.B), could be the result of the mixed disulfide formation between C618 and C467 residues of ATF6 or between the ATF6 molecule and the disulfide exchange protein(s) in the PDI families such as ERp18.

In accordance with the results of our study and the information accumulated from numerous other studies, the post-processes modification of ATF6 after the releasing of BiP has a critical role in packaging of ATF6 into COP II vesicles and trafficking. The potential modifications include the glycosylation and redox status within the luminal domain of ATF6 (Oka et al., 2019; Higa et al., 2014; Lynch et al., 2012; Honore, 2009; Jeong et al., 2008; Ye et al., 2000; Haze et al., 1999). Therefore, the disruption of these modification processes will lead to the non-trafficking of ATF6 in the presence of ER stress. The altered conformation of our non-trafficking mutants ATF6, ATF6(D564G) and ATF6(Y567N), may disrupt these modification processes after the release of BiP. Even though we are still not sure how the disruption occurs, our hypothesis is the altered conformation of the ATF6 mutants might obscure specific binding sites or the binding sites might not be exposed in the right way. Hence the proteins involved with ATF6 modification cannot access the ATF6 luminal domain. Moreover, the altered conformation of the ATF6 mutants might be recognised as

one of the unfolded proteins. Therefore, BiP or other chaperone association might occur in the same way as when these proteins bind to unfolded proteins, rather than the way it binds to the wild type ATF6.

6. 2. The non-trafficking mutants ATF6 are forming a complex with others ER resident proteins differently from the wild type ATF6

Since our study suggested that disulfide formation of the non-trafficking mutants ATF6 was different from the wild type of protein and that an altered conformation might affect the binding of other ER resident proteins to the luminal domain of ATF6, we decided to establish whether there were differences in the ATF6 complexes as determined by density gradient analysis. It was reported that the ATF6 could go through modification after release of BiP and association with some specific proteins such as ERp18, PDIR, glucosidase II. Subsequently, the modified ATF6 could package into COP II vesicles and traffic from the ER to the Golgi during ER stress (Oka et al., 2019; Higa et al., 2014; Lynch et al., 2012; Honore, 2009; Jeong et al., 2008; Ye et al., 2000; Haze et al., 1999). Results of our study suggested that the ATF6 mutants, both ATF6(D564G) and ATF6(Y567N), form a complex with the other ER proteins differently from the wild type ATF6 in both resting stage and during ER stress (Chapter 4.1 and 4.2). The sucrose gradient approach was not ideal since the results were inconsistent. However, we still could see differences between the sedimentation patterns between the wild type ATF6 and the mutant, as well as the differences between complexes from cells in the absence or presence of ER-stress (Fig. 4.1). Moreover, the results of our mass spectrometry also supported the results of our sucrose gradients in that the wild type and the ATF6 mutants form a complex with other proteins differently. Numerous proteins were found in the ATF6-proteins complex as a result of mass spectrometry (Table 4.1), however we chose only 4 promising proteins for our future investigation at this time, 14-3-3E, protein TFG, Neudesin, and ERdj3. These proteins became the promising candidates in the ATF6 trafficking regulation in our study since some of them such as 14-3-3E and ERdj3 are already reported to have a role involved with ER stress response. Meanwhile the proteins TFG and Neudesin have a broad range of function in cells, hence it might be worth investigating these too (Hanafusa, Wada, and Hosokawa, 2019; Romine and

Wiseman, 2019; Pennington et al., 2018; Kanadome et al., 2017; Genereux et al., 2015; Johnson et al., 2015; Beetz et al., 2013).

To verify the mass spectrometry results we carried out immunoisolation of the ATF6 complex and western blot analysis to determine the presence of our most promising hits (Chapter 4.3). Unfortunately, we could not see any interaction between ATF6 and our identified proteins in our first attempt. However, we know that mass spectrometry is a very sensitive method, it could detect even a small amount of protein in the sample. Therefore, our inability to detect an interaction-by western blotting might be due to the low level of our proteins in the sample. For this reason we adapted our immunoisolation and western blot protocol and focused only for one particular protein, the ERdj3, instead of investigating all four proteins at the same time, since ERdj3 is an ER chaperone in DnaJ family which has been reported to be involved with the regulation of BiP function in the UPR, therefore, it seemed to be the most promising protein from the four identified proteins (Hanafusa, Wada, and Hosokawa, 2019; Romine and Wiseman, 2019; Genereux et al., 2015; Shen and Hendershot, 2005). After some adaptations in the immunoisolation protocol, we could confirm that ERdj3 can interact with ATF6 (Fig. 4.2.C) and the reason we cannot detected it in the earlier experiments is might due to the weak binding between ATF6 and ERdj3, hence a harsh washing step during immunoisolation protocol could cause the loss of protein interaction.

Recently, several studies suggested that the ERdj3 is also involved with the UPR, mainly in the protein's folding processes. ERdj3 is found to assist BiP by transferring the unfolded proteins to BiP after the dissociation of BiP from ATF6 upon ER stress (Hanafusa, Wada, and Hosokawa, 2019; Romine and Wiseman, 2019; Genereux et al., 2015; Shen and Hendershot, 2005). However, there is no report of an interaction between ATF6 and ERdj3 until now. According to our previous study, ERdj3 interacts with ATF6, however it is still a challenge to demonstrate a role for ERdj3 in ATF6 trafficking at this point, it could be involved in either retention or translocation regulation. Subsequent investigation of the role of ERdj3, showed that in the absence of ER stress ERdj3 associated with ATF6 and dissociated from ATF6 when ER stress was induced (Chapter 4.4). However, the dissociation of ERdj3 seems to be insufficient to drive the trafficking of ATF6,

since the dissociation of ERdj3 was also seen in the non-trafficking ATF6 mutants in the presence of ER stress and the mutants still remained in the ER. This could suggest that the interaction of ERdj3 might play a retention role toward the wild type ATF6, or it might recognise and interact with the altered conformation of the ATF6 mutants as a misfolded protein.

The absence of ERdj3 shows no significant effect toward ATF6 function in the UPR, since the expression of the UPR downstream products of ATF6 activation, such as BiP, the appearance of the Golgi form of ATF6 and the cleavage form of ATF6, are all similar in both the wild type ERdj3 and the ERdj3-KO cells during ER stress (Chapter 4.6 and 4.7). Thus, we can suggest that ERdj3 had no regulatory role toward ATF6 during the UPR since the absence of ERdj3 did not disrupt induction of the ATF6 pathway (Fig 4.8 and 4.9). In addition, our results showed no difference in BiP expression during ER stress in the presence and absence of ERdj3 and BiP was still released from the UPR sensers like ATF6 and PERK in the absence of ERdj3 (Fig. 4.7). According to previous studies the role of ERdj3 with BiP in the protein folding process, is to recruit the unfolded protein to BiP (Genereux et al., 2015; Jin, Zhuang and Hendershot., 2009). However, from our study, it is clear that the role of ERdj3 can be replaced by the other co-factor(s), since the absence of ERdj3 show no effect toward releasing BiP. Interestingly, while ERdj3 shows no direct regulatory effect toward ATF6 in the UPR, ATF6 itself seems to regulate the function of ERdj3 in ER stress response, since the absence of ATF6 can affect the expression of ERdj3 during stress. We found that in the ATF6-KO cells, the removal of ATF6 can inhibit the expression of ERdj3 in the cells, while the level of ERdj3 secretion increases during the stress response (Fig. 4.5). Our result is in contrast with the study of another ER stress response mediator, PERK, which regulates the secretion of the ERdj3-unfolded protein complex. The absence of PERK can cause the accumulation of the complex in the ER lumen (Romine and Wiseman., 2019). Therefore, it is likely to be that the association ATF6 is not related to the secretion of ERdj3 in the presence of ER stress, without ATF6, ERdj3 still simply could be secreted from the cells with the increasing of unfolded proteins in the ER lumen. Some studies suggested that secretion will appear after the association of ERdj3 with the unfolded proteins in the presence of ER stress (Pobre, Poet, and Hendershot, 2019; Genereux et al., 2015), however, it is clear that the increase of unfolded proteins in the ER lumen alone is enough

to lead the secretion of ERdj3 from the cells, it is not required an additional factor of ATF6 to complete the process. Moreover, our study also suggested that the expression of ERdj3 is significantly involved with the presence of ATF6, since in the wild-type ATF6 cells, ERdj3 level is increased in the cells during ER stress. Meanwhile, in the ATF6-KO cells the level of ERdj3 remained unchanged. It would be interesting to see if we could observe the secretion of ERdj3 and the expression level in the cells expressing just the ATF6 mutants in future studies. This would test our earlier hypothesis about ER resident proteins involved with the protein folding processes, and whether they might recognise the non-trafficking ATF6 mutants as unfolded proteins due to the altered conformation of the luminal domain.

6. 3. The lipotoxic stress response of ATF6 by the inducing of DHS and DHC

For this part of our work, we focused on lipotoxic stress, a new inducer of the ER stress response, hoping for more understanding of the role of ATF6 in the ER lipid homeostasis. Lipotoxic stress is a newly studied area of ER stress, which has its own pathway distinctly different from the proteotoxic stress pathway. Proteotoxic stress activates the UPR sensers like ATF6 via the luminal domain, whereas lipotoxic stress activates the UPR sensors via the transmembrane motif (Tam et al., 2019; Halbleib et al., 2017; Volmer and Ron, 2015; Volmer et al., 2013; Promlek et al., 2011). There is still a lack of knowledge about this pathway compared to the common proteotoxicity pathway, however, there was a recent report showed that specific lipids such as DHS and DHC could induce ER-lipotoxic stress response directly via the ATF6 pathway (Tam et al., 2019). Therefore, we decided to use DHS and DHC, the intermediators of sphingolipid biosynthetic pathway, as an ER stress inducer in our study. We aimed to generate lipotoxic stress in our cells expressing ATF6 mutants and compare the results to those that we generated from the normal proteotoxic stress inducers like DTT or TG. Since our ATF6 mutants have a point mutation in the luminal domain they should affect the way of ATF6 luminal domain senses proteotoxic stress, however the mutation in the luminal domain might not affect the response of ATF6 to lipotoxic stress since it is reported to be activated via the transmembrane domain.

To begin with, we induced lipotoxic stress in the wild type ATF6 cell line by using DHS and DHC to see whether it could induce the stress response in the cells, before using these lipids to induce the lipotoxic stress in the cells expressing ATF6 mutants. After several experiments, our results are not consistent with the results of Tam's group, who reported that the DHS and DHC could induce ER stress response via ATF6 (Tam et al., 2019). Our results suggested that the DHS and DHC do not induce ER stress compared with ER stress inducers like DTT or TG (Chapter 6.1 and 6.2). The DHS and DHC do not induce any downstream products of ER stress response such as the Golgi form or the nuclear form of ATF6, or BiP induction (Fig. 5.2.A). Even for ACOX1, the specific protein involved with lipid synthesis which was reported could be upregulated by DHS and DHC via ER stress, the expression of ACOX1 remained unchanging in our study (Fig. 5.2.B). The results of the DHS and DHC induced ER stress in the wild type ATF6 cells convincingly show that DHS and DHC could not induce ER stress and upregulate the ATF6 stress response pathway in our hands. Despite our results contrasting with the previous study, it still a possibility that our results are of value, since the study of lipotoxic stress is very new, the data or the information might be changed from time to time when more experiments are performed to obtain more information. It is possibility that the conditions that we used in our experiment are different from the conditions which were used in the published paper in some specific details, even though we tried to reproduce their experiments as close as possible and used the DHS and DHC reagent from the same supplier. In addition, the cell-line specificity is also a concern for the comparison of our results and the publication results since we used different cell types for the experiments. Moreover, we also need to verify the method that we used to treat our cells with DHS and DHC since we do not have a positive control that would allow us to confirm that the added lipids actually do get into the cells. Therefore, it is necessary to do more experiments to determine the basis for the discrepancy in the results obtained.

CHAPTER VII: MITIGATION PLAN - To investigate the mechanism by which disease mutants of ATF6 are prevented from ER to Golgi trafficking.

7. 1. Introduction and aims

According to the situation of the Covid pandemic during the time of my study, the impact of disruption is high since my study is lab based/object-based research. Therefore, when the pandemic occurred, I had to stop all my research work for several months because of the full lockdown. After the full lockdown there was also a restriction and social distancing requirement for working in laboratory and I cannot do the experiment full time as usual, so the disruption is still continuous as a medium Impact for several months after the lockdown. Thus, this chapter was added as a compensation for the lost lab time.

Recent studies provide strong evidence that ATF6 has an important role in the unfolded protein response, which regulates proteins synthesis in the ER lumen. Malfunctional ATF6 can lead to ER stress and cell death, which can cause multiple pathological conditions such as cancer, diabetes, ischemic disease and achromatopsia (Glembotski, Rosarda and Wiseman, 2019; Hillary and FitzGerald, 2018; Chiang et al., 2017; Kohl et al., 2015; Glembotski, 2014; Usui et al., 2012; Schewe and Aguirre-Ghiso, 2008). ATF6 is a type II ER transmembrane protein, which was identified as a member of the basic leucine zipper (bZIP) family (Haze et al., 1999 and 2001). The C-terminal luminal domain of ATF6 is unstructured, contains disulfide bonds and senses changes to the redox conditions within the ER. The N-terminal cytosolic domain is a DNA binding domain, which works as a transcription factor to upregulate the ER stress response element (ERSE) such as BiP, XBP1, glucose-regulated protein 94 (GRP94), and protein disulfide isomerase (Okada et al., 2002; Haze et al., 1999; Yoshida et al., 1998). Signal transduction of ATF6 is thought to be regulated by BiP which binds to the luminal domain of ATF6. Upon stress, BiP is released from ATF6 to bind with unfolded proteins, which accumulate in the ER lumen and used to count as a higher affinity substrate for BiP than the UPR mediators. The dissociation of BiP is thought to lead to the formation of a reduced monomer of ATF6 which can be packaged into the coat protein complex II (COPII) vesicles and migrate to the Golgi complex (Schindler and Schekman, 2009; Nadanaka et al., 2004). There, ATF6 is cleaved by site 1 protease (S1P) and site 2 protease (S2P), and the cleaved soluble ATF6

translocates to the nucleus where it will upregulate the transcription of ER chaperone and folding enzymes (Shen and Prywes, 2004; Ye et al., 2000; Haze et al., 1999). Meanwhile, during chronic stress ATF6 is also responsible for apoptosis by upregulating genes involved in cell death such as CHOP and the endoplasmic reticulum protein 29 (ERp29) (Hirsch et al., 2014; Tabas and Ron, 2011; Yoshida et al., 2000).

Despite these previous studies, the process of ATF6 trafficking from the ER to the Golgi is not straightforward and requires a number of additional elements, for instance, ATP, COPII cargo protein, protein disulfide isomerases (PDI), and thrombospondin (Thbs). ATP has been identified to be required for protein quality-control by BiP, therefore, lack of ATP inhibits the dissociation of BiP from ATF6 under stress conditions (Vishnu et al., 2014; Mirazimi and Svensson, 2000; Dorner and Kaufman, 1994; Braakman, Helenius, and Helenius 1992). In addition, the dissociation of the BiP-ATF6 complex does not mean that ATF6 will translocate to the Golgi or undergo proteolysis (Nadanaka et al., 2004; Antonny and Schekman, 2001). A recent study demonstrated that the reduced monomer form of ATF6, which is thought to form only after dissociation from BiP, is the most preferable form for packaging into COPII vesicles and also the most preferable substrate form of S1P enzyme. This may prevent unnecessary activation of the UPR when ATF6 migrates by mistake to the Golgi in the absence of ER stress (Schindler and Schekman, 2009; Nadanaka et al., 2007). The reduction of ATF6 is likely to be accomplished by proteins in the PDI family such as the protein disulfide isomerase A5 (PDIA5 or PDIR), (Higa et al., 2014; Nadanaka et al., 2004). Specifically, PDI participates in inter- and intra-molecular disulfide bond rearrangement to activate ATF6. Furthermore, vesicles packaging of ATF6 is thought to involve proteins in the Thbs group, in particular Thbs4, which binds to the luminal domain of ATF6 and promotes vesicles formation and the migration of ATF6 to the Golgi (Brodya et al., 2016; Lynch et al., 2012). In addition, other studies suggested that the luminal domain of ATF6 plays an important role in stress sensing and trafficking. Several types of luminal domain mutants, such as Y567N, D564G, and G512Lfs*39, lead to a decrease or prevention of downstream signal in the ATF6 pathway by blocking the trafficking of ATF6 from the ER to the Golgi. Thus, when ER stress occurs, ATF6 with these mutations is retained in the ER and

cannot upregulate the UPR genes (Chianga et al., 2017). The mechanisms and proteins in facilitating these processes remain elusive.

Although, our knowledge of the UPR and ATF6 activation pathway has increased, it is important to understand the mechanism of ATF6 in every aspect to allow novel therapeutic approaches to be developed. This project will focus on the proteins involved with trafficking of ATF6 from the ER to the Golgi by studying the disease mutants of ATF6, ATF6 (D564G) and ATF6 (Y567N), which can prevent the trafficking of ATF6 (Chianga et al., 2017). Therefore, we can compare the absence or the present of specific proteins in the mutant cells with proteins in wild type ATF6 cells during ER stress. The results of this study will provide a clearer idea of the regulatory mechanism of ATF6 and the role of additional proteins in the process. Our specific aims are:

- To investigate the role of the proteins which are found in the complex with ATF6.
- To examine the redox status of the ATF6 luminal domain and the role of disulfide bridges in controlling trafficking.
- To study the role of the glycosylation status of ATF6 in trafficking.

7. 2. Experimental design and methods to be used

7.2.1. The siRNA knockdown of target genes associated with regulation of ATF6 trafficking

Recent reports indicate that BiP is insufficient to regulate the trafficking of ATF6 from the ER to the Golgi and the process requires additional proteins. Previously we have found by mass spectrometry that several proteins interact differently with either the wild type or ATF6 mutants during ER stress. In this project we want to evaluate whether these proteins are involved in ATF6 trafficking. If BiP dissociates from the mutants but they are not trafficked, then the expectation is that they interact (or not) with downstream factors that are involved in retention (or forward trafficking). Hence the proteins that we found through mass spectrometry could be involved in retention (or selection for forward

trafficking), consequently, the knockdown experiments would be carried out to test the roles of the proteins.

Once the interactions of ATF6 or BiP with all of the proteins of our interest ERdj3, 14-3-3E, TGF, or Neudesin, have been verified, we will address the consequence of knocking down specific genes on the activation and trafficking of the ATF6 mutants. Individual genes will be knocked down using siRNA to examine the effect of reducing protein expression on the translocation of ATF6 from the ER to the Golgi. If the proteins are playing an important role, the trafficking of ATF6 should be decreased or completely prevented after knockdown. For this experiment, siRNA will be specifically designed for the target genes so the siRNA will selectively adjust the level of individual proteins. The wild type ATF6 stable cell-line will be transfected with siRNA targeting specific gene and then screened for knockdown efficiency by qPCR or western blotting. High efficiency of knockdown will be selected and treated with ER stress inducer such as tunicamycin, thapsigargin, or DTT. The treated cells will be lysed, immunoprecipitated with anti-V5 antibody which is specific to the V5 tagged C-terminal of ATF6, and then the level of the cleaved ATF6 will be analyse by western blotting with anti-ATF6. The results of this study will show the level of the cleaved ATF6 in the knockdown cells, if the cleaved form of ATF6 is not showing after ER stress induction, therefore we can confirm that the unexpressed protein in the knockdown cells is playing an importance role for ATF6 trafficking. Meanwhile, we can consider that the knocked down protein is selectively working only for ATF6 regulation, or it could be regulating the other UPR reporters, like IRE1 and PERK by doing the same experiment that we use for investigated ATF6. The knockdown cells will be treated with ER stress inducers such as tunicamycin, thapsigargin, or DTT, and then will be lysed. The cells lysate will be immunoprecipitated with anti-IRE1 or anti-PERK antibody, and then the expression level of IRE1 and PERK will be analysed by western blotting with anti-p-IRE1 or anti-p-PERK antibody. If the results show that the expression of p-IRE1 and p-PERK are still increasing after the knockdown cells were induced ER stress, it means that the knockdown protein has not affected IRE1 or PERK, and specifically regulated only the ATF6 pathway. In other way, after roughly screening to find the most promising gene(s) from our protein candidates, ERdj3, 14-3-3E, TGF, or Neudesin, by knockdown method, we can evaluate the role of the proteins of our interest by creating the knockout cell

lines. Moreover, for the knockout-cells, we can restore the expression of the proteins by transfection to recheck its function, meanwhile the knockdown-cells would prevent the cell from compensating for the reduction of protein level. The proteins will be knocked out by CRISPR/Cas9 method using vectors expressed specific guide RNA for individual protein of interest. Then the knockout cells will be used to investigate the consequence of restoring the expression of the identified proteins. However, for the knockout experiment, we already have some data for ERdj3 and the data suggested that the expression of ERdj3 during stress response seemed to be regulated by ATF6, rather than the ATF6 or BiP regulated or activated by ERdj3. Therefore, it is still worth examining the other proteins; 14-3-3E, TGF and Neudesin, which we did not have enough time to check determine.

7.2.2. Changing of redox status of the ATF6 luminal domain and the role of disulfide bridges

According to our studies, the non-trafficking mutants ATF6, D564G and Y567N, are found in different redox states compared to the wild type ATF6. It is already well known that the two conserved cysteines in the luminal domain of wild type ATF6 can form inter- and intramolecular disulfide bridges appearing in oligomeric, dimeric, and monomeric forms. However, our experiments show that the D564G mutant appears in all forms as the wild type in normal conditions, while the dimeric form rapidly disappears during ER stress compared with the wild type. Additionally, the Y567N mutant is only present as a monomer in non-stressed ER but forms an alternative dimer to the wild type protein following stress. Even though D564G and Y567N are not close to the position of the conserved cysteine residues, the mutations affect the formation of disulfides in the luminal domain of ATF6. Recent studies suggest that ATF6 leaves the ER in the form of a reduced monomer following stress (Kroeger et al., 2018; Schindler and Schekman, 2009; Nadanaka et al., 2007), so the redox status of the non-trafficking mutants ATF6 should be considered.

As it was stated in the precious paragraph, in the non-reducing gels the untreated wild type ATF6 has 3 specific forms, oligomer, dimer and monomer,

meanwhile, the Y567N mutation only has monomer and the D564G mutation has 3 forms with the rapid disappearance of the dimer after exposing with stress. Therefore, to investigate the formation of disulfides in the ATF6 mutants, the thiol-reactive probe 4-acetamido-4'-maleimidylstilbene-2,2;-disulfonate (AMS) will be used. The untreated wild type and ATF6 mutant cell-lines will be lysed with or without N-ethylmaleimide (NEM), then proteins will be precipitated with trichloroacetic acid (TCA) and reduced with DTT. Consequently, the reduced proteins will be incubated with or without AMS for covalent modification on the thiol group of cysteine residues and analysed by immunoblotting using an anti-ATF6 antibody. The results will demonstrate the presence or absence of the free thiols in the luminal domain of ATF6 mutants, so we can determine if the monomeric form of the mutants is oxidized or reduced (Fig. 7.1.A).

Furthermore, it was clear that the mutants ATF6, D564G and Y567N, formed the disulfide bond in a different way from the wild type ATF6, however the reason why it formed differently is unclear and it might significantly affect the trafficking of ATF6 during stress. We can determine whether mutants ATF6 are disulfide bonded with another ATF6 or other ER proteins by immunoprecipitating the lysates of the untreated ^{35}S-labeled cells with anti-ATF6 antibody and immunoblotting analysis under reducing and non-reducing condition (Fig. 7.1.B). The difference of the ATF6 migration will indicate oligomeric and redox status of the mutants (Fig. 7.1.C).

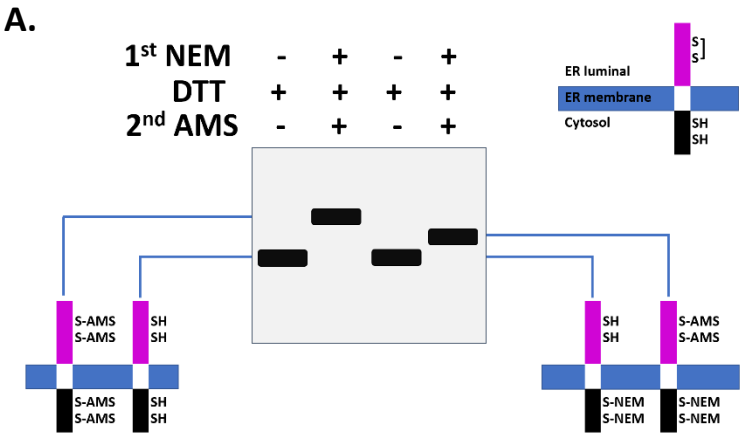

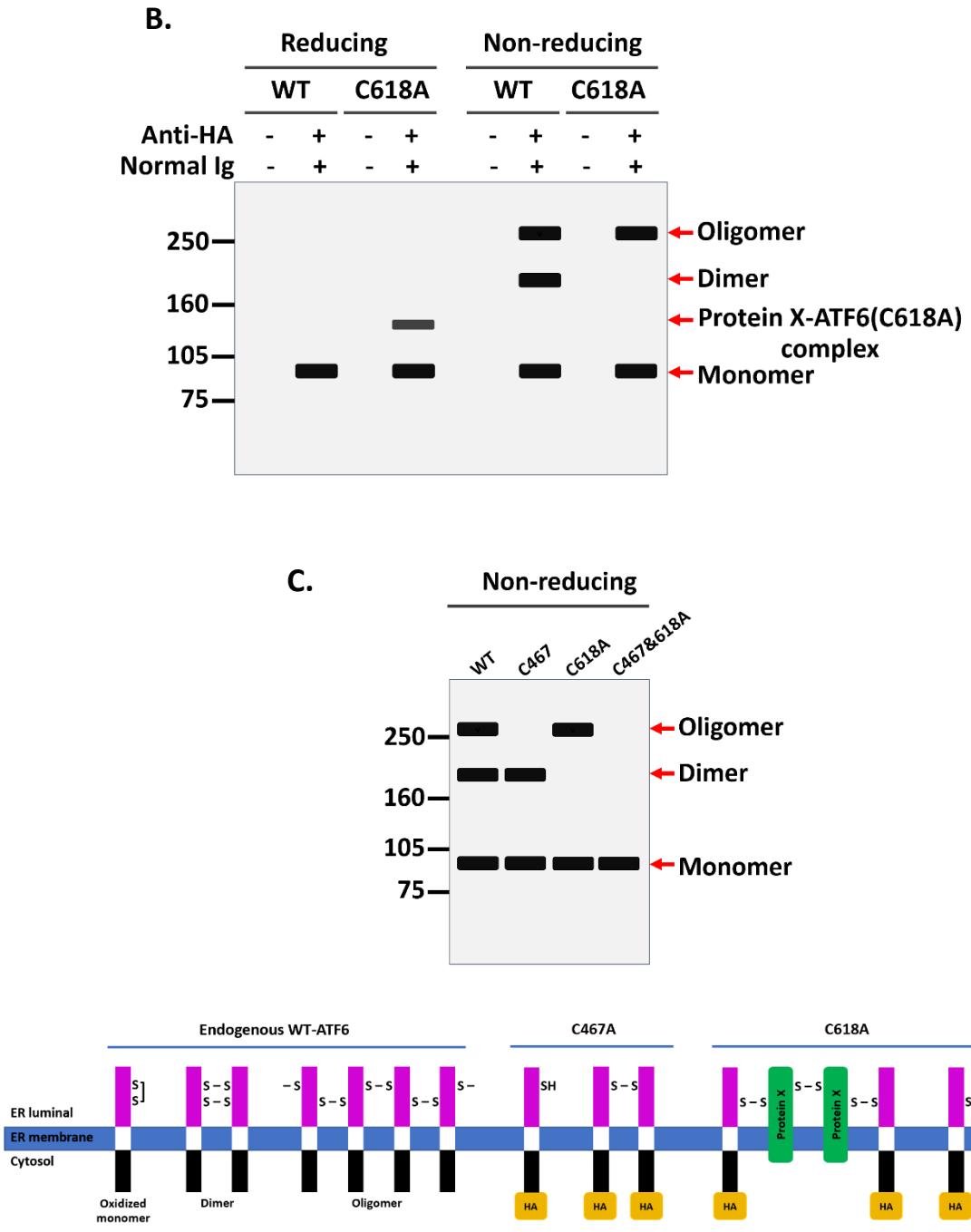

Fig. 7.1. The presence of the disulfide bonds in ATF6. The figure is adapted from the publication of Nadanaka S. and colleagues in 2007 (Nadanaka et al., 2007). (A) ATF6(WT) cells with four cysteine residues, two in the luminal domain and two in the cytosolic domain, were harvested with PBS contained or not contained NEM. Then the proteins lysate was precipitated with TCA and reduced with DTT, followed by incubation with or without AMS. Proteins were then separated by SDS-PAGE under reducing condition and analyzed by immunoblotting using anti-ATF6 antibody. Cysteines with free SH or disulfide bonded as well as those covalently modified with NEM or AMS are illustrated. (B) ATF6(WT) cells or the cysteine mutant ATF6 cells, ATF6(C618A), were pulse-labeled with [35S]methionine and cysteine. The SDS-PAGE results under reducing and nonreducing conditions shown difference forms of ATF6, which formed the disulfide bonds between molecules

of ATF6 or between ATF6 and unknown proteins (protein X). (C) Non-reducing SDS-page shown the difference disulfide formations on the luminal domain of ATF6(WT) compared with the disulfide mutants of ATF6, C467A, C618A and C467&618. The disulfide formations are also illustrated under the SDS-page figure.

7.2.3. Glycosylation status of ATF6

Since there is still lack of evidence and understanding of the trafficking mechanism of ATF6, except the co-proteins which assisted ATF6 to traffic, one of the possible control factors of ATF6 trafficking is the glycosylation status of ATF6. Recently, the information we have suggested that the glycosylated ATF6 with high mannose N-glycan was established in the ER and transported to the Golgi when ER stress occurred. Therefore, in Golgi, the glycosylated ATF6 was modified by glycosidases to form an Endo H-resistant ATF6 before undergoing S1P and S2P protease cleavage (Kroeger et al., 2018; Ye et al., 2000; Haze et al., 1999). However, the glycosylation status of the non-trafficking mutants ATF6, such as D567G and Y567N, remains undetermined. Thus, the aim of this study is to examine the glycosylation status of the mutants ATF6 to see whether it is similar or different from the wild type ATF6 because these point mutations clearly affect disulfide formation, so it might be also to charge the conformation of ATF6 leading to unusual glycosylation of ATF6. Firstly, the sensitivity of the glycosylated ATF6 with Endo H will be tested. The untreated wild type ATF6 and the mutants AT6 cell-lines will be lysated and then treated with Endo H. If the mutants ATF6 are glycosylated as the wild type in the non-stress condition, the western blotting analysis will show a single band of the deglycosylated ATF6. Afterwards, the conversion of Asparagine to aspartate after deglycosylation will be monitored by mass spectrometry to identify the glycosylation site in the wild type and mutants ATF6 peptides. The ER fraction will be prepared by sucrose gradient from the untreated wild type and mutants ATF6 cell-lines and then treated with the labelled $H_2{}^{18}O$ during PNGase F digestion. After deglycosylated by PNGase F, asparagine residues of the ATF6 luminal domain will be converted to aspartate with ^{18}O incorporation and this change will be analysed by mass spectrometry. Moreover, we can also create cell-line with the glycosylation site mutants of ATF6 and then induce cells with ER stress inducers to examine the effect of the

mutation in the ATF6 trafficking. The data should unveil more information of the role of the glycosylation in ATF6 transport.

7. 3. Conclusion

The mechanism of the UPR has been explored throughout this decade, however there are so many aspects of this mechanism that still remain obscure, including the regulation of the ATF6 pathway. It has been reported that ATF6 has its own mechanism which works differently from other UPR reporters like PERK and IRE1, to respond to unfolded protein and ER stress. Initially, it was shown that BiP an ER chaperone plays a key role in the downstream regulation of ATF6. Only after BiP is released from ATF6 following stress is the protein packaged into COP II vesicles and trafficked from the ER to the Golgi. Recent studies show that BiP release from ATF6 is insufficient to drive the translocation of ATF6 from the ER to the Golgi. In addition, it is unclear what role of disulfide bonds has in regulating ATF6 trafficking control. However, it has been shown that the luminal domain of ATF6 is the most important part of ATF6 which regulates the mechanism of trafficking. Several mutations which occur in the luminal domain, can prevent trafficking of ATF6 and inhibit the downstream signal for the UPR during ER stress. From our previous study, the results shown that specific mutation types of ATF6 luminal domain, such as D564G and Y567N, still can be released from BiP during stress induction, despite that trafficking is blocked. Thereby, there may be other factors which have a crucial role in terms of trafficking control. There are other results from our experiments which indicated some proteins in PDI family, ER chaperone group, and the group of trafficking-control proteins, like ERdj3, ERp18, and ERO1, as a candidate protein in trafficking control. According to the knowledge we have, if we can continue our research as described above to test all the hypothesis. The results will improve our understanding about ATF6 pathway, and we may discover the way to control or boost it in patients who are suffering with different kinds of diseases.

LIST OF RERERENCES

Adachi, N., Nawata, K., Maeta, M., and Kurozawa, Y. (2008). Relationship of the menstrual cycle phase to anterior cruciate ligament injuries in teenaged female athletes. Arch. Orthop. Trauma Surg., 128(5), 473-478.

Adams, B. M., Canniff, N. P., Guay, K. P., and Hebert, D. N. (2021). The Role of Endoplasmic Reticulum Chaperones in Protein Folding and Quality Control. Prog. Mol. Subcell. Biol., 59, 27-50.

Adams, C. J., Kopp, M. C., Larburu, N., Nowak, P. R., and Ali, M. M. U. (2019). Structure and Molecular Mechanism of ER Stress Signaling by the Unfolded Protein Response Signal Activator IRE1. Front. Mol. Biosci., 6, 11.

Alder, M. N., Rogozin, I. B., Iyer, L. M., Glazko, G. V., Cooper, M. D., Pancer, Z. (2005). Diversity and function of adaptive immune receptors in a jawless vertebrate. Science., 310(5756), 1970-1973.

Almanza, A., Carlesso, A., Chintha, C., Creedican, S., Doultsinos, D., Leuzzi, B., Luís, A., McCarthy, N., Montibeller, L., More, S., Papaioannou, A., Püschel, F., Sassano, M. L., Skoko, J., Agostinis, P., de Belleroche, J., Eriksson, L. A., Fulda, S., Gorman, A. M., Healy, S., Kozlov, A., Muñoz-Pinedo, C., Rehm, M., Chevet, E., and Samali, A. (2019). Endoplasmic reticulum stress signalling - from basic mechanisms to clinical applications. FEBS. J., 286(2), 241-278.

Antonny, B. and Schekman, R. (2001). ER export: public transportation by the COPII coach. Curr. Opin. Cell. Biol., 13, 438-443.

Appenzeller-Herzog, C. and Ellgaard, L. (2008). The human PDI family: versatility packed into a single fold. Biochim. Biophys. Acta., 1783(4), 535-48.

Arai, K., Takei, T., Okumura, M., Watanabe, S., Amagai, Y., Asahina, Y., Moroder, L., Hojo, H., Inaba, K., and Iwaoka, M. (2017). Preparation of Selenoinsulin as a Long-Lasting Insulin Analogue. Angew. Chem. Int. Ed. Engl., 56, 5522-5526.

Ariyasu, R., Horiike, A., Yoshizawa, T., Dotsu, Y., Koyama, J., Saiki, M., Sonoda, T., Nishikawa, S., Kitazono, S., Yanagitani, N., and Nishio, M. (2017). Adrenal Insufficiency Related to Anti-Programmed Death-1 Therapy. Anticancer Res., 37(8), 4229-4232.

Baumann, O., and Walz, B. (2001). Endoplasmic reticulum of animal cells and its organization into structural and functional domains. Int. Rev. Cytol., 205, 149-214.

Bertolotti, A., Wang, X., Novoa, I., Jungreis, R., Schlessinger, K., Cho, J. H., West, A. B., and Ron, D. (2001). Increased sensitivity to dextran sodium sulfate colitis in IRE1β-deficient mice. J. Clin. Invest., 107, 585–593.

Bertolotti, A., Zhang, Y., Hendershot, L. M., Harding, H. P., and Ron, D. (2000). Dynamic interaction of BiP and ER stress transducers in the unfolded-protein response. Nat. Cell. Biol., 2, 326–332.

Bhardwaj, M., Leli, N. M., Koumenis, C., and Amaravadi, R. K. (2020). Regulation of autophagy by canonical and non-canonical ER stress responses. Semin. Cancer Biol., 66, 116–128.

Blobel, G. (1980). Intracellular protein topogenesis. Proc. Natl. Acad. Sci. USA., 77(3), 1496-1500.

Braakman, I., and Bulleid, N. J. (2011). Protein folding and modification in the mammalian endoplasmic reticulum. Annu. Rev. Biochem., 80, 71-99.

Braakman, I., and Hebert, D. N. (2013). Protein folding in the endoplasmic reticulum. Cold Spring Harbor Perspectives in Biology., 5(5):a013201.

Brodya, M. J., Schipsa, T. G., Vanhouttea, D., Kanisicaka, O., Karcha, J., Bryan D. Malikena, N. Scott Blaira, Sargenta, M. A., Prasada, V., and Molkentin, J. D. (2016). Dissection of thrombospondin-4 domains involved in intracellular adaptive endoplasmic reticulum stress-responsive signaling. Mol. Cell. Biol., 36, 2-12.

Calfon, M., Zeng, H., Urano, F., Till, J. H., Hubbard, S. R., Harding, H. P., Clark, S. G., and Ron, D. (2002). IRE1 couples endoplasmic reticulum load to

secretory capacity by processing the XBP-1 mRNA. Nature., 415(6867), 92-96.

Chalmers, F., Van Lith, M., Sweeney, B., Cain, K., and Bulleid, N. J. (2017). Inhibition of IRE1a-mediated XBP1 mRNA cleavage by XBP1 reveals a novel regulatory process during the unfolded protein response. Wellcome Open Research., 2, 36.

Chen, K. C., Qu, S., Chowdhury, S., Noxon, I. C., Schonhoft, J. D., Plate, L., Powers, E. T., Kelly, J. W., Lander, G. C., and Wiseman, R. L. (2017). The endoplasmic reticulum HSP40 co-chaperone ERdj3/DNAJB11 assembles and functions as a tetramer. EMBO. J., 36(15), 2296-2309.

Chen, Y., and Brandizzi, F. (2013). IRE1: ER stress sensor and cell fate executor. Trends in Cell Biology., 23(11):547-555.

Chiang, W. C., Chan, P., Wissinger, B., Vincent, A., Skorczyk-Werner, A., Krawczyński, M. R., Kaufman, R. J., Tsang, S. H., Héon, E., Kohl, S., and Lin, J. H. (2017). Achromatopsia mutations target sequential steps of ATF6 activation. Proc. Natl. Acad. Sci. USA., 114(2), 400-405.

Correll, R. N., Grimes, K. M., Prasad, V., Lynch, J. M., Khalil, H., and Molkentin, J. D. (2019). Overlapping and differential functions of ATF6a versus ATF6ß in the mouse heart. Sci. Rep., 9(1), 2059.

Credle, J. J., Finer-Moore, J. S., Papa, F. R., Stroud, R. M., and Walter, P. (2005). On the mechanism of sensing unfolded protein in the endoplasmic reticulum. Proc. Natl. Acad. Sci. USA., 102(52), 18773-18784.

Cuevas, E. P., Eraso, P., Mazón, M. J., Santos, V., Moreno-Bueno, G., Cano, A., and Portillo, F. (2017). LOXL2 drives epithelial-mesenchymal transition via activation of IRE1-XBP1 signalling pathway. Sci. Rep., 27, 44988.

Dandekar, A., Mendez, R., and Zhang, K. (2015). Cross talk between ER stress, oxidative stress, and inflammation in health and disease. Methods Mol. Biol.,1292, 205-214.

Deponte, M. (2013). Glutathione catalysis and the reaction mechanisms of glutathione-dependent enzymes. Biochim. Biophys. Acta., 1830(5), 3217-66.

Deshaies, R. J., Sanders, S. L., Feldheim, D. A., Schekman, R. (1991). Assembly of yeast Sec proteins involved in translocation into the endoplasmic reticulum into a membrane-bound multisubunit complex. Nature., 349(6312), 806-808.

Dorner, A. J., and Kaufman, R. J. (1994). The levels of endoplasmic reticulum proteins and ATP affect folding and secretion of selective proteins. Biologicals., 22(2), 103-112.

DuRose, J. B., Tam, A. B., and Niwa, M. (2006). Intrinsic capacities of molecular sensors of the unfolded protein response to sense alternate forms of endoplasmic reticulum stress. Mol. Biol. Cell., 17, 3095-3107.

Eletto, D., Eletto, D., Dersh, D., Gidalevitz, T., and Argon, Y. (2014). Protein disulfide isomerase A6 controls the decay of IRE1a signaling via disulfide-dependent association. Mol. Cell., 53, 562–576.

Ellgaard, L., and Helenius, A. (2003). Quality control in the endoplasmic reticulum. Nat. Rev. Mol. Cell. Biol., 4, 181-191.

English, A. R., and Voeltz, G. K. (2013). Endoplasmic reticulum structure and interconnections with other organelles. Cold Spring Harb Perspect Biol., 5(4), a013227.

English, A. R., Zurek, N., and Voeltz, G. K. (2009). Peripheral ER structure and function. Curr. Opin. Cell Biol., 21(4), 596-602.

Fass, D. (2019). Going for the Golgi: small PDI protein helps ATF6 perform better under stress. EMBO. J., 38(15), e102743.

Fagone, P., and Jackowski, S. (2009). Membrane phospholipid synthesis and endoplasmic reticulum function. J. Lipid Res., 50 Suppl(Suppl), S311-316.

Flynn, G. C., Pohl, J., Flocco, M. T., and Rothman, J. E. (1991). Peptide-binding specificity of the molecular chaperone BiP. Nature., 353(6346), 726-730.

Friedlander, R., Jarosch, E., Urban, J., Volkwein, C., and Sommer, T. (2000). A regulatory link between ER-associated protein degradation and the unfolded-protein response. Nat. Cell. Biol., 2, 379-384.

Fu, X., Cui, J., Meng, X., Jiang, P., Zheng, Q., Zhao, W., and Chen, X. (2021). Endoplasmic reticulum stress, cell death and tumor: Association between endoplasmic reticulum stress and the apoptosis pathway in tumors (Review). Oncol. Rep., 45(3), 801-808.

Gestaut, D., Roh, S. H., Ma, B., Pintilie, G., Joachimiak, L. A., Leitner, A., Walzthoeni, T., Aebersold, R., Chiu, W., and Frydman, J. (2019). The Chaperonin TRiC/CCT Associates with Prefoldin through a Conserved Electrostatic Interface Essential for Cellular Proteostasis. Cell., 177(3), 751-765.e15.

Gilmore, R., Walter, P., and Blobel, G. (1982). Protein translocation across the endoplasmic reticulum. II. Isolation and characterization of the signal recognition particle receptor. J. Cell. Biol., 95(2 Pt 1), 470-477.

Glembotski, C. C. (2014). Roles for ATF6 and the sarco/endoplasmic reticulum protein quality control system in the heart. J. Mol. Cell Cardiol., 71, 11-15.

Glembotski, C. C., Rosarda, J. D., and Wiseman, R. L. (2019). Proteostasis and Beyond: ATF6 in Ischemic Disease. Trends Mol. Med., 25(6), 538-550.

Glick, B. S., and Nakano, A. (2009). Membrane traffic within the Golgi apparatus. Annu. Rev. Cell. Dev. Biol., 25, 113-132.

Guo, F., and Snapp, E. L. (2013). ERdj3 regulates BiP occupancy in living cells. J. Cell. Sci., 126, 1429–1439.

Gao, R., Peterson, E. J., and Voytek, B. (2017). Inferring synaptic excitation/inhibition balance from field potentials. Neuroimage., 158, 70-78.

Guo, Y., Sirkis, D. W., and Schekman, R. (2014). Protein sorting at the trans-Golgi network. Annu. Rev. Cell Dev. Biol., 30, 169-206.

Han, J., Back, S. H., Hur, J., Lin, Y., Gildersleeve, R., Shan, J., Yuan, C. L., Krokowski, D., Wang, S., Hatzoglou, M., Kilberg, M. S., Sartor, M. A., and Kaufman, R. J. (2013). ER-stress-induced transcriptional regulation increases protein synthesis leading to cell death. Nat. Cell. Biol., 15(5), 481–490.

Han, J., and Kaufman, R. J. (2016). The role of ER stress in lipid metabolism and lipotoxicity. J. Lipid Res., 57(8), 1329-38.

Harding, H. P., Zhang, Y., Bertolotti, A., Zeng, H., and Ron, D. (2000). Perk is essential for translational regulation and cell survival during the unfolded protein response. Mol. Cell., 5, 897–904.

Harding, H. P., Zhang, Y., and Ron, D. (1999). Protein translation and folding are coupled by an endoplasmic-reticulum-resident kinase. Nature., 397(6716), 271-274.

Haze, K., Okada, T., Yoshida, H., Yanagi, H., Yura, T., Negishi, M., and Mori, K. (2001). Identification of the G13 (cAMP-response-element-binding protein-related protein) gene product related to activating transcription factor 6 as a transcriptional activator of the mammalian unfolded protein response. Biochem. J., 355, 19-28.

Haze, K., Yoshida, H., Yanagi, H., Yura, T., and Mori, K. (1999). Mammalian transcription factor ATF6 is synthesized as a transmemmbrane protein and activated by proteolysis in response to endoplasmic reticulum stress. Mol. Biol. Cell., 10,, 3787-3799.

Hebert, D. N., and Molinari, M. (2007). In and out of the ER: protein folding, quality control, degradation, and related human diseases. Physiol. Rev., 87(4), 1377-1408.

Helenius, A., Marquardt, T., and Braakman, I. (1992). The endoplasmic reticulum as a protein-folding compartment. Trends Cell Biol., 2(8), 227-231.

Hetz, C., and Papa, F. R. (2018). The Unfolded Protein Response and Cell Fate Control. Mol. Cell., 69(2),169-181.

Higa, A., Taouji, S., Lhomond, S., Jensen, D., Fernandez-Zapico, M. E., Simpson, J. C., Pasquet, J. M., Schekman, R., and Chevet, E. (2014). Endoplasmic reticulum stress-activated transcription factor ATF6a requires the disulfide isomerase PDIA5 to modulate chemoresistance. Mol. Cell. Biol., 34, 1839-1849.

Hillary, R. F., and FitzGerald, U. (2018). A lifetime of stress: ATF6 in development and homeostasis. J. Biomed. Sci., 25(1), 48.

Hiramatsu, N., Messah, C., Han, J., LaVail, M. M., Kaufman, R. J., and Lin, J. H. (2014). Translational and posttranslational regulation of XIAP by eIF2a and ATF4 promotes ER stress-induced cell death during the unfolded protein response. Mol. Biol. Cell., 25, 1411–1420.

Hirsch, I., Weiwad, M., Prell, E., and Ferrari, D. M. (2014). ERp29 deficiency affects sensitivity to apoptosis via impairment of the ATF6–CHOP pathway of stress response. Apoptosis , 19, 801–815.

Honjo, Y., Ayaki, T., Tomiyama, T., Horibe, T., Ito, H., Mori, H., Takahashi, R., and Kawakami, K. (2017). Decreased levels of PDI and P5 in oligodendrocytes in Alzheimer's disease. Neuropathology., 37(6), 495-501.

Hosoda, A., Kimata, Y., Tsuru, A., and Kohno, K. (2003). JPDI, a novel endoplasmic reticulum-resident protein containing both a BiP-interacting J-domain and thioredoxin-like motifs. J. Biol. Chem., 278, 2669-2676.

Hotamisligil, G. S. (2010). Endoplasmic reticulum stress and the inflammatory basis of metabolic disease. Cell., 140(6), 900-917.

Hu, H., Tian, M., Ding, C., and Yu, S. (2019). The C/EBP Homologous Protein (CHOP) Transcription Factor Functions in Endoplasmic Reticulum Stress-Induced Apoptosis and Microbial Infection. Front. Immunol., 9, 3083.

Iwakoshi, N. N., Lee, A. H., Vallabhajosyula, P., Otipoby, K. L., Rajewsky, K., and Glimcher, L. H. (2003). Plasma cell differentiation and the unfolded

protein response intersect at the transcription factor XBP-1. Nat. Immunol., 4(4), 321-329.

Iwawaki, T., Akai, R., Yamanaka, S., and Kohno, K. (2009). Function of IRE1 alpha in the placenta is essential for placental development and embryonic viability. Proc. Natl. Acad. Sci. USA, 106, 16657–16662.

Iwawaki, T., Hosoda, A., Okuda, T., Kamigori, Y., Nomura-Furuwatari, C., Kimata, Y., Tsuru, A., and Kohno, K. (2001). Translational control by the ER transmembrane kinase/ribonuclease IRE1 under ER stress. Nat. Cell. Biol., 3, 158–165.

Jan, C. H., Williams, C. C., Weissman, J. S. (2014). Principles of ER cotranslational translocation revealed by proximity-specific ribosome profiling. Science., 346(6210), 1257521.

Jha, V., Kumari, T., Manickam, V., Assar, Z., Olson, K. L., Min, J. K., and Cho, J. (2021). ERO1-PDI Redox Signaling in Health and Disease. Antioxid Redox Signal., 35(13), 1093-1115.

Jin, J. K., Blackwood, E. A., Azizi, K., Thuerauf, D. J., Fahem, A. G., Hofmann, C., Kaufman, R. J., Doroudgar, S., Glembotski, C. C. (2017). ATF6 Decreases Myocardial Ischemia/Reperfusion Damage and Links ER Stress and Oxidative Stress Signaling Pathways in the Heart. Circ Res., 120(5), 862-875.

Karagöz, G. E., Acosta-Alvear, D., Nguyen, H. T., Lee, C. P., Chu, F., and Walter, P. (2017). An unfolded protein-induced conformational switch activates mammalian IRE1. Elife., 6, e30700.

Karlin, S., and Brocchieri, L. (1998). Heat shock protein 70 family: Multiple sequence comparisons, function, and evolution. Journal of Molecular Evolution., 47(5), 565-577.

Kaufman, R. J. (1999). Stress signaling from the lumen of the endoplasmic reticulum: coordination of gene transcriptional and translational controls. Genes Dev., 13(10), 1211-1233.

Kim, Y. E., Hipp, M. S., Bracher, A., Hayer-Hartl, M., and Hartl, F. U. (2013). Molecular chaperone functions in protein folding and proteostasis. Annu. Rev. Biochem., 82, 323–355.

Kopp, M. C., Larburu, N., Durairaj, V., Adams, C. J., and Ali, M. M. U. (2019). UPR proteins IRE1 and PERK switch BiP from chaperone to ER stress sensor. Nat. Struct. Mol. Biol., 26(11), 1053-1062.

Kozlov, G., Maattanen, P., Thomas, D. Y., and Gehring, K. (2010). A structural overview of the PDI family of proteins. FEBS J., 277, 3924–3936.

Lai, E., Teodoro, T., and Volchuk, A. (2007). Endoplasmic reticulum stress: signaling the unfolded protein response. Physiology (Bethesda)., 22, 193-201.

Lee, I. C., Ho, X. Y., George, S. E., Goh, C. W., Sundaram, J. R., Pang, K. K. L., Luo, W., Yusoff, P., Sze, N. S. K., and Shenolikar, S. (2017). Oxidative stress promotes SIRT1 recruitment to the GADD34/PP1a complex to activate its deacetylase function. Cell Death Differ., 25, 255–267.

Lin, J. H., Li, H., Yasumura, D., Cohen, H. R., Zhang, C., Panning, B., Shokat, K. M., Lavail, M. M., and Walter, P. (2007). IRE1 signaling affects cell fate during the unfolded protein response. Science, 318, 944-949.

Lippert, U., Diao, D., Barak, N. N., Ferrari, D. M. (2007). Conserved structural and functional properties of D-domain containing redox-active and -inactive protein disulfide isomerase-related protein chaperones. J. Biol. Chem., 282, 11213-11220.

Liu, J., Xiao, M., Li, J., Wang, D., He, Y., He, J., Gao, F., Mai, L., Li, Y., Liang, Y., Liu, Y., and Zhong, X. (2017). Activation of UPR signaling pathway is associated with the malignant progression and poor prognosis in prostate cancer. Prostate., 77(3), 274-281.

Lynch, J. M., Maillet, M., Vanhoutte, D., Schloemer, A., Sargent, M. A., Blair, N. S., Lynch, K. A., Okada, T., Aronow, B. J., Osinska, H., Prywes, R., Lorenz, J. N., Mori, K., Lawler, J., Robbins, J., and Molkentin, J. D. (2012). A

thrombospondin-dependent pathway for a protective ER stress response. Cell., 149, 1257-1268.

Maattanen, P., Kozlov, G., Gehring, K., Thomas D. Y. (2006). ERp57 and PDI: multifunctional protein disulfide isomerases with similar domain architectures but differing substrate-partner associations. Biochem. Cell Biol., 84, 881-889.

Malhi, H., and Kaufman, R. J. (2011). Endoplasmic reticulum stress in liver disease. J. Hepatol., 54(4), 795-809.

Martínez, I. M., and Chrispeels, M. J. (2003). Genomic analysis of the unfolded protein response in Arabidopsis shows its connection to important cellular processes. Plant. Cell., 15, 561-576.

Martino, M. B., Jones, L., Brighton, B., Ehre, C., Abdulah, L., Davis, C. W., Ron, D., O'Neal, W. K., and Ribeiro, C. M. P. (2013). The ER stress transducer IRE1β is required for airway epithelial mucin production. Mucosal Immunol., 6, 639–654.

Mathew, A. (2015). The P5 disulfide switch: taming the aging unfolded protein response. Cell Stress Chaperones., 20(5), 743-751.

Matsusaki, M., Kanemura, S., Kinoshita, M., Lee, Y. H., Inaba, K., Okumura, M. (2020). The Protein Disulfide Isomerase Family: From proteostasis to pathogenesis. Biochim. Biophys. Acta Gen. Subj., 2020, 1864, 129338.

McQuiston, A., and Diehl, J. A. (2017). Recent insights into PERK-dependent signaling from the stressed endoplasmic reticulum. F1000Research, 6, 1897.

Meldolesi, J., and Pozzan, T. (1998). The endoplasmic reticulum Ca2+ store: a view from the lumen. Trends Biochem Sci., 23(1), 10-14.

Mirazimi, A., and Svensson, L. (2000). ATP is required for correct folding and disulfide bond formation of rotavirus VP7. J. Virol., 74, 8048-8052.

Morris, J. A., Dorner, A. J., Edwards, C. A., Hendershot, L. M., and Kaufman, R. J. (1997). Immunoglobulin binding protein (BiP) function is required to

protect cells from endoplasmic reticulum stress but is not required for the secretion of selective proteins. J. Biol. Chem., 272(7), 4327-4334.

Mrowiec, T., and Schwappach, B. (2006). 14-3-3 proteins in membrane protein transport. Biol Chem., 387(9), 1227-36.

Munro, S., and Pelham, H. R. (1986). An Hsp70-like protein in the ER: identity with the 78 kd glucose-regulated protein and immunoglobulin heavy chain binding protein. Cell., 46(2), 291-300.

Nadanaka, S., Okada, T., Yoshida, H., and Mori, K. (2007). Role of disulfide bridges formed in the luminal domain of ATF6 in sensing endoplasmic reticulum stress. Mol. Cell. Biol., 27, 1027-1043.

Nadanaka, S., Yoshida, H., Kano,F., Murata, M., and Mori, K. (2004). Activation of mammalian unfolded protein response is compatible with the quality control system operating in the endoplasmic reticulum. Mol. Biol. Cell., 15, 2537–2548.

Nillegoda, N. B., and Bukau, B. (2015). Metazoan Hsp70-based protein disaggregases: emergence and mechanisms. Front. Mol. Biosci., 2: 57.

Oikawa, D., Kimata, Y., and Kohno, K. (2007). Self-association and BiP dissociation are not sufficient for activation of the ER stress sensor Ire1. J. Cell. Sci., 120(Pt 9), 1681-1688.

Oka, B. O., Lith, V. M., Rudolf, J., Tungkum, W., Pringle, A. M., Bulleid, J. N., (2019). ER p18 regulates activation of ATF 6a during unfolded protein response. EMBO. J., 38(15).

Oka, O. B., Pringle, M. A., Schopp, I. M., Braakman, I., and Bulleid, N. J. (2013). ERdj5 is the ER reductase that catalyzes the removal of non-native disulfides and correct folding of the LDL receptor. Mol. Cell., 50(6), 793-804.

Okada, S., Matsusaki, M., Arai, K., Hidaka, Y., Inaba, K., Okumura, M., and Muraoka, T. (2019). Coupling effects of thiol and urea-type groups for

promotion of oxidative protein folding. Chem. Commun. (Camb.), 55, 759-762.

Okada, T., Yoshida, H., Akazawa, R., Negishi, M., and Mori, K. (2002). Distinct roles of activating transcription factor 6 (ATF6) and double-stranded RNA-activated protein kinase-like endoplasmic reticulum kinase (PERK) in transcription during the mammalian unfolded protein response. Biochem J., 366, 585-594.

Okumura, M., Kadokura, H., and Inaba, K. (2015). Structures and functions of protein disulfide isomerase family members involved in proteostasis in the endoplasmic reticulum. Free. Radic. Biol. Med., 83, 314–322.

Otero, J. H., Lizák, B., and Hendershot, L. M. (2010). Life and death of a BiP substrate. Seminars in Cell & Developmental Biology., 21(5), 472-478.

Ozcan, L., and Tabas, I. (2012). Role of endoplasmic reticulum stress in metabolic disease and other disorders. Annu. Rev. Med., 63, 317–328.

Pakula, T. M., Laxell, M., Huuskonen, A., Uusitalo, J., Saloheimo, M., and Penttilä, M. (2003). The effects of drugs inhibiting protein secretion in the filamentous fungus Trichoderma reesei. Evidence for down-regulation of genes that encode secreted proteins in the stressed cells. J. Biol. Chem., 278, 45011-45020.

Pincus, D., Chevalier, M. W., Aragón, T., van Anken, E., Vidal, S. E., El-Samad, H., and Walter, P. (2010). BiP binding to the ER-stress sensor Ire1 tunes the homeostatic behavior of the unfolded protein response. PLoS. Biol., 8(7), e1000415.

Poet, G. J., Oka, O. B., van Lith, M., Cao, Z., Robinson, P. J., Pringle, M. A., Arnér, E. S., and Bulleid, N. J. (2017). Cytosolic thioredoxin reductase 1 is required for correct disulfide formation in the ER. EMBO. J., 36(5), 693-702.

Potter, M. D., and Nicchitta, C. V. (2002). Endoplasmic reticulum-bound ribosomes reside in stable association with the translocon following termination of protein synthesis. J. Biol. Chem., 277(26), 23314-23320.

Prinz, W.A., Grzyb, L., Veenhuis, M., Kahana, J.A., Silver, P.A. and Rapoport, T.A. (2000). Mutants affecting the structure of the cortical endoplasmic reticulum in Saccharomyces cerevisiae. J. Cell. Biol., 150, 461– 474.

Prischi, F., Nowak, P. R., Carrara, M., and Ali, M. M. U. (2014). Phosphoregulation of Ire1 RNase splicing activity. Nat. Commun., 5, 3554.

Rajapaksa, G., Nikolos, F., Bado, I., Clarke, R., Gustafsson, J. Å., and Thomas, C. (20015). ERB decreases breast cancer cell survival by regulating the IRE1/XBP-1 pathway. Oncogene, 34, 4130–4141.

Rajesh, K., Krishnamoorthy, J., Kazimierczak, U., Tenkerian, C., Papadakis, A. I., Wang, S., Huang, S., and Koromilas, A. E. (2015). Phosphorylation of the translation initiation factor eIF2a at serine 51 determines the cell fate decisions of Akt in response to oxidative stress. Cell Death Dis, 6, e1591.

Rapoport, T. A. (2007). Protein translocation across the eukaryotic endoplasmic reticulum and bacterial plasma membranes. Nature., 450(7170), 663-669.

Read, A., and Schröder, M. (2021). The Unfolded Protein Response: An Overview. Biology (Basel)., 10(5), 384.

Reid, D. W., and Nicchitta, C. V. (2015). Diversity and selectivity in mRNA translation on the endoplasmic reticulum. Nat. Rev. Mol. Cell Biol., 16(4), 221-231.

Reimold, A. M., Iwakoshi, N. N., Manis, J., Vallabhajosyula, P., Szomolanyi-Tsuda, E., Gravallese, E. M., Friend, D., Grusby, M. J., Alt, F., and Glimcher, L. H. (2001). Plasma cell differentiation requires the transcription factor XBP-1. Nature, 412, 300-307.

Ron, D. (2002). Translational control in the endoplasmic reticulum stress response. J. Clin. Invest, 110, 1383-1388.

Ron, D., and Walter, P. (2007). Signal integration in the endoplasmic reticulum unfolded protein response. Nat. Rev. Mol. Cell. Biol., 8, 519-529.

Ruggiano, A., Foresti, O., and Carvalho, P. (2014). Quality control: ER-associated degradation: protein quality control and beyond. J. Cell. Biol., 204(6), 869-879.

Rutkevich, L. A., Cohen-Doyle, M. F., Brockmeier, U., Williams, D. B. (2010). Functional relationship between protein disulfide isomerase family members during the oxidative folding of human secretory proteins. Mol. Biol. Cell., 21(18), 3093-3105.

Schewe. D. M., and Aguirre-Ghiso, J. A. (2008). ATF6alpha-Rheb-mTOR signaling promotes survival of dormant tumor cells in vivo. Proc. Natl. Acad. Sci. USA., 105(30), 10519-1024.

Schindler, S. J., and Schekman, R. (2009). In vitro reconstitution of ER-stress induced ATF6 transport in COPII vesicles. Proc. Natl. Acad. Sci. USA., 106, 17775–17780.

Schröder, M., and Kaufman, R. J. (2005). ER stress and the unfolded protein response. Mutat. Res., 569(1-2), 29-63.

Schröder, M., and Kaufman, R. J. (2005). The mammalian unfolded protein response. Annu. Rev. Biochem., 74, 739-789.

Schuck, S., Prinz, W. A., Thorn, K. S., Voss, C., and Walter, P. (2009). Membrane expansion alleviates endoplasmic reticulum stress independently of the unfolded protein response. J. Cell Biol., 187, 525-536.

Seiser, R. M., and Nicchitta, C. V. (2000). The fate of membrane-bound ribosomes following the termination of protein synthesis. J. Biol. Chem., 275(43), 33820-33827.

Sevier, C. S., and Kaiser, C. A. (2006). Conservation and diversity of the cellular disulfide bond formation pathways. Antioxid. Redox Signal., 8, 797-811.

Shen, J., and Prywes, R. (2004). Dependence of site-2 protease cleavage of ATF6 on prior site-1 protease digestion is determined by the size of the luminal domain of ATF6. J Biol Chem. , 279, 43046-43051.

Shen, J., Chen, X., Hendershot, L., and Prywes, R. (2002). ER stress regulation of ATF6 localization by dissociation of BiP/GRP78 binding and unmasking of Golgi localization signals. Dev. Cell., 3, 99-111.

Sheng, X., Nenseth, H. Z., Qu, S., Kuzu, O. F., Frahnow, T., Simon, L., Greene, S., Zeng, Q., Fazli, L., Rennie, P. S., Mills, I. G., Danielsen, H., Theis, F., Patterson, J. B., Jin, Y., Saatcioglu, F. (2019). IRE1a-XBP1s pathway promotes prostate cancer by activating c-MYC signaling. Nat. Commun., 10(1), 323.

Shibata, Y., Shemesh, T., Prinz, W. A., Palazzo, A. F., Kozlov, M. M., and Rapoport, T. A. (2010). Mechanisms determining the morphology of the peripheral ER. Cell., 143(5), 774-788.

Shibata, Y., Voeltz, G. K., and Rapoport, T. A. (2006). Rough sheets and smooth tubules. Cell., 126(3), 435-439.

Simon, S. M., and Blobel, G. (1991). A protein-conducting channel in the endoplasmic reticulum. Cell., 65(3), 371-380.

Sitia, R., and Braakman, I. (2003). Quality control in the endoplasmic reticulum protein factory. Nature., 426(6968), 891-894.

Smith, M. H., Ploegh, H. L., and Weissman, J. S. (2011). Road to ruin: targeting proteins for degradation in the endoplasmic reticulum. Science, 334, 1086-1090.

Sun, L., Zhang, S. S., Lu, S. J., and Liu, J. X. (2015). Site-1 protease cleavage site is important for the ER stress-induced activation of membrane-associated transcription factor bZIP28 in Arabidopsis. Sci China Life Sci., 58(3), 270-275.

Sweeney, P., Park, H., Baumann, M., Dunlop, J., Frydman, J., Kopito, R., McCampbell, A., Leblanc, G., Venkateswaran, A., Nurmi, A., and Hodgson,

R. (2017). Protein misfolding in neurodegenerative diseases: implications and strategies. Transl. Neurodegener., 6, 6.

Tabas, I., and Ron, D. (2011). Integrating the mechanisms of apoptosis induced by endoplasmic reticulum stress. Nat. Cell. Biol., 13, 184-190.

Tam, B. A., Roberts, S. L., Chandra, V., Rivera, I. G., Nomura, K. D., Forbes, J. D., Niwa, M. (2018). The UPR Activator ATF6 Responds to Proteotoxic and Lipotoxic Stress by Distinct Mechanisms. Dev. Cell., 46(3), 327–343.e7.

Terrab, L., and Wipf, P. (2020). Hsp70 and the Unfolded Protein Response as a Challenging Drug Target and an Inspiration for Probe Molecule Development. ACS. Med. Chem. Lett., 11(3), 232-236.

Thorpe, C., and Coppock, D.L., (2007). Generating disulfides in multicellular organisms: emerging roles for a new flavoprotein family. J. Biol. Chem., 282, 13929-13933.

Tirasophon, W., Lee, K., Callaghan, B., Welihinda, A., and Kaufman, R. J. (2000). The endoribonuclease activity of mammalian IRE1 autoregulates its mRNA and is required for the unfolded protein response. Genes. Dev., 14, 2725-2736.

Tirasophon, W., Welihinda, A. A., and Kaufman, R. J. (1998). A stress response pathway from the endoplasmic reticulum to the nucleus requires a novel bifunctional protein kinase/endoribonuclease (Ire1p) in mammalian cells. Genes. Dev., 12, 1812–1824.

Travers, K. J., Patil, C. K., Wodicka, L., Lockhart, D. J., Weissman, J. S., and Walter, P. (2000). Functional and genomic analyses reveal an essential coordination between the unfolded protein response and ER-associated degradation. Cell., 101, 249-258.

Usui, M., Yamaguchi, S., Tanji, Y., Tominaga, R., Ishigaki, Y., Fukumoto, M., Katagiri, H., Mori, K., Oka, Y., and Ishihara, H. (2012). Atf6a-null mice are glucose intolerant due to pancreatic β-cell failure on a high-fat diet but

partially resistant to diet-induced insulin resistance. Metabolism, 61(8), 1118-1128.

van Lith, M., Karala, A. R., Bown, D., Gatehouse, J. A., Ruddock, L. W., Saunders, P. T., and Benham, A. M. (2007). A developmentally regulated chaperone complex for the endoplasmic reticulum of male haploid germ cells. Mol Biol. Cell., 18(8), 2795-804.

Vishnu, N., Jadoon Khan, M., Karsten, F., Groschner, L. N., Waldeck-Weiermair, M., Rost, R., Hallström, S., Imamura, H., Graier, W. F., and Malli, R. (2014). ATP increases within the lumen of the endoplasmic reticulum upon intracellular Ca2+ release. Mol. Biol. Cell., 25, 368-379.

Vitale, A., and Denecke, J. (1999). The endoplasmic reticulum-gateway of the secretory pathway. Plant Cell., 11(4), 615-628.

Voeltz, G. K., Rolls, M. M., Rapoport, T. A. (2002). Structural organization of the endoplasmic reticulum. EMBO Rep., 3(10), 944-950.

Walter, P., Ibrahimi, I., and Blobel, G. (1981). Translocation of proteins across the endoplasmic reticulum. I. Signal recognition protein (SRP) binds to in-vitro-assembled polysomes synthesizing secretory protein. J. Cell. Biol., 91(2 Pt 1), 545-550.

Walter, P., and Ron, D. (2011). The unfolded protein response: from stress pathway to homeostatic regulation. Science, 334, 1081-1086.

Watson, M. L. (1955). The nuclear envelope; its structure and relation to cytoplasmic membranes. J Biophys Biochem Cytol., 1(3), 257-270.

Westrate, L. M., Lee, J. E., Prinz, W. A., and Voeltz, G. K. (2015). Form follows function: the importance of endoplasmic reticulum shape. Annu. Rev. Biochem., 84, 791-811.

West, M., Zurek, N., Hoenger, A., and Voeltz, G. K. (2011). A 3D analysis of yeast ER structure reveals how ER domains are organized by membrane curvature. J. Cell Biol., 193, 333–346.

Woehlbier, U., and Hetz, C. (2011). Modulating stress responses by the UPRosome: a matter of life and death. Trends Biochem Sci., 36(6), 329-337.

Wu,. J, and Kaufman, R. J. (2006). From acute ER stress to physiological roles of the Unfolded Protein Response. Cell Death Differ., 13(3), 374-84.

Xu, F., Du, W., Zou, Q. Wang, Y., Zhang, X., Xing, X., Li, Y., Zhang, D., Wang, H., Zhang, W., Hu, X., Liu, X., Liu, X., Zhang, S., Yu, J., Fang, J., Li, F., Zhou, Y., Yue, T., Mi, N., Deng, H., Zou, P., Chen, X., Yang, X., and Yu, L. (2021). COPII mitigates ER stress by promoting formation of ER whorls. Cell Res 31, 141–156.

Ye, J., Rawson, R. B., Komuro, R., Chen, X., Davé, U. P., Prywes, R., Brown, M. S., Goldstein, J. L. (2000). ER stress induces cleavage of membrane-bound ATF6 by the same proteases that process SREBPs. Mol. Cell., 6, 1355-1364.

Yoshida, H. (2007). ER stress and diseases. FEBS J., 274, 630-658.

Yoshida, H., Okada, T., Haze, K., Yanagi,H., Yura, T., Negishi, M., and Mori, K. (2000). ATF6 activated by proteolysis binds in the presence of NF-Y(CBF) directly to the cis-acting element responsible for the mammalian unfolded protein response. Mol. Cell. Biol., 20, 6755–6767.

Yoshida, H., Haze., Yanagi, H., Yura, T., and Mori, K. (1998). Identification of the cis-acting endoplasmicreticulum stress response element responsible for transcriptional induction of mammalian glucose-regulated proteins. Involvement of basic leucine zipper transcription factors. J. Biol. Chem., 273, 33741-33749.

Zeng, Y., Li, B., Zhang, W., Jiang, L. (2019). ER-Phagy and ER Stress Response (ERSR) in Plants. Front Plant Sci., 10, 1192.

Zhang, Z., Zhang, L., Zhou, L., Lei, Y., Zhang, Y., Huang, C. (2019). Redox signaling and unfolded protein response coordinate cell fate decisions under ER stress. Redox Biol., 25, 101047.